CANADIAN THESES ON MICROFICHE

THÈSES CANADIENNES SUR MICROFICHE

National Library of Canada
Collections Development Branch

Canadian Theses on
Microfiche Service

Ottawa, Canada
K1A 0N4

Bibliothèque nationale du Canada
Direction du développement des collections

Service des thèses canadiennes
sur microfiche

NOTICE

The quality of this microfiche is heavily dependent upon the quality of the original thesis submitted for microfilming. Every effort has been made to ensure the highest quality of reproduction possible.

If pages are missing, contact the university which granted the degree.

Some pages may have indistinct print especially if the original pages were typed with a poor typewriter ribbon or if the university sent us an inferior photocopy.

Previously copyrighted materials (journal articles, published tests, etc.) are not filmed.

Reproduction in full or in part of this film is governed by the Canadian Copyright Act, R.S.C. 1970, c. C-30. Please read the authorization forms which accompany this thesis.

AVIS

La qualité de cette microfiche dépend grandement de la qualité de la thèse soumise au microfilmage. Nous avons tout fait pour assurer une qualité supérieure de reproduction.

S'il manque des pages, veuillez communiquer avec l'université qui a conféré le grade.

La qualité d'impression de certaines pages peut laisser à désirer, surtout si les pages originales ont été dactylographiées à l'aide d'un ruban usé ou si l'université nous a fait parvenir une photocopie de qualité inférieure.

Les documents qui font déjà l'objet d'un droit d'auteur (articles de revue, examens publiés, etc.) ne sont pas microfilmés.

La reproduction, même partielle, de ce microfilm est soumise à la Loi canadienne sur le droit d'auteur, SRC 1970, c. C-30. Veuillez prendre connaissance des formules d'autorisation qui accompagnent cette thèse.

THIS DISSERTATION
HAS BEEN MICROFILMED
EXACTLY AS RECEIVED

LA THÈSE A ÉTÉ
MICROFILMÉE TELLE QUE
NOUS L'AVONS REÇUE

Canada

NL 339 (r. 86/09)

0-315-19610-6

National Library
of Canada

Bibliothèque nationale
du Canada

271

Canadian Theses Division

Division des thèses canadiennes

Ottawa, Canada
K1A 0N4

67518

PERMISSION TO MICROFILM — AUTORISATION DE MICROFILMER

- Please print or type — Écrire en lettres moulées ou dactylographier

Full Name of Author — Nom complet de l'auteur

Robert Arthur Hux

Date of Birth — Date de naissance February 15, 1983	Country of Birth — Lieu de naissance CANADA

Permanent Address — Résidence fixe

35 Forsyth Dr., Blenheim Ontario N0P 1A0

Title of Thesis — Titre de la thèse

LIQUID CHROMATOGRAPHY AND TWO-PHASE POTENTIOMETRIC TITRATIONS

University — Université

University of Alberta, Edmonton, Alberta

Degree for which thesis was presented — Grade pour lequel cette thèse fut présentée

Ph.D.

Year this degree conferred — Année d'obtention de ce grade 1983	Name of Supervisor — Nom du directeur de thèse Dr. F. F. Cantwell

Permission is hereby granted to the NATIONAL LIBRARY OF CANADA to microfilm this thesis and to lend or sell copies of the film.

The author reserves other publication rights, and neither the thesis nor extensive extracts from it may be printed or otherwise reproduced without the author's written permission.

L'autorisation est, par la présente, accordée à la BIBLIOTHÈQUE NATIONALE DU CANADA de microfilmer cette thèse et de prêter ou de vendre des exemplaires du film.

L'auteur se réserve les autres droits de publication; ni la thèse ni de longs extraits de celle-ci ne doivent être imprimés ou autrement reproduits sans l'autorisation écrite de l'auteur.

Date October 5, 1983	Signature Robert Hux

NL-91 (4/77)

THE UNIVERSITY OF ALBERTA

LIQUID CHROMATOGRAPHY AND TWO-PHASE POTENTIOMETRIC TITRATIONS

by

© ROBERT A. HUX

A THESIS

SUBMITTED TO THE FACULTY OF GRADUATE STUDIES AND RESEARCH

IN PARTIAL FULFILMENT OF THE REQUIREMENTS FOR THE DEGREE

DOCTOR OF PHILOSOPHY

DEPARTMENT OF CHEMISTRY

EDMONTON, ALBERTA

FALL 1983

THE UNIVERSITY OF ALBERTA

RELEASE FORM

NAME OF AUTHOR ROBERT A. HUX

TITLE OF THESIS LIQUID CHROMATOGRAPHY AND TWO-PHASE POTENTIOMETRIC TITRATIONS

DEGREE FOR WHICH THESIS WAS PRESENTED Ph.D.

YEAR THIS DEGREE GRANTED 1983

Permission is hereby granted to THE UNIVERSITY OF ALBERTA LIBRARY to reproduce single copies of this thesis and to lend or sell such copies for private, scholarly or scientific research purposes only.

The author reserves other publication rights, and neither the thesis nor extensive extracts from it may be printed or otherwise reproduced without the author's written permission.

(Signed) Robert Hux

PERMANENT ADDRESS:

35 Forsyth Dr.
Blenheim, Ontario
NOP 1A0

2

DATED October 5, 1983

THE UNIVERSITY OF ALBERTA

FACULTY OF GRADUATE STUDIES AND RESEARCH

The undersigned certify that they have read, and recommend to the Faculty of Graduate Studies and Research, for acceptance, a thesis entitled LIQUID CHROMATOGRAPHY AND TWO-PHASE POTENTIOMETRIC TITRATIONS

submitted by ROBERT A. HUX
in partial fulfilment of the requirements for the degree of
DOCTOR OF PHILOSOPHY.

Frederick F. Cantwell
F.F. Cantwell, Supervisor

Gary Horlick
G. Horlick

Dallas L Rabenstein
D.L. Rabenstein

W.A. Ayer

R.A. Locock
R.A. Locock

Peter W. Carr
P.W. Carr, External Examiner

DATE Sept 30, 1983

ABSTRACT

The first part of this thesis presents the results of an investigation of the acid-base titration behaviour of weak acids in vigorously stirred aqueous/immiscible organic solvent mixtures. Weak acids of the H_2A^+ charge type (e.g. the conjugate acids of aminophenols) whose first and second ionization constants are close show a sharp potentiometric pH "break" at the first equivalence point. Theoretical titration equations for H_2A^+ acids in such two-phase systems are derived and experimentally verified. Mixtures of a BH^+ type acid (e.g. organic ammonium ion) and an HA type acid (e.g. a phenol) with similar ionization constants can be differentiated by such two-phase titrations. The two-phase titrations can be performed with the same speed and precision (i.e. 1-2 ppt) of conventional aqueous potentiometric titrations.

The second part of this thesis describes the development of a liquid chromatographic method for the determination of the sedative drug, methaqualone (MTQ), in human blood plasma. A small pre-column (2 cm × 0.2 cm) packed with Amberlite XAD-2 (XAD) and placed before the analytical column allows direct injection of relatively large volumes (up to 4 mL) of untreated plasma. A pH 9.3 buffer washes out the plasma components and an

acetonitrile/water solvent subsequently elutes the MTQ from the pre-column through the analytical column. Pre-column parameters such as particle size and solvent flowrate are studied. MTQ detection limit is 0.3-0.6 ng/mL and analysis time is 7.5 min. Other common drugs do not interfere.

In the third and final part of this thesis, an on-stream pre-column equilibration technique has been used to measure the ionic strength dependence of the distribution coefficients, K, for the sorption of ionic samples on surface sulfonated Amberlite XAD-2 (SXAD). The method allows measurement of K for the sample to be made in the linear region of the sorption isotherm (trace conditions) even for very strongly retained samples (i.e. $K > 10^3$ L/Kg). The retention of m-nitrobenzyltrimethylammonium chloride (NBTACl) on SXAD can be quantitatively ascribed to two processes: cation exchange in the diffuse part of the electrical double layer at the SXAD/solution interface, and surface adsorption. While K for ion exchange varies inversely with ionic strength, surface adsorption depends on the electrical potential at the surface of the resin, ψ_o, which has a more complex dependence on ionic strength. The relative contribution of ion exchange to the overall retention of NBTACl on SXAD increases with ion exchange capacity over the range 0.01

to 0.06 meq/g. The relevance of these studies to "ion-pair" chromatography is discussed.

ACKNOWLEDGEMENTS

The author wishes to express his sincere gratitude to Dr. Frederick F. Cantwell for his guidance and encouragement during the course of this work.

Sincere thanks are also extended to Miss A. Wiseman for her excellent work in typing and proof reading this manuscript.

Finally, the author would like to thank Dr. Leslie Chatten of the College of Pharmacy, University of Alberta, and C.F. Hiskey of Endo Laboratories, Inc., for their supply of sample drugs.

TABLE OF CONTENTS

CHAPTER PAGE

PART I. TWO-PHASE POTENTIOMETRIC TITRATIONS......... 1

1. INTRODUCTION.. 2

2. THEORY.. 8

    2.1 Diprotic Acid H_2A^+.......................... 8

        2.1.1 Titration Equations...................... 8

        2.1.2 Predicted Titration Behaviour............ 17

3. EXPERIMENTAL.. 24

    3.1 Apparatus...................................... 24

    3.2 Chemicals...................................... 26

    3.3 Reagents and Solvents.......................... 28

    3.4 Aqueous Buffers................................ 29

    3.5 Titration Procedure............................ 31

    3.6 Distribution Coefficients...................... 32

4. RESULTS AND DISCUSSION.............................. 34

    4.1 Dissociation Constants......................... 36

    4.2 Distribution Coefficients...................... 42

    4.3 Quantitative Evaluation of Model............... 47

    4.4 Applications to Quantitative Analysis.......... 49

        4.4.1 Naloxone Hydrochloride................... 49

        4.4.2 Mixture of Molindone Hydrochloride and m-Nitrophenol.................... 49

CHAPTER PAGE

4.4.3 Naloxone Hydrochloride and Ammonium Chloride........................ 53

5. CONCLUSIONS.................................... 56

PART II. PRECOLUMNS OF AMBERLITE XAD-2 FOR DIRECT INJECTION LIQUID CHROMATOGRAPHIC DETERMINATION OF METHAQUALONE IN BLOOD PLASMA........ 58

1. INTRODUCTION.................................. 59

2. EXPERIMENTAL.................................. 65

2.1 Chromatograph............................. 65

2.2 Resins 68

2.3 Chemicals and Solutions................... 69

2.4 Standards and Samples..................... 70

2.5 Chromatographic Procedure................. 71

2.6 System Characterization................... 73

3. RESULTS AND DISCUSSION........................ 74

3.1 Chromatography of Plasma.................. 76

3.2 Chromatography of MTQ..................... 79

3.3 Recovery from Plasma...................... 80

3.4 Column Efficiency......................... 85

3.5 Quantitative Analysis..................... 88

3.6 Other Compounds........................... ~~90~~

CHAPTER PAGE

PART III. CHROMATOGRAPHIC RETENTION MECHANISM OF ORGANIC IONS ON A LOW CAPACITY CATION EXCHANGER........ 92

1. INTRODUCTION........ 93
2. THEORY........ 97
    - 2.1 Proposed Model........ 98
        - 2.1.1 Electrical Double Layer Theory........ 98
        - 2.1.2 Sorption on a Low Capacity Cation Exchanger........ 109
            - 2.1.2.1 Ion Exchange of a Counterion........ 109
            - 2.1.2.2 Surface Adsorption of a Counterion........ 114
            - 2.1.2.3 Surface Adsorption of a Coion........ 118
            - 2.1.2.4 Exclusion of a Coion........ 119
        - 2.1.3 Dependence of Sorption on Ionic Strength........ 120
            - 2.1.3.1 Sorption of a Counterion........ 120
            - 2.1.3.2 Sorption of a Coion........ 121
    - 2.2 Sorption Isotherms........ 123
3. EXPERIMENTAL........ 133
    - 3.1 Procedure........ 133

CHAPTER PAGE

3.2 Apparatus.................................. 136

3.3 Chemicals.................................. 139

3.4 Reagents and Solvents...................... 140

3.5 Sample Solutions........................... 141

3.6 Sorbent Preparation........................ 142

3.7 Mobile Phases and Columns.................. 143

3.8 Equipment Calibration...................... 145

3.9 Ion Exchange Capacity Measurements......... 148

4. RESULTS AND DISCUSSION........................ 151

4.1 Void Volume Measurements................... 151

4.1.1 XAD Resin............................. 151

4.1.2 Low Capacity Cation Exchanger (SXAD)............................. 155

4.2 Ion Exchange Capacity Measurements on SXAD.. 156

4.3 Sorption Isotherm Measurements............. 166

4.3.1 Acetaminophen on XAD Resin........... 166

4.3.2 Counterion on SXAD Resin............. 169

4.3.3 Coion on SXAD Resin.................. 173

4.4 Dependence of Sorption on Ionic Strength.... 174

4.4.1 Sorption of a Counterion on SXAD Resin.............................. 174

4.4.2 Sorption of a Coion on SXAD Resin.... 186

4.5 Relevance to Ion-Pair Chromatography....... 188

PAGE

*****

BIBLIOGRAPHY.. 195

APPENDIX I: Theoretical Derivation of the Titration Equations for H_2A^+ in a Two-Phase System................................. 213

APPENDIX II: Tables of Data used in Figures 25-32... 222

LIST OF TABLES

TABLE PAGE

1. Equilibrium constant and distribution coefficient expressions for H_2A^+ in a two-phase system.................................... 11
2. Distribution ratio of Naloxone as a function of pH.. 44
3. Percent of component by three titration methods based on weight taken......................... 50
4. Effect of XAD particle size and pre-column flow direction on overall efficiency................ 87
5. Recovery of MTQ added to blood plasma.......... 89
6. Measured values of V_m for XAD-packed column C_1 as a function of sodium nitrate concentration... 154
7. Characteristics of resin-packed pre-columns..... 157
8. Effect of flowrate of water eluent and sodium hydroxide concentration on the apparent ion exchange capacity.............................. 162
9. Calculation of ion exchange capacity for SXAD-packed column C_1. SXAD resin #2................ 164
10. Calculation of ion exchange capacity for SXAD-packed column C_1. SXAD resin #3................ 165

TABLE PAGE

11. Ion exchange equilibrium constants and standard chemical potentials of adsorption for Q^+ on SXAD resins.................................... 181
12. Sorption isotherm data for acetaminophen on XAD in aqueous 1.0×10^{-3} $\underline{M}$ NaCl (data for Figure 25).. 223
13. Sorption isotherm data for $NBTA^+$ on 54.5 μeq/g SXAD resin from aqueous 0.1 $\underline{M}$ NaCl (data for Figure 26).................................... 224
14. Sorption isotherm data for $NBTA^+$ on 54.5 μeq/g SXAD resin from aqueous 1.0 $\underline{M}$ NaCl (data for Figure 26).................................... 225
15. Sorption isotherm and distribution coefficient data for $NBTA^+$ on 54.5 μeq/g SXAD resin from aqueous NaCl solutions (data for Figures 27 and 28)....................................... 226
16. Distribution coefficient data for the sorption of $NBTA^+$ on 54.5 μeq/g SXAD resin from aqueous KCl solutions (data for Figure 29)...... 227
17. Distribution coefficient data for the sorption of $NBTA^+$ on 54.5 μeq/g SXAD resin from aqueous LiCl solutions (data for Figure 30)............. 228

TABLE PAGE

18. Distribution coefficient data for the sorption of $NBTA^+$ on 9.7 µeq/g SXAD resin from aqueous NaCl solutions (data for Figure 31)............. 229

19. Distribution coefficient data for the sorption of NBS^- on 54.5 µeq/g SXAD resin from aqueous NaCl solutions (data for Figure 32)............. 230

LIST OF FIGURES

FIGURE PAGE

1. Theoretical titration curves for an H_2A^+ acid... 18
2. Diagram of the titration apparatus............... 25
3. Titration of Naloxone ·HCl with NaOH............ 35
4. Effect of γ_{OH} on the fit of the titration equations to aqueous phase titration data for Naloxone·HCl.................................. 38
5. Comparison of pK^{th}_{a,H_2A} and $pK^{th}_{a,HA}$ values for Naloxone·HCl with literature data obtained at 20°C, 30°C and 37°C............................. 41
6. Distribution ratio of Naloxone between chloroform and aqueous solution as a function of pH.. 43
7. Plot of $D(a_H^2 + K_{a,H_2A} \cdot a_H + K_{a,H_2A} \cdot K_{a,HA})$ versus a_H used to evaluate K_{HA}........................ 46
8. Plot of $D(a_H^2 + K_{a,H_2A} \cdot a_H + K_{a,H_2A} \cdot K_{a,HA})$ versus a_H used to evaluate $K_{I,MA}$...................... 48
9. Titration of a mixture of Molindone·HCl and m-nitrophenol with NaOH......................... 51
10. Titration of a mixture of ammonium chloride and Naloxone·HCl with NaOH......................... 54
11. Diagram of liquid chromatograph used in the MTQ determination................................. 66

FIGURE PAGE

12. Elution of blood plasma from XAD and breakthrough study of MTQ as a function of volume of Solvent 1 pumped through pre-column... 77

13. Chromatograms of 500 μL of blood plasma and 500 μL of MTQ spiked blood plasma.................... 78

14. Effect of XAD particle size and Solvent 1 flowrate on recovery of MTQ from spiked plasma (10.7 μg/mL) by pre-column..................... 81

15. Effect of flowrate of Solvent 1 on recovery of MTQ from an aqueous 2.3 mM bovine albumin solution.. 83

16. Diagram of the interfacial region between a sulfonated Amberlite XAD-2 bead and an aqueous electrolyte solution........................... 99

17. Concentration of counterions and coions as a function of distance from the Outer Helmholtz Plane.. 106

18. Dependence of electrical potential at the charge surface, ψ_o, on ionic strength c......... 110

19. Hypothetical sorption isotherm.................. 124

20. Breakthrough profile for sample component assuming the sorption isotherm is linear........ 129

21. Liquid chromatograph used to measure distribution coefficients by the column equilibration method................................. 134

FIGURE PAGE

22. Pre-column for small weights of sorbent......... 137

23. Liquid chromatograph used to measure ion exchange capacities.............................. 149

24. Specific conductance versus time profile observed during measurement of ion exchange capacity of SXAD resin........................... 159

25. Isotherm for sorption of acetaminophen from aqueous 1.0 × 10^{-3} M sodium chloride onto XAD at 25.5°C.. 168

26. Isotherms for the sorption of $NBTA^+$ from aqueous NaCl solution onto 54.5 μeq/g SXAD resin at 25.0°C................................. 171

27. Linear region of isotherms for sorption of $NBTA^+$ from aqueous NaCl solutions onto 54.5 μeq/g SXAD resin at 25.0°C...................... 172

28. Distribution coefficient for the sorption of $NBTA^+$ on 54.5 μeq/g SXAD resin as a function of NaCl concentration........................... 175

29. Distribution coefficient for the sorption of $NBTA^+$ on 54.5 μeq/g SXAD resin as a function of KCl concentration.............................. 176

30. Distribution coefficient for the sorption of $NBTA^+$ on 54.5 μeq/g SXAD resin as a function of LiCl concentration............................. 177

FIGURE PAGE

31. Distribution coefficient for the sorption of $NBTA^+$ on 9.7 µeq/g SXAD resin as a function of NaCl concentration.............................. 178

32. Distribution coefficient for the sorption of NBS^- on 54.5 µeq/g SXAD resin as a function of NaCl concentration.............................. 187

LIST OF SYMBOLS

a_i	activity of species i
α	fraction of surface charge density neutralized by positive surface excess of counterions
c	ionic strength (moles/L)
C_m	concentration of sample compound in mobile phase solution (moles/L)
C_s	concentration of sample compound sorbed on stationary phase (moles/kg)
C_1	specific capacitance of compact part of electrical double layer (Farads/cm^2)
C_2	specific capacitance of diffuse part of double layer (Farads/cm^2)
$[i]$	concentration of species in in solution (moles/L)
d	distance (cm) between charge surface and Outer Helmholtz Plane
D	distribution ratio of a sample in a two-phase system
ε	dielectric constant for pure bulk solvent
ε°	permittivity of a vacuum (Farads/cm)
F	Faraday constant (96,487 coul/eq)
γ_i	aqueous phase ionic activity coefficient of i
$\gamma_{i,ADS}$	activity coefficient of adsorbed solute ion i

$\Gamma_{i,ADS}$	moles of solute i adsorbed on the charge surface per square centimeter
$\Gamma_{i,DL}$	surface excess of species in in the diffuse part of the double layer (moles/cm^2)
K	distribution coefficient
$K_{i/j}$	equilibrium constant or selectivity coefficient for the exchange of ions i and j
$K_{Q^+,IEX}$	distribution coefficient (L/Kg) for the ion exchange sorption of Q^+
κ	inverse of "thickness" of the diffuse part of the double layer (cm^{-1})
$\mu^{\circ}_{i,ADS}$	standard chemical potential for the transfer of solute i from the bulk solution to the charge surface (Joule/mole)
$\mu^{\circ}_{i,DL}$	standard chemical potential for the transfer of i into the diffuse layer
ψ_o	electrical potential at charge surface (volts)
ψ_{OHP}	electrical potential at Outer Helmholtz Plane (volts)
Q_{wgt}	ion exchange capacity (meq/g)
R	universal gas constant (8.314 Joule $K^{-1}mole^{-1}$)
σ_o	surface charge density (coulombs/cm^2)
T	absolute temperature (K)
Z	valence of sample ion (no sign)
$Z_{\pm}$	valence of sample ion, including sign

Z_R	valence (with sign) of fixed charge sites on resin

PART I

TWO-PHASE POTENTIOMETRIC TITRATIONS

CHAPTER 1

INTRODUCTION

A knowledge of the dissociation constants of acidic and basic substances in aqueous solution and their purity is important in a wide variety of problems in chemistry. For example, the therapeutic effect obtained following ingestion of a drug depends upon the dosage taken and the rate and extent to which the drug is absorbed by the human body. The former depends on the assay value of the drug while the latter is a function of the dissociation constants of the acidic and basic functional groups of the compound.

Potentiometric acid-base titration is one of the techniques commonly used to obtain this information. The theoretical and practical aspects of acid-base titrations in aqueous solution are well covered in the literature [1-4]. Accurate assay of a weak acid by this method requires that the compound is a significantly stronger acid than water (i.e. $K_a > 10^{-8}$) and that the concentration of the acid is large relative to the concentration of hydrogen ions from the autoprotolysis of water (i.e. $c >> \sqrt{K_w}$). Analogous requirements apply for bases. Further, due to the "leveling effect" of water [4] and to residual liquid junction potentials [3], accurate measurements of the dissociation constants for acids or bases can only be made when the condition $3 < pK_a < 11$ is met.

Selection of a solvent other than water will often overcome these limitations. Nonaqueous solvents exhibiting small autoprotolysis constants and which are either less acidic than water (titration of acids) or less basic than water (titration of bases) can be used for titrimetric determinations [5,6]. Aprotic solvents [5,6], mixed aqueous-organic solvents [7-9] and aqueous solutions containing a high concentration of an inert electrolyte [9] have also been investigated.

An alternate approach to circumventing these limitations to titrimetric acid-base determinations in water involves titrating the acidic or basic sample in a vigorously stirred mixture of water and an insoluble second phase. Systems have been described in which the second phase is an ion exchange resin [10-12], a nonionic resin [13,14], surfactant micelles [15-20] or an organic solvent [21-42]. The removal of one or more chemical species from the aqueous phase due to sorption by the second phase perturbs the acid dissociation equilibria. If the phase distribution removes the conjugate base formed by dissociation of an acid, then according to Le Chatelier's principle equilibrium will be reestablished by increasing the dissociation of the acid. The net effect in a titration is that the compound behaves as if it were a stronger acid. Alternately, if the acid itself is more extensively sorbed by the second phase than its conjugate base, then it will titrate as though it were a weaker acid.

Dyrssen [21] and subsequent workers [22 cites earlier work,23-25] have used two-phase potentiometric titration to evaluate distribution coefficients of acids and bases between aqueous solution and immiscible solvents. Alternately, the perturbing effect of an organic solvent on titration curves has been utilized in the measurement of overlapping pK_a values or of pK_a values outside the range $3 < pK_a < 11$ [23-29]. Several of these studies assume that only the uncharged conjugate acid or base species is extracted by the organic solvent. More general treatments have considered the effect of ion-pair formation and other competing equilibria [22,23,30]. Komar [31] has derived expressions for the potentiometric titration curve, the buffer capacity as a function of pH, and the relative precision in locating the first equivalence point in a two-phase titration of a mixture of HA type acids. Acids of this charge type (e.g. phenols and carboxylic acids) exhibit an apparent decrease in strength in such two-phase systems compared to their behaviour in water [32-35]. The technique has been applied to the assay of mixtures of weak acids of differing molecular weights [32-35].

In contrast to the apparent decrease in strength which is observed for HA type acids, monoprotic acids of the BH^+ charge type (e.g. organic ammonium ions) show an apparent increase in strength in aqueous solution/immiscible organic solvent systems [36]. Two-phase titrations of other charge type acids, such as the diprotic acids H_2A [28] and BH_2^{2+} [23] and salts of the type BH^+A^- [37], have also been examined.

Considerable change in the titration behaviour of an acid or base in a heterogeneous solvent system can result from enhancing the extraction of ion-pair species. For example, organic ammonium ions, BH^+, have been quantitatively titrated with sodium hydroxide in a two-phase system consisting of an aqueous phase and an organic phase composed of pentachlorophenol (PCP) dissolved in dichloromethane. The anionic conjugate base of PCP forms a highly extractable ion-pair with BH^+, thereby liberating protons which are titrated [38]. Similarly, the apparent weakening of a base, B, in two-phase systems can be counteracted by addition of an aprotic surfactant Y^- which extracts the conjugate acid of the compound as the ion-pair BHY [39]. Gur'ev and coworkers [40,41) have analyzed mixtures of strong acids such as perchloric and hydrochloric by titration with strong base using trioctylamine in toluene as the organic phase.

One of the advantages of a two-phase system is its ability to enhance the differentiating character of a titration. This advantage is most pronounced when the acids or bases in the mixture to be titrated are of opposite charge type [14]. An important category of diprotic acid which combines, in one component, both cationic and anionic species is the charge type H_2A^+, which includes the conjugate acids of aminophenols. These lose one proton to form HA and a second to form A^-. This category includes many of the major naturally occurring and synthetic narcotics and narcotic antagonists.

In the present study the theoretical titration equation is derived for H_2A^+ charge type acids and its validity is tested for Naloxone Hydrochloride, a narcotic antagonist. The consequences of ion pair formation between cationic and anionic conjugate species are considered in detail for this charge type. Titration behaviour is also evaluated for mixtures of BH^+ and HA acids with similar ionization constants. In both systems studied the chloroform:water titration medium produces a large "break" at the first equivalence point where none is discernable for titrations with water alone as solvent.

The proposed titration method is simple, rapid and does not require special equipment or modified electrodes.

CHAPTER 2

THEORY

In this section, a model is presented for the behaviour of diprotic acid H_2A^+ when titrated with strong base in a two-phase system consisting of an aqueous solution and an immiscible organic solvent. The treatment given here follows from a model previously proposed (but not tested) to describe the titration behaviour of H_2A^+ acids in the presence of a nonionic resin [13,14]. Details of the derivation may be found in Appendix I. The titration behaviour of monoprotic acids of charge types HA and BH^+ with strong base in aqueous solution/immiscible solvent mixtures is also described by analogy to the titration behaviour of H_2A^+.

2.1 Diprotic Acid H_2A^+

2.1.1 Titration Equations

The equilibria involved in the two-phase titration of a diprotic acid H_2A^+ with strong base MOH are given below:

$$H_2A^+ + H_2O \xrightleftharpoons{K_{a,H_2A}} HA + H_3O^+ \quad (1)$$

$$HA + H_2O \xrightleftharpoons{K_{a,HA}} A^- + H_3O^+ \quad (2)$$

$$H_2A^+ + X^- \xrightleftharpoons{K_{I,H_2AX}} (H_2AX)_o \quad (3)$$

$$HA \xrightleftharpoons{K_{HA}} (HA)_o \quad (4)$$

$$A^- + M^+ \xrightleftharpoons{K_{I,MA}} (MA)_o \quad (5)$$

$$H_2A^+ + A^- \xrightleftharpoons{K_{I,H_2A\cdot A}} (H_2A\cdot A)_o \quad (6)$$

$$2H_2O \xrightleftharpoons{K_w} H_3O^+ + OH^- \quad (7)$$

Here it is assumed that H_2A^+ is added as the salt H_2AX, where X^- is the conjugate base of a strong acid (e.g. Cl^-) which does not enter into the acid-base equilibria. In addition, M^+ is assumed to be an aprotic cation (e.g. Na^+). Species without a subscript are in the aqueous phase and those with a subscript "o" are in the organic phase.

In addition to the neutral species HA, it is assumed that the ion-pairs H_2AX, MA, and $H_2A{\cdot}A$ can partition into the organic phase. In the present treatment formation of ion-pairs in the aqueous phase and their dissociation in the organic phase [43], dimerization and the formation of higher aggregates of any species in the organic phase [38,43-45], adduct formation between ion-pairs and HA [38,45], and the formation of half-salts [46] have all been neglected, since they are unlikely to occur to a significant extent at the concentrations used in a titration, with a moderately polar solvent such as chloroform as the organic phase. Also neglected as being unlikely when non-surface-active compounds are involved is adsorption onto the liquid-liquid interface [47].

The equilibrium constant and distribution coefficient expressions corresponding to equilibria 1-7 are listed in Table 1. The dissociation constants have been written as mixed concentration-activity constants by incorporating activity coefficients for the H_2A^+, HA and A^- species into the value of the constants K_{a,H_2A} and $K_{a,HA}$. The titrations are performed in the presence of a large excess of the electrolyte MX which ensures that the activity coefficients for all species remain constant. The distribution coefficients K_{I,H_2AX} and $K_{I,MA}$ are conditional constants whose values depend on $[X^-]$ and

Table 1

Equilibrium Constant and Distribution Coefficient Expressions for H_2A^+ in a Two-Phase System

Constant Used	Thermodynamic Constant
$K_{a,H_2A} = \frac{[HA].a_H}{[H_2A^+]}$	$K^{th}_{a,H_2A} = K_{a,H_2A}\left(\frac{\gamma_{HA}}{\gamma_{H_2A}}\right)$
$K_{a,HA} = \frac{[A^-].a_H}{[HA]}$	$K^{th}_{a,HA} = K_{a,HA}\left(\frac{\gamma_A}{\gamma_{HA}}\right)$
$K_{I,H_2AX} = \frac{[H_2AX]_o}{[H_2A^+]}$	$K^{th}_{I,H_2AX} = \frac{K_{I,H_2AX}}{[X^-]\gamma_X}\left(\frac{\gamma_{(H_2AX)_o}}{\gamma_{H_2A}}\right)$
$K_{HA} = \frac{[HA]_o}{[HA]}$	$K^{th}_{HA} = K_{HA}\left(\frac{\gamma_{(HA)_o}}{\gamma_{HA}}\right)$
$K_{I,MA} = \frac{[MA]_o}{[A^-]}$	$K^{th}_{I,MA} = \frac{K_{I,MA}}{[M^+]\gamma_M}\left(\frac{\gamma_{(MA)_o}}{\gamma_A}\right)$
$K_{I,H_2A.A} = \frac{[H_2A.A]_o}{[H_2A^+][A^-]}$	$K^{th}_{I,H_2A.A} = K_{I,H_2A.A}\left(\frac{\gamma_{(H_2A.A)_o}}{\gamma_{H_2A}\cdot\gamma_A}\right)$

$$K_w = a_H \cdot a_{OH}$$

$[M^+]$. Thus addition of excess MX also serves to maintain constant the distribution coefficients K_{I,H_2AX} and $K_{I,MA}$.

The titration behaviour of H_2A^+ in such a two-phase system can be qualitatively understood by considering Le Chatelier's principle. Assume for simplicity that extraction of the neutral species HA is the only phase distribution of importance. Since HA is a product of the first dissociation step (equilibrium 1), its removal from the aqueous phase by extraction into the organic phase enhances the dissociation of H_2A^+. Consequently, in the two-phase system H_2A^+ behaves as a stronger acid than it does in water. At the same time extraction of HA into the organic phase suppresses the second dissociation step (equilibrium 2) resulting in an apparent weakening of the HA acid. Similar reasoning can be applied to predict the effect which the other phase distribution equilibria have on the titration curve.

The equations for the two-phase titration of H_2A^+ can be written in the simplest form, by defining "apparent dissociation constants" [48-50] which include the perturbing effect of phase distribution equilibria on the dissociation constants K_{a,H_2A} and $K_{a,HA}$. The apparent dissociation constants for H_2A^+ and HA can be written:

$$K^{app}_{a,H_2A} = \frac{a_H \cdot C^{app}_{HA}}{C^{app}_{H_2A}} \qquad (8)$$

$$K_{a,HA}^{app} = \frac{a_H \cdot C_A^{app}}{C_{HA}^{app}} \quad (9)$$

where the "apparent concentrations" [48-50] of the diprotonated, monoprotonated and unprotonated species are given by:

$$C_{H_2A}^{app} = [H_2A^+] + \frac{V_o}{V}[H_2AX]_o \quad (10)$$

$$C_{HA}^{app} = [HA] + \frac{V_o}{V}[HA]_o \quad (11)$$

$$C_A^{app} = [A^-] + \frac{V_o}{V}[MA]_o \quad (12)$$

The V and V_o terms are the respective volumes of the aqueous and organic phases. Substituting equations 10-12 into equations 8 and 9, and using the dissociation constant expression from Table 1:

$$K_{a,H_2A}^{app} = K_{a,H_2A}\left[\frac{1+(\frac{V_o}{V}).K_{HA}}{1+(\frac{V_o}{V}).K_{I,H_2AX}}\right] \quad (13)$$

$$K_{a,HA}^{app} = K_{a,HA}\left[\frac{1+(\frac{V_o}{V}).K_{I,MA}}{1+(\frac{V_o}{V}).K_{HA}}\right] \quad (14)$$

Combining the expressions in Table 1 with the mass balance and electroneutrality equations, and substituting equations 11, 13, and 14 gives the equations for the potentiometric titration of n_{H_2A} moles of a H_2A^+ acid with a strong base MOH (Appendix I, equation I-24 through I-27).

$$n_{OH} = n_{H_2A} + V\left[\frac{K^{app}_{a,HA}}{a_H} C^{app}_{HA} - \frac{a_H}{K^{app}_{a,H_2A}} C^{app}_{HA}\right] + \frac{K_w \cdot V}{a_H \gamma_{OH}} - \frac{a_H \cdot V}{\gamma_H} \qquad (15)$$

where C^{app}_{HA} is found from the positive root of the quadratic equation:

$$a'(C^{app}_{HA})^2 + b'C^{app}_{HA} - n_{H_2A} = 0 \qquad (16)$$

and where

$$a' = 2 \cdot V_o \cdot K_{I,H_2A} \cdot A\left(\frac{K_{a,HA}}{K_{a,H_2A}}\right)\left(1 + \left(\frac{V_o}{V}\right)K_{HA}\right)^{-2} \qquad (17)$$

$$b' = V\left(\frac{K^{app}_{a,HA}}{a_H} + \frac{a_H}{K^{app}_{a,H_2A}} + 1\right) \qquad (18)$$

In these equations γ_i are aqueous phase ionic activity coefficients, and n_{OH} is the moles of titrant added. The effect of dilution of the aqueous phase is neglected in the above treatment, since the total volume of titrant delivered from the microburet is only 1-2% of the initial volume of the aqueous phase.

The significance of the "apparent dissociation constants" defined above can be appreciated by comparing equations 15-18 to the corresponding equations describing the titration of H_2A^+ in a single phase aqueous system. If V_o is set to zero, K_{a,H_2A}^{app}, $K_{a,HA}^{app}$ and C_{HA}^{app} in equations 15-18 can be replaced by K_{a,H_2A}, $K_{a,HA}$ and [HA] (equations 11, 13 and 14), and the quadratic term in equation 16 can be dropped. Consequently, the equations describing the titration of H_2A^+ in a single phase aqueous system with strong base can be written:

$$n_{OH} = n_{H_2A} + V\left[\frac{K_{a,HA}}{a_H}[HA] - \frac{a_H}{K_{a,H_2A}}[HA]\right] + \frac{K_w \cdot V}{a_H \cdot \gamma_{OH}} - \frac{a_H \cdot V}{\gamma_H} \qquad (19)$$

where [HA] is calculated from:

$$b''[HA] - n_{H_2A} = 0 \tag{20}$$

with

$$b'' = V\left(\frac{K_{a,HA}}{a_H} + \frac{a_H}{K_{a,H_2A}} + 1\right) \tag{21}$$

Provided extraction of the ion-pair $H_2A{\cdot}A$ is negligible (see below), in which case a' in equation 17 is zero; the two-phase titration equations have exactly the same form as those for titration of H_2A^+ in a single phase aqueous solution (compare equations 15, 16 and 18 with equations 19-21). The first three terms on the right side of equations 15 and 19 give the number of moles of strong base titrant consumed by the sample acid H_2A^+, as a function of a_H, for the respective titrations in two-phase and single-phase media. These terms give rise to the "proton binding curve" [51] which is a plot of pH versus the average number of protons bound to the Naloxonate ion A^-. The fourth and fifth terms on the right side in equations 15 and 19 arise because water is an amphiprotic solvent which exerts a "leveling effect" [52] on the strength of acidic compounds (term 5) and their conjugate bases (term 4).

2.1.2 Predicted Titration Behaviour

The behaviour predicted by equations 13-18 is shown in Figure 1 for a hypothetical acid with $K_{a,H_2A} = 1.0 \times 10^{-6}$, $K_{a,HA} = 5.0 \times 10^{-8}$, $K_{I,H_2AX} = 1.0$, $K_{I,MA} = 1.0$, $V = 0.060$ L, $n_T = 5.0 \times 10^{-4}$ mole and $\gamma_H = \gamma_{OH} = 1$. Curve 1, for titration in the absence of an organic phase shows no "pH-break" at the first equivalence point because K_{a,H_2A} and $K_{a,HA}$ differ by only a factor of 20. Since HA is both a product of the first titration step and a reactant in the second step, its removal from the aqueous phase by extraction into the organic solvent shifts the portion of the titration curve prior to the first equivalence point to lower pH, making H_2A^+ appear to be a stronger acid. Simultaneously, the second half of the titration curve is shifted to higher pH, making HA appear to be a weaker acid. The larger the value of K_{HA}, the more pronounced are these shifts (compare curves 2 and 3) and the sharper the break at the first equivalence point.

The influence of the ion-pair extraction constants K_{I,H_2AX} and $K_{I,MA}$ on titration curve shape can similarly be explained [13,14]. Increasing values of K_{I,H_2AX} cause more extensive removal of H_2A^+ from the aqueous phase, shifting the first half of the titration curve to higher pH values, while an increase in $K_{I,MA}$ shifts the second half of the curve to lower pH. Consequently, increases in

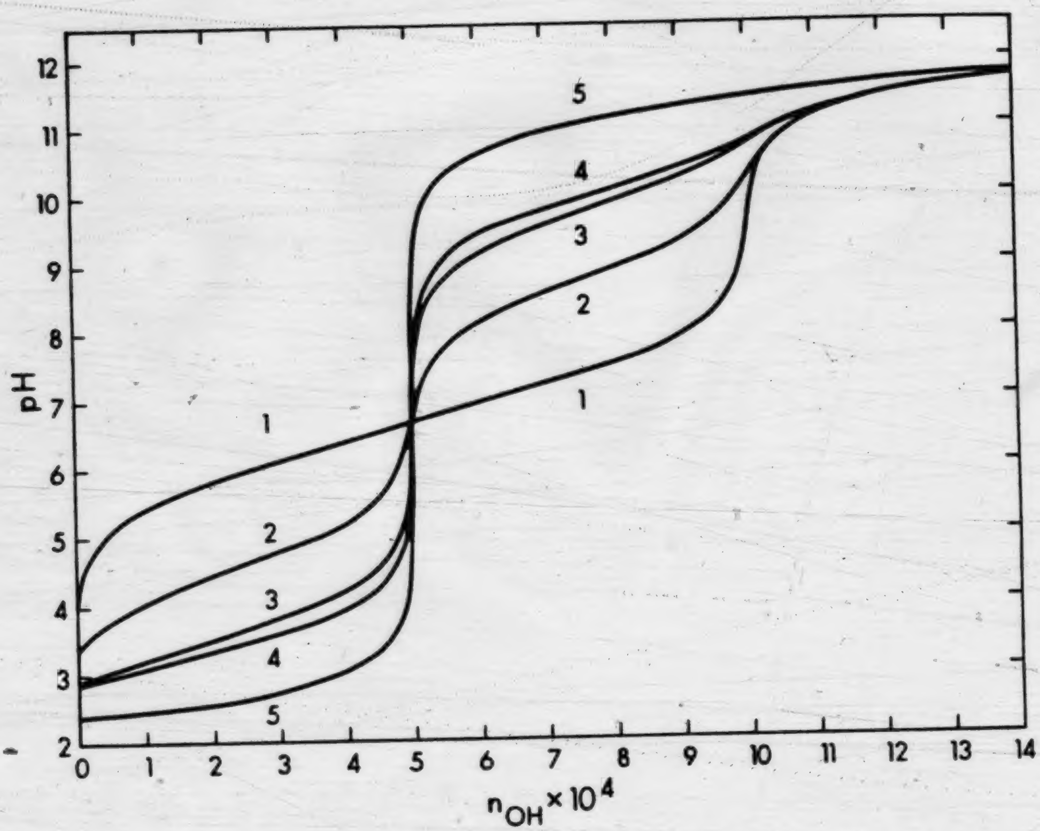

Figure 1. Theoretical titration curves for an H_2A^+ acid. Effect of K_{HA} and $K_{I,H_2A \cdot A}$. Curves calculated from equations 13-18. $K_{a,H_2A} = 1.0 \times 10^{-6}$; $K_{a,HA} = 5.0 \times 10^{-8}$; $K_{I,H_2AX} = 1.0$; $K_{I,MA} = 1.0$; $V = 0.060$ L; $n_{H_2A} = 5.0 \times 10^{-4}$ mole; $\gamma_H = \gamma_{OH} = 1$. Values of ($V_o$; K_{HA}; $K_{I,H_2A \cdot A}$) for Curve 1 (0.0 L, -, -); Curve 2 (0.020 L, 10^2, 0); Curve 3 (0.020 L, 10^3, 0); Curve 4 (0.020 L, 10^3, 10^9); Curve 5 (0.020 L, 10^3, 10^{12}).

K_{I,H_2AX} and $K_{I,MA}$ have the opposite effect of K_{HA} and diminish the magnitude of the first equivalence point break. Therefore, K_{I,H_2AX} and $K_{I,MA}$ should be minimized when it is desired to accurately locate the first endpoint. This can be done, for example, by avoiding unnecessarily high concentrations of inert salt MX. In most cases, when M^+ and X^- are small inorganic ions, K_{HA} is expected to be much greater than both K_{I,H_2AX} and $K_{I,MA}$.

The effect of the ion-pair distribution coefficient, $K_{I,H_2A \cdot A}$, on the titration curve for H_2A^+ is shown in Figure 1, curves 4 and 5. The values of all constants are given in the caption. Three important conclusions can be drawn from these curves. First, unless $K_{I,H_2A \cdot A}$ is very large (i.e. $K_{I,H_2A \cdot A} > 10^7$) it has a negligible effect on the shape of the titration curve. Second, increasing $K_{I,H_2A \cdot A}$ sharpens the first endpoint break and diminishes the second break as does an increase in K_{HA}. Finally, the existence of this "self ion-pair" equilibrium does not cause the location of the first "pH-break" to deviate from the true equivalence point, as happens when half-salt formation (i.e. $H_2A \cdot HA$) occurs [46]. No effect on the titration curve is observed until $K_{I,H_2A \cdot A}$ becomes very large because large concentrations of H_2A^+ and A^- are not simultaneously present in solution. If K_{a,H_2A} and $K_{a,HA}$

had values closer to one another than the values in Figure 1, then the influence of "self ion-pair" formation would be observed for smaller values of $K_{I,H_2A\cdot A}$.

2.2 Monoprotic Acids HA and BH^+

Previous workers have described the titration behaviour of weak acids of charge type HA and BH^+ in the presence of a second phase. Titration equations analogous to equations 13 to 18 have been developed and are applicable to this work [13,14]. Hence, for the purposes of this study, a qualitative description of the two-phase titration behaviour of HA and BH^+ is sufficient.

The equilibria which are involved when a weak monoprotic acid HA (e.g. a phenol) is titrated with strong base MOH in a two-phase system are exactly the same as those describing the titration of the second proton of the diprotic acid H_2A^+:

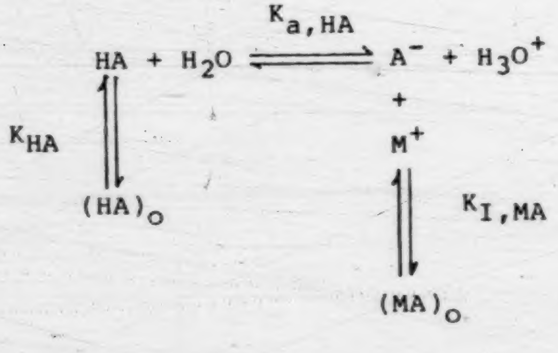

(22)

$$2H_2O \overset{K_w}{\rightleftharpoons} H_3O^+ + OH^- \qquad (23)$$

The pH shift in the proton-binding curve of A^-, due to the presence of an organic phase, is given by the difference between the values of $pK_{a,HA}$ and $pK^{app}_{a,HA}$. Taking logarithms on both sides of equation 14 and rearranging gives:

$$pK_{a,HA} - pK^{app}_{a,HA} = \log\left[\frac{1 + (\frac{V_o}{V})\ K_{I,MA}}{1 + (\frac{V_o}{V})\ K_{HA}}\right] \qquad (24)$$

In the case of a monoprotic weak acid BH^+ (e.g. an organic ammonium ion), the equilibria are analogous to those describing the titration of the first proton of the diprotic acid H_2A^+:

$$\begin{tikzcd}
BH^+ + H_2O \arrow[rr, rightleftharpoons, "K_{a,BH}"] & & B + H_3O^+ \arrow[d, rightleftharpoons, "K_B"] \\
+ & & (B)_o \\
X^- \arrow[d, rightleftharpoons, "K_{I,BHX}"] & & \\
(BHX)_o & &
\end{tikzcd} \qquad (25)$$

$$2H_2O \xrightleftharpoons{K_w} H_3O^+ + OH^- \qquad (26)$$

An expression analogous to equation 13 may be used to derive the pH shift in the proton-binding curve, due to the presence of an organic phase.

$$pK_{a,BH} - pK_{a,BH}^{app} = \log\left[\frac{1 + (\frac{V_o}{V})\, K_B}{1 + (\frac{V_o}{V}) K_{BHX}}\right] \qquad (27)$$

Thus, titration of either HA or BH^+ monoprotic acids separately in a two-phase system gives behaviour which could be predicted by analogy with the titration behaviour of diprotic acids H_2A^+. Assuming that the neutral species is much more highly extracted into the organic phase, a monoprotic BH^+ acid should show enhanced ionization in a two-phase system (eqn 27) and a monoprotic HA acid suppressed ionization (eqn 26).

Titration of mixtures of monoprotic acids BH^+ and HA in a two-phase system introduces an additional equilibrium:

$$BH^+ + A^- \xrightleftharpoons{K_{I,BHA}} (BHA)_o \qquad (28)$$

This is analogous to the extraction of the ion-pair $H_2A{\cdot}A$ discussed in the titration of H_2A^+. An important difference between the two cases should be mentioned. Extraction of the ion-pair $H_2A{\cdot}A$ can only become significant for very large values of $K_{I,H_2A{\cdot}A}$ because the ratio of the dissociation constants, $K^{th}_{a,H_2A}/K^{th}_{a,HA}$, must be 4 or greater [53] resulting in only a small fraction of the compound being simultaneously present as the H_2A^+ and A^- species. However, the values of the dissociation constants for BH^+ and HA are independent of each other. Thus a weak acid HA (e.g. benzoic acid) may be fully dissociated at a pH where a BH^+ acid (e.g. an organic ammonium ion) is fully protonated. Consequently, extraction of the ion-pair $BH{\cdot}A$ may be more significant than extraction of the corresponding $H_2A{\cdot}A$.

CHAPTER 3

EXPERIMENTAL

3.1 Apparatus

All potentiometric titrations were performed using the equipment shown in Figure 2. The 100 mL borosilicate glass titration vessel was fitted with a Teflon lid which had holes drilled to accommodate a glass electrode, a ceramic junction saturated calomel electrode (Cat. no. 13-639-3 and 13-639-51, Fisher Scientific Co.) and a glass buret tip. Two additional holes in the lid allowed a stream of nitrogen to be passed through the container for deaerating the solution. A 9 in. × 9 in. magnetic stirrer (no. 4815, Cole Parmer Instruments Co., Chicago, Illinois) was used with a 1-in. Teflon coated magnetic stirring bar to vigorously aggitate the two-phase mixture during a titration. The titration vessel was placed in a glass jacketed beaker filled with water and thermostatted at 25 ± 0.5°C using a circulating constant temperature bath. Measurements of pH were made using an Accumet Model 320 pH meter (Fisher Scientific Co.).

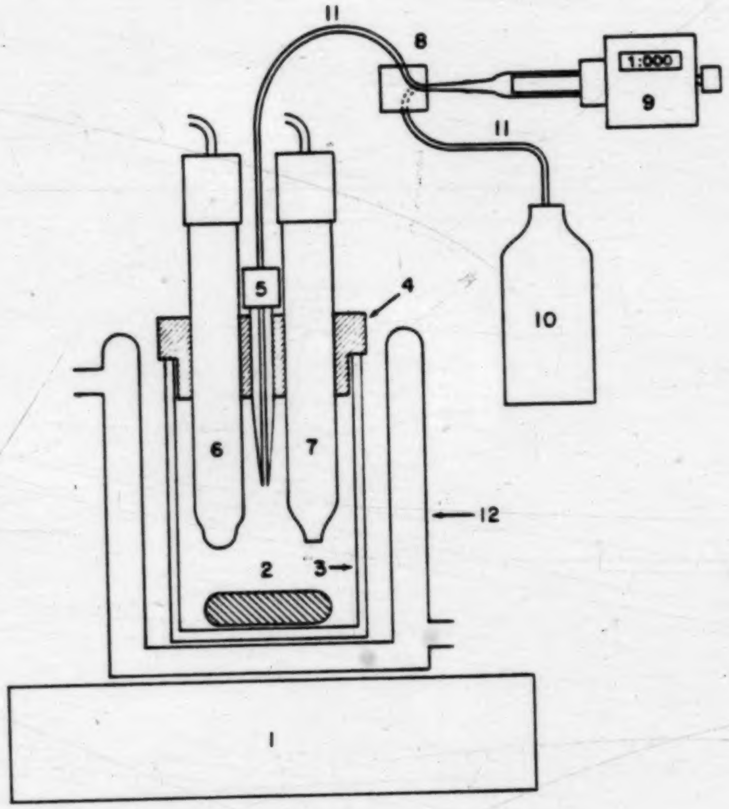

Figure 2. Diagram of the titration apparatus.

1. Magnetic stirrer, 2. Stirring bar, 3. Titration vessel, 4. Lid, 5. Buret tip, 6. Glass electrode, 7. Reference electrode, 8. Three way valve, 9. Micrometer buret, 10. Titrant reservoir, 11. 1/16" O.D. Teflon tubing, 12. Water-jacketed beaker.

Titrant was delivered from a 2 mL micrometer buret (Roger Gilmont Instruments, Great Neck, N.Y.). The buret is connected to a three-way valve (Model CAV 3031, Laboratory Data Control, Riviera Beach, Florida) via Teflon tubing. Another length of Teflon tubing directs the titrant from the three-way valve to the titration vessel. The third valve port is connected via Teflon tubing to a polyethylene bottle containing the titrant. This arrangement allows the rapid refilling of the buret by switching the valve and retracting the piston of the buret.

Determination of the distribution coefficients K_{HA} and $K_{I,MA}$ required pH measurements to be made on small volumes (<5 mL) of solution. For these measurements a miniature combination glass and saturated calomel electrode (no. 13-639-90, Fisher Scientific Co.) was used.

Spectrophotometric measurements were made on a Cary 118 spectrophotometer (Varian Instruments, Palo Alto, California).

3.2 Chemicals

Naloxone Hydrochloride and Molindone Hydrochloride were supplied by Endo Laboratories, Garden City, New York. They were assayed without drying, by the mercuric acetate method of nonaqueous titration, using perchloric acid in glacial acetic acid as titrant and crystal violet indicator [54] and also by potentiometric titration with sodium hydroxide in n-Propanol/water (3:1 v/v) mixed solvent [8].

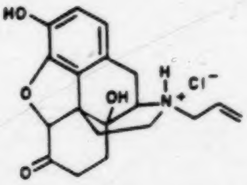

NALOXONE · HCL

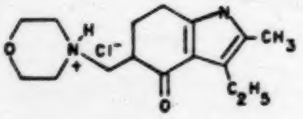

MOLINDONE · HCL

m-Nitrophenol (Eastman Kodak Co., Rochester, N.Y.) was recrystallized once from water and dried several hours over magnesium perchlorate. The pale yellow crystalline solid had a melting point of 96.7-97.0°C.

Other Chemicals including sodium chloride, sodium hydroxide, sodium carbonate, sodium bicarbonate, ammonium chloride, ammonium hydroxide, hydrochloric acid, perchloric acid, acetic acid and acetic anhydride were all analytical reagent grade. Potassium acid phthalate was primary standard grade.

3.3 Reagents and Solvents

Chloroform used in the measurements of distribution coefficients was analyzed reagent grade (J.T. Baker Chemical Co.) and was distilled before use to remove uv-absorbing impurities (boiling point (760 torr) 60.1-61.2°C). Chloroform used in the two-phase titrations was not distilled but it was washed with double distilled water to remove ethanol preservative (see below).

Double Distilled Water was prepared by distilling the laboratory distilled water from alkaline permanganate in an all-glass still. The first 20% of the distillate was discarded and the middle fraction was used. This water was used to prepare all aqueous solutions.

0.4 Molar Sodium Hydroxide Titrant was prepared by diluting 1:1 (w/w) aqueous sodium hydroxide solution with an appropriate volume of freshly boiled and cooled double distilled water. The sodium hydroxide solution was stored in a polyethylene bottle and standardized by potentiometric titration of 0.1 g portions of primary standard potassium acid phthalate using the 2 mL micrometer buret. This titrant was used for the two-phase titrations and for titrations of samples dissolved in the 1-propanol/water mixed solvent.

0.1 Molar Perchloric Acid in glacial acetic acid was prepared by combining, in a one liter volumetric flask, several hundred mL of glacial acetic acid, 8.5 mL of 70% perchloric acid and 20 mL acetic anhydride. The solution was allowed to cool for one half hour, was diluted to volume with glacial acetic acid and was allowed to stand overnight before use. This solution was standardized against primary standard potassium acid phthalate using the 2 mL micrometer buret and crystal violet indicator.

3.4 Aqueous Buffers

In measurements of the distribution ratio of Naloxone•HCl between chloroform and aqueous solutions, the aqueous phase was prepared by adding a 10 mL aliquot of an aqueous solution of Naloxone•HCl to a 50 mL aliquot of either a buffer solution (NH_4Cl/NH_3 or $Na_2CO_3/NaHCO_3$), a strong acid (HCl) or a strong base (NaOH). With the exception of the sodium carbonate-bicarbonate buffer (see below), all buffer, strong acid and strong base solutions had an ionic strength of 0.130. Consequently, in most cases the aqueous phases used in the batch equilibrations had an ionic strength within a few percent of 0.108. Rather than calculating or measuring the initial pH of the buffer, strong acid or strong base solution, pH measurements were obtained, subsequent to the distribution ratio measurements (Section 3.6), using a small portion (<5 mL) of the equilibrated aqueous phase. In all solutions at pH > 10, for which the extraction of the ion-pair MA might be expected to be significant, the concentration of Na^+ ion was adjusted to 0.108 M by the addition of NaCl.

0.130 Molar Hydrochloric Acid used in the measurement of the ion-pair distribution constant K_{I,H_2AX}, was prepared from the concentrated reagent and standardized by titration with standard 0.1 M sodium hydroxide using phenolphthalein indicator.

Ammonium Chloride/Ammonia Buffers were prepared by combining in a one liter volumetric flask 6.95 g NH_4Cl and either 1.9 mL, 3.8 mL or 9.4 mL of 6 M NH_3 and diluting to volume with distilled water.

Carbonate Buffer was prepared by combining 0.240 g anhydrous Na_2CO_3, 0.060 g $NaHCO_3$ and 1.592 g NaCl in a 250 mL volumetric flask and diluting to volume with distilled water. The resultant solution contained 0.130 M Na^+ ion and had an ionic strength of 0.139.

Sodium Hydroxide Solutions were prepared by combining either 1.00 mL, 1.10 mL, 1.31 mL, 3.00 mL, 5.00 mL or 50.0 mL of 0.130 M sodium hydroxide with 0.130 M sodium chloride to give solutions with a final volume of 50.0 mL and an ionic strength of 0.130.

Commercial Buffers (Fisher Scientific Co.) of pH 7.00 ± 0.02 and pH 10.00 ± 0.02 were used to standardize the pH meter. An additional buffer of pH 4.00 ± 0.02 was used as a check on the two-point calibration.

3.5 Titration Procedure

Chloroform was shaken in a separatory funnel immediately before use with an equal volume of distilled water to remove the ethanol preservative and traces of HCl. It was then filtered through dry Whatman No. 2 filter paper to remove entrained water, purged with nitrogen to remove dissolved carbon dioxide and warmed to 25°C.

Aliquots of aqueous stock solutions containing 0.2-0.3 millimoles of the sample acids were pipetted into the titration vessel. Sodium chloride solution was added to adjust the salt concentration to 0.108 M and the aqueous volume to 60.0 mL. The Teflon lid with glass and reference electrodes in place was fitted over the titration vessel and the solution de-oxygenated with a stream of nitrogen for 10 min while stirring vigorously. A 20.00 mL volume of chloroform was added and the glass buret tip inserted through a hole in the Teflon lid. Stable pH measurements on the vigorously stirred two-phase mixture were usually obtained within 10-15 seconds after addition of an increment of titrant. Equivalence points were evaluated from first derivative plots.

3.6 Distribution Coefficients

The distribution coefficient of Naloxone hydrochloride K_{I,H_2ACl}, was determined by magnetically stirring 30.00 mL of 0.108 M HCl containing 2.7×10^{-5} mole of Naloxone hydrochloride with 150.0 mL of chloroform in a 250 mL ground glass stoppered conical flask for 10 minutes at 25 ± 0.5°C. (Longer equilibration times produced no change in the measured value of K_{I,H_2ACl}.) The Naloxone content of the aqueous phase was determined by measuring the absorbance at 281 nm. The Naloxone content of the organic phase was determined by extracting a 140.0 mL portion with 7.00 mL of 0.13 M HCl and measuring the absorbance of the aqueous layer after centrifugation.

The distribution coefficients of the neutral Naloxone species, K_{HA}, and of the anionic species, $K_{I,MA}$, were determined by a graphical procedure described later. For this purpose the distribution ratio of Naloxone (see equation 29 below) was measured between chloroform and solutions having equilibrium pH values of: 8.10, 8.44 and 8.80 (NH_4Cl/NH_3 buffers); 10.11 ($Na_2CO_3/NaHCO_3$ buffer); and 10.75, 10.92, 11.10, 11.64, 11.95 and 13.08 (NaOH solutions). Appropriate volumes of chloroform and the aqueous solution, 1.0×10^{-3} M in Naloxone•HCl and containing either NH_4Cl/NH_3 buffer, $Na_2CO_3/NaHCO_3$ buffer or NaOH to adjust the pH, were combined and vigorously stirred for 10 min at 25 ± 0.5°C in a glass stoppered flask. The separated chloroform phase was filtered through Whatman No. 2 paper, the filtered chloroform extracted with 0.1 M HCl, and the Naloxone concentration of the 0.1 M HCl extract determined by uv spectrophotometry.

An aliquot of the aqueous phase was adjusted to pH 8.6 with HCl and NH_3/NH_4Cl buffer and extracted with 4 portions of chloroform. The combined chloroform extracts were diluted to volume, an aliquot of this solution back-extracted with 0.1 M HCl, and the Naloxone concentration of the centrifuged aqueous extract measured spectrophotometrically.

Quantitative recovery (mass balance) of Naloxone was verified for both phases by comparison with a diluted aliquot of the original Naloxone•HCl stock solution.

CHAPTER 4

RESULTS AND DISCUSSION

The validity of the titration equations for an H_2A^+ acid was tested by titrating Naloxone Hydrochloride with aqueous sodium hydroxide in both the presence and absence of chloroform. Naloxone Hydrochloride is a narcotic antagonist drug which contains both tertiary ammonium and phenolic functional groups. Since the thermodynamic pK_a values, $pK^{th}_{a,H_2A} = 8.03$ and $pK^{th}_{a,HA} = 9.32$ (see below), differ by only 1.3 units, titration of Naloxone Hydrochloride in aqueous solution yields a titration curve with a single "pH break", at the second equivalence point (Figure 3, curve A). Repeating the titration in the presence of chloroform (Figure 3, curve B), results in a titration curve with a sharp pH break at the first equivalence point. Comparison of curve B to curve A indicates that in the presence of a second phase, the proton binding region prior to the first equivalence point is shifted towards lower pH and the proton binding region between the first and second equivalence points is shifted to higher pH. Thus the experimental data are in qualitative agreement with the proposed model.

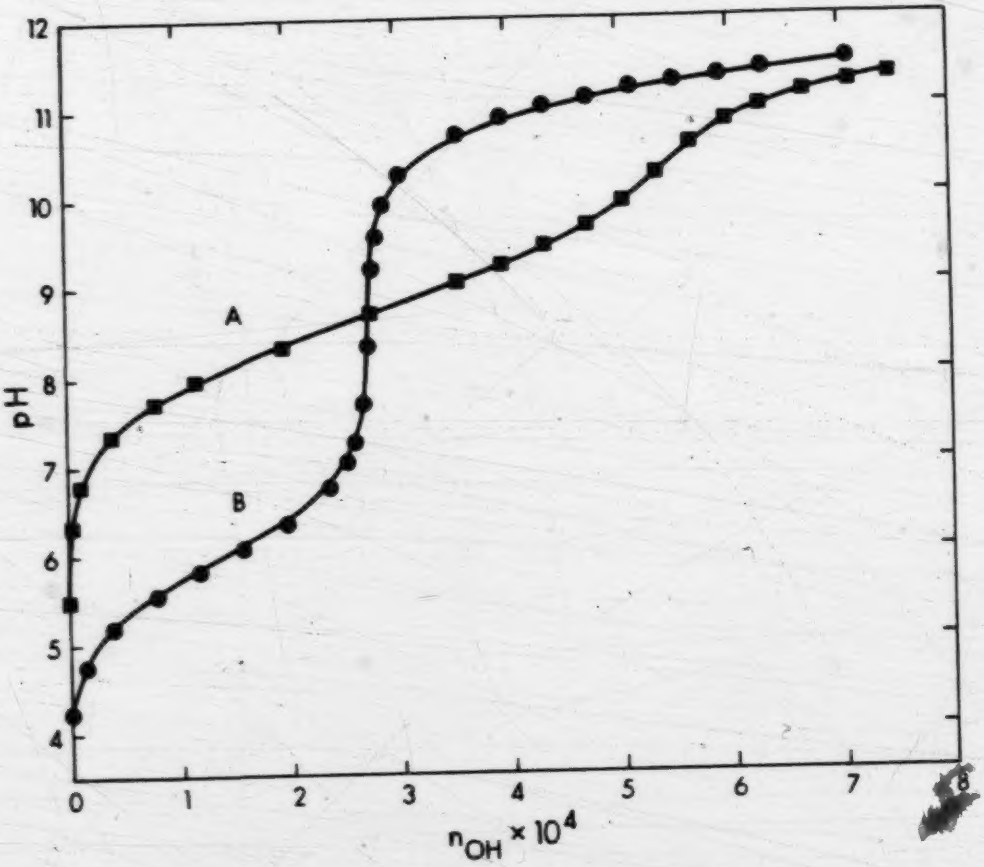

Figure 3. Titration of Naloxone•HCl with NaOH. Points are experimental and lines are calculated from equations 13-18 using the following values for constants: $K_{a,H_2A} = 7.53 \times 10^{-9}$; $K_{a,HA} = 5.87 \times 10^{-10}$; $K_{HA} = 433$; $K_{I,H_2A\cdot A} = 0$; $K_{I,H_2AX} = 0$; $K_{I,MA} = 0.14$; V = 0.060 L of 0.108 M NaCl; $n_{H_2A} = 2.72 \times 10^{-4}$ moles; $\gamma_H = 0.83$; $\gamma_{OH} = 0.63$; Curve A: $V_o = 0.0$ L; Curve B: $V_o = 0.020$ L of chloroform.

In order to quantitatively evaluate the model it is necessary to first obtain accurate values of the dissociation constants and the distribution coefficients. These values are substituted into equations 13-18 to obtain a theoretically predicted titration curve which is then compared with the experimentally obtained titration data. This is done in sections 4.1 to 4.3 below. In Section 4.4 some examples of the use of two-phase titrations for the assay of mixtures of acids are presented.

4.1 Dissociation Constants

The dissociation constants K_{a,H_2A} and $K_{a,HA}$ were determined by using the nonlinear least-squares program "KINET" [55] to fit equations 19-21 to the titration data for Naloxone•HCl in the absence of chloroform (Figure 3, curve A). Twenty-two data values in the buffer regions (i.e. $7.0 \leq pH \leq 10.6$) were used in the evaluation of K_{a,H_2A} and $K_{a,HA}$. Many of these data points are not shown in curve A, to allow a clear comparison of experimental data and the drawn curve.

Values for the activity coefficients of H^+ and OH^- required in equation 19 were obtained as follows. The value of γ_H was calculated to be 0.83 using the extended Debye-Huckel equation [56] for an ionic strength of 0.108

and using an ion-size parameter of 8×10^{-8} cm [57]. The value used for γ_H is not critical because it is only involved in the final term of equation 19 which is negligible at pH values greater than 4.

Since $pK_{a,H_2A} > 9$ the value used for γ_{OH} can be expected to have a significant effect on the fitted values of K_{a,H_2A} and $K_{a,HA}$. Initially, the activity coefficient of OH^- ($\gamma_{OH} = 0.76$) was calculated from the extended Debye-Huckel equation using an ion-size parameter of 3.5×10^{-8} [57]. However, if $\gamma_{OH} = 0.76$ is used in fitting equations 19-21 to the experimental data for the titration of Naloxone•HCl in the absence of chloroform (Figure 3, curve A), the standard deviations of the fitted dissociation constants is relatively large; $K_{a,H_2A} = (7.42 \pm 0.24) \times 10^{-9}$ and $K_{a,HA} = (6.14 \pm 0.11) \times 10^{-10}$ and the fitted titration curve lies slightly above the data points at $pH > 10.6$. Curve A of Figure 4 is a portion of the aqueous titration curve of Naloxone•HCl calculated from the fitted dissociation constants, with $\gamma_{OH} = 0.76$. Though the discrepancy between the experimental data points and the calculated titration curve is less than 0.1 pH unit, the theoretical curve falls above the experimental data points, suggesting a (small) systematic error.

In view of this and of the uncertainties involved in

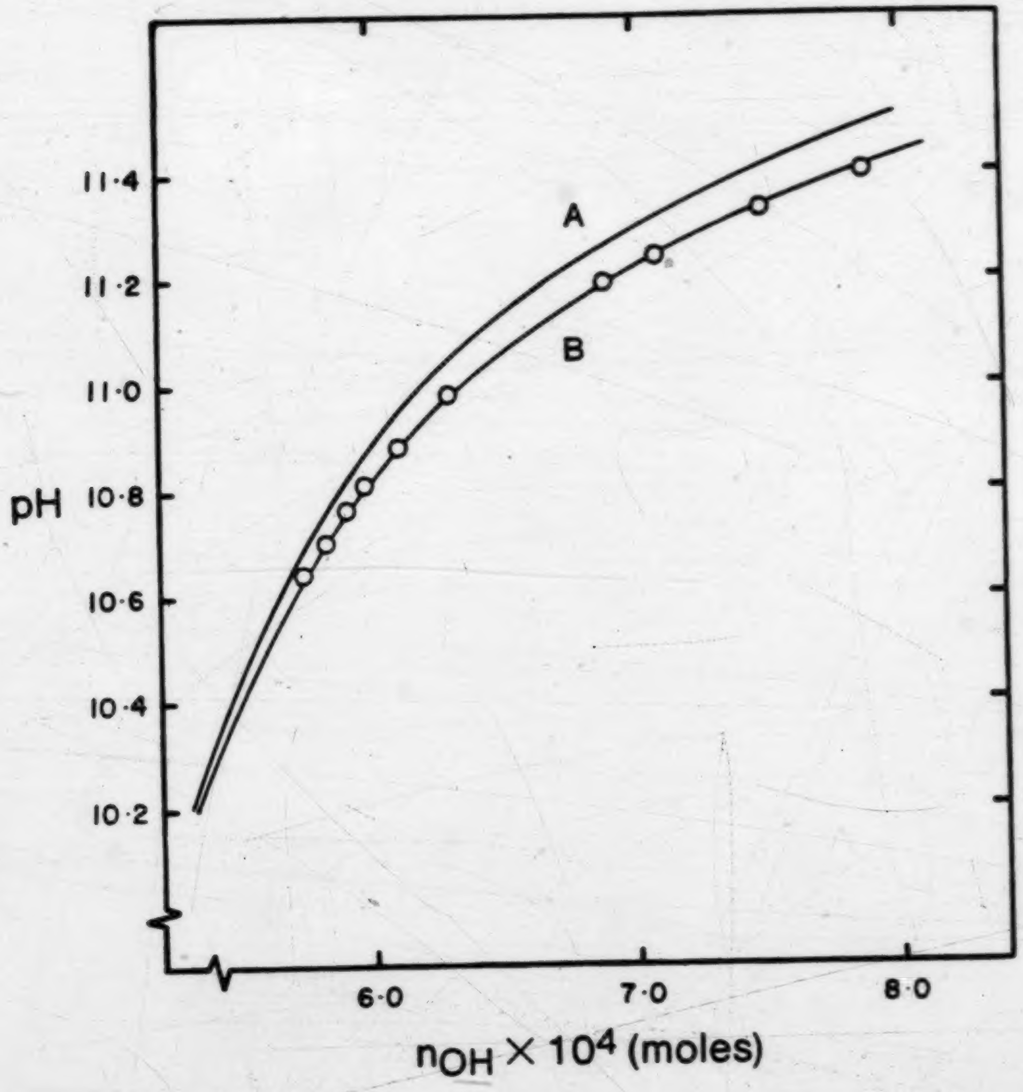

Figure 4. Effect of γ_{OH} on the fit of the titration equations (19-21) to aqueous phase titration data for Naloxone•HCl. Curve A: $\gamma_{OH} = 0.76$; fitted constants $K_{a,H_2A} = (7.42 \pm 0.24) \times 10^{-9}$ and $K_{a,HA} = (6.14 \pm 0.11) \times 10^{-10}$; Curve B: $\gamma_{OH} = 0.63$, fitted constants $K_{a,H_2A} = (7.53 \pm 0.05) \times 10^{-9}$ and $K_{a,HA} = (5.87 \pm 0.02) \times 10^{-10}$.

calculating activity coefficients at ionic strengths as high as 0.1 [58], it was decided to determine γ_{OH} from experimental data for titration of H_2A^+ in aqueous solution. Equations 19-21, with γ_{OH} as an adjustable parameter and all other parameters held constant, were fitted by KINET to the high pH portion of the aqueous titration curve of Naloxone•HCl beyond the second equivalence point (Figure 4, curve B). The value of γ_{OH} obtained in this manner ($\gamma_{OH} = 0.63$) was used as a constant in all subsequent work.

The solid line in curve A of Figure 3 is the nonlinear least-squares fit of equations 19 to 21 to the aqueous titration data in the buffer regions ($7.0 < pH < 10.6$) using $\gamma_H = 0.83$ and $\gamma_{OH} = 0.63$. It yields values for the dissociation constants: $K_{a,H_2A} = (7.53 \pm 0.05) \times 10^{-9}$ and $K_{a,HA} = (5.87 \pm 0.02) \times 10^{-10}$. The error limits, which are estimates of the linear standard deviations calculated by the nonlinear least-squares program, are relatively small indicating that the scatter of the data points about the fitted curve is small. However, the pH values of the buffer solutions used to standardize the pH meter are not known to better than ±0.02 pH units, thus a more realistic estimate of the uncertainties in pK_{a,H_2A} and $pK_{a,HA}$ is ±0.04 pH units.

The mixed (concentration-activity) dissociation constants K_{a,H_2A} and $K_{a,HA}$ found for Naloxone•HCl must be converted to thermodynamic activity constants K^{th}_{a,H_2A} and $K^{th}_{a,HA}$ before comparison with literature values can be made. The activity coefficient of the neutral species HA at the ionic strength of 0.11 M was assumed to equal unity [59]. The activity coefficients for the H_2A^+ and A^- species were both assumed to equal 0.813, as calculated from the extended Debye-Huckel equation with the ion-size parameter assumed to be 8×10^{-8} cm, the same as that for diphenylacetate [57]. Applying the activity coefficient corrections given in Table 1, the thermodynamic constants at 25°C are $pK^{th}_{a,H_2A} = 8.03 \pm 0.04$ and $pK^{th}_{a,HA} = 9.32 \pm 0.04$. Literature values at 25°C are $pK^{th}_{a,H_2A} = 7.92 \pm 0.06$ and $pK^{th}_{a,HA} = 9.38 \pm 0.06$. They were obtained from a linear least-squares fit (Figure 5) to literature values measured at 20°C, 37°C [24] and 30°C [60]. The error estimates on the literature values are 95% confidence limits [61] evaluated at a single point (25°C) after pooling the estimates of the variances of the points about the two fitted lines [62]. Comparisons of values are shown graphically in Figure 5. The values obtained for K^{th}_{a,H_2A} and $K^{th}_{a,HA}$ in this study compare reasonably well with the literature values, especially in view of the uncertainties in activity coefficients calculated at an ionic strength of 0.1.

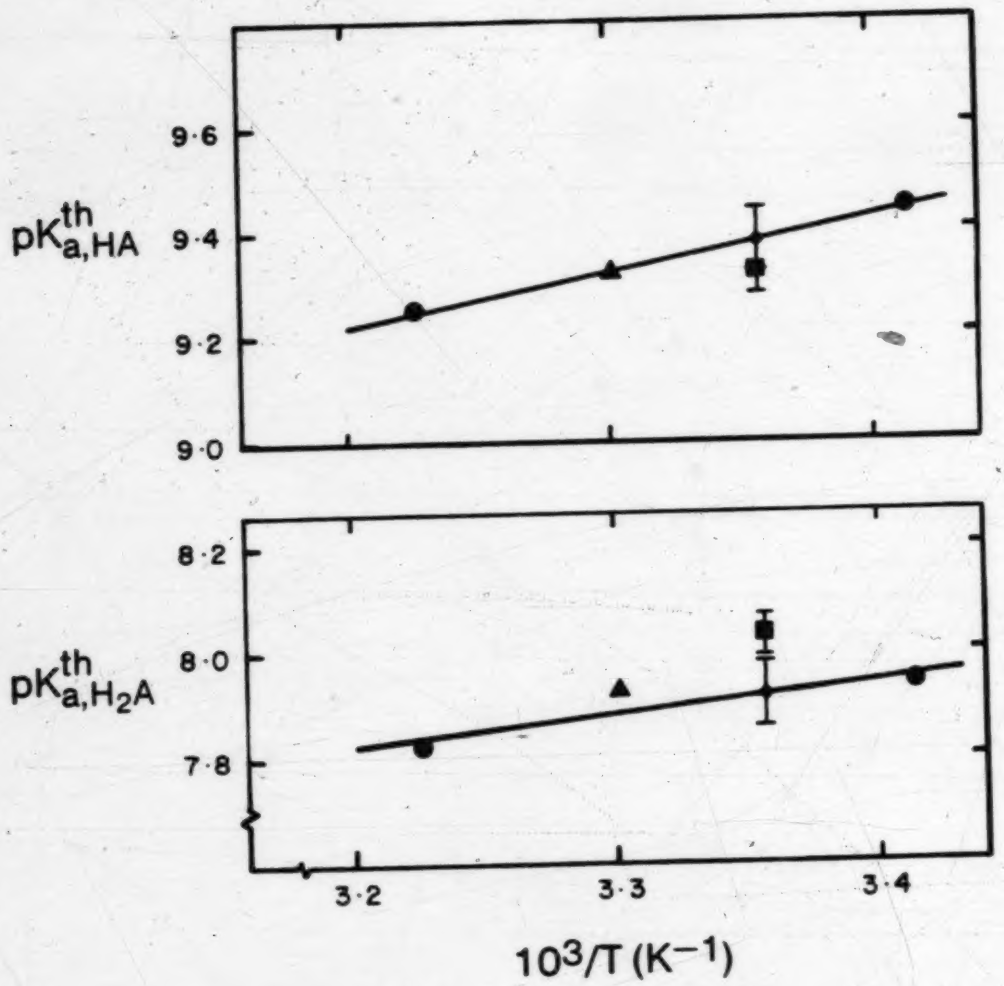

Figure 5. Comparison of pK^{th}_{a,H_2A} and $pK^{th}_{a,HA}$ for Naloxone•HCL (■, this study) with literature values obtained at 20°C and 37°C (●, ref. 24) and 30°C (▲, ref 60). Literature values of pK^{th}_{a,H_2A} and $pK^{th}_{a,HA}$ at 25°C and their 95% confidence limits indicated by (•) and error bars.

4.2 Distribution Coefficients

The distribution coefficients K_{I,H_2A}, K_{HA} and $K_{I,MA}$ were obtained from batch equilibration studies. The distribution ratio of Naloxone, D, defined as:

$$D = \frac{[H_2AX]_o + [HA]_o + [MA]_o + 2[H_2A.A]_o}{[H_2A] + [HA] + [A]} \qquad (29)$$

was measured as a function of pH (Figure 6, Table 2). Substituting for the species concentrations in equation 29 from the equilibrium constants in Table 1 yields:

$$D = \frac{K_{I,H_2AX} \cdot a_H^2 + K_{HA} \cdot K_{a,H_2A} \cdot a_H + K_{I,MA} \cdot K_{a,H_2A} \cdot K_{a,HA}}{a_H^2 + K_{a,H_2A} \cdot a_H + K_{a,H_2A} \cdot K_{a,HA}}$$

$$+ \frac{2K_{I,H_2A.A} \cdot K_{a,HA} \cdot [HA].a_H}{a_H^2 + K_{a,H_2A} \cdot a_H + K_{a,H_2A} \cdot K_{a,HA}} \qquad (30)$$

where [HA] is obtained from equations 11 and 16-18. At low pH (e.g. pH 1) all terms but the first in the numerator and denominator of equation 30 are negligible and the distribution coefficient K_{I,H_2AX} is equal to the distribution ratio D. The value of K_{I,H_2AX} was found to be zero within experimental error (Table 2).

Although the value of K_{I,H_2AX} could be obtained from a single measurement of the distribution ratio at low pH,

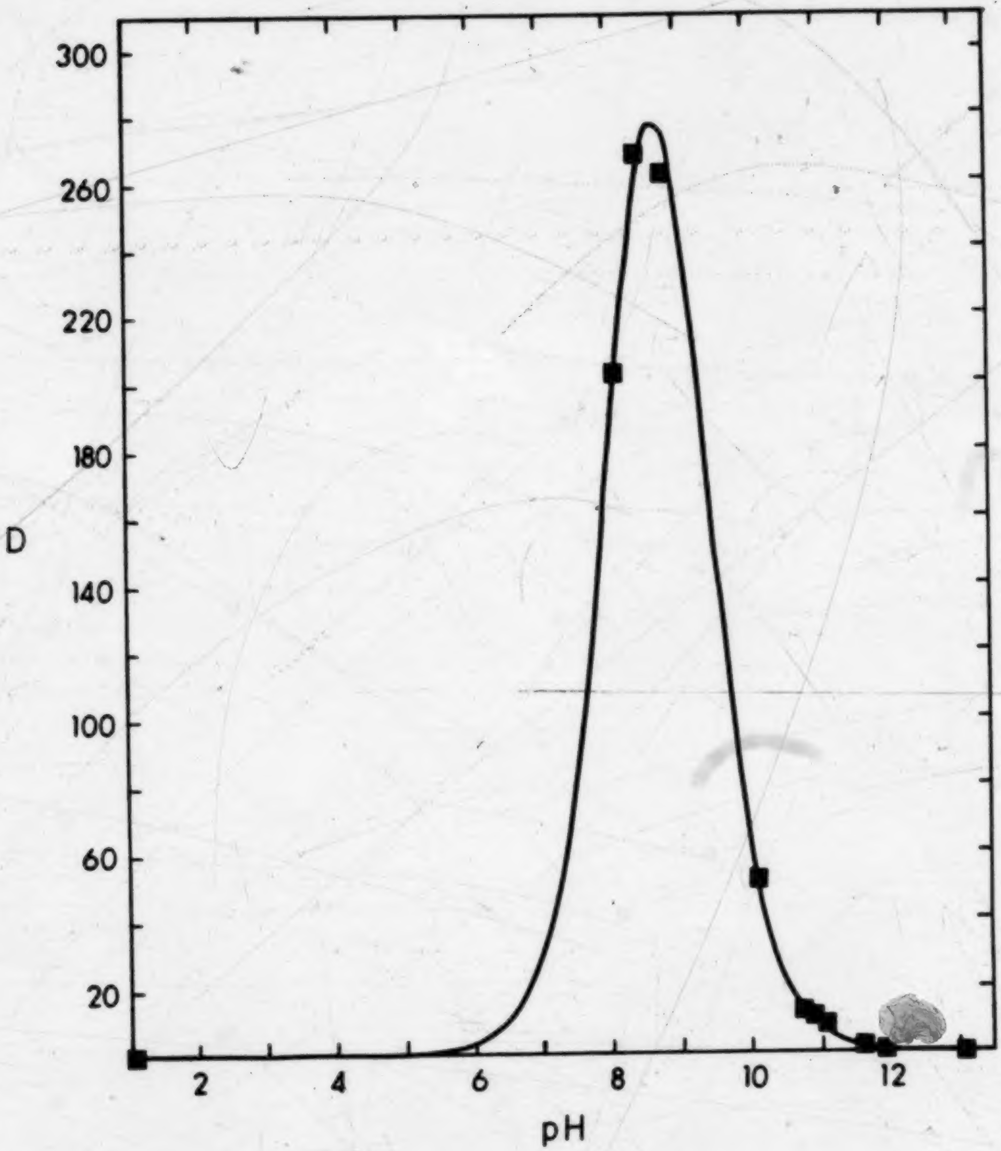

Figure 6. Distribution ratio of Naloxone between chloroform and aqueous solution as a function of pH. Squares are experimental data and curve is calculated from equation 30 using $V_o = 0.020$ L. The values of all other constants are given in the caption to Figure 3.

TABLE 2

Distribution Ratio of Naloxone[a] as a Function of pH

pH	D
1.05	$< 1 \times 10^{-4}$
8.10	203 ± 1
8.44	269 ± 2
8.80	263 ± 2
10.11	52.2 ± 0.4
10.75	13.9 ± 0.1
10.92	12.0 ± 0.2
11.10	9.20 ± 0.08
11.64	2.77 ± 0.02
11.95	1.56 ± 0.01
13.08	0.130 ± 0.001

[a] Error limits are standard deviations calculated from uncertainties in absorbance measurements and tolerances for glassware.

the values of $K_{I,MA}$ and K_{HA} could not be so easily determined because of the closeness of the dissociation constants and their low values. The values of $K_{I,MA}$ and K_{HA} were determined from the distribution ratio vs pH data as follows. Making the first approximation that $K_{I,H_2A\cdot A}$ is small enough to be ignored (see below), the last term in the numerator of equation 30 can be dropped. In addition, the measured value of K_{I,H_2AX} is sufficiently small that the first term in the numerator can also be neglected at pH > 5. Incorporating these approximations, equation 30 can be rewritten as:

$$D(a_H^2 + K_{a,H_2A} \cdot a_H + K_{a,H_2A} \cdot K_{a,HA}) = (K_{HA} \cdot K_{a,H_2A})a_H$$

$$+ K_{I,MA} \cdot K_{a,H_2A} \cdot K_{a,HA} \qquad (31)$$

Thus K_{HA} and $K_{I,MA}$ can be obtained from the slope and intercept of a plot of $D(a_H^2 + K_{a,H_2A} \cdot a_H + K_{a,H_2A} \cdot K_{a,HA})$ vs a_H.

An example of such a plot made in the pH range 8.1 to 10.1 is shown in Figure 7. The line is a linear least squares fit to the four points. In this pH range the concentration of the species HA is relatively high so that the most accurate value of K_{HA} can be obtained. On the

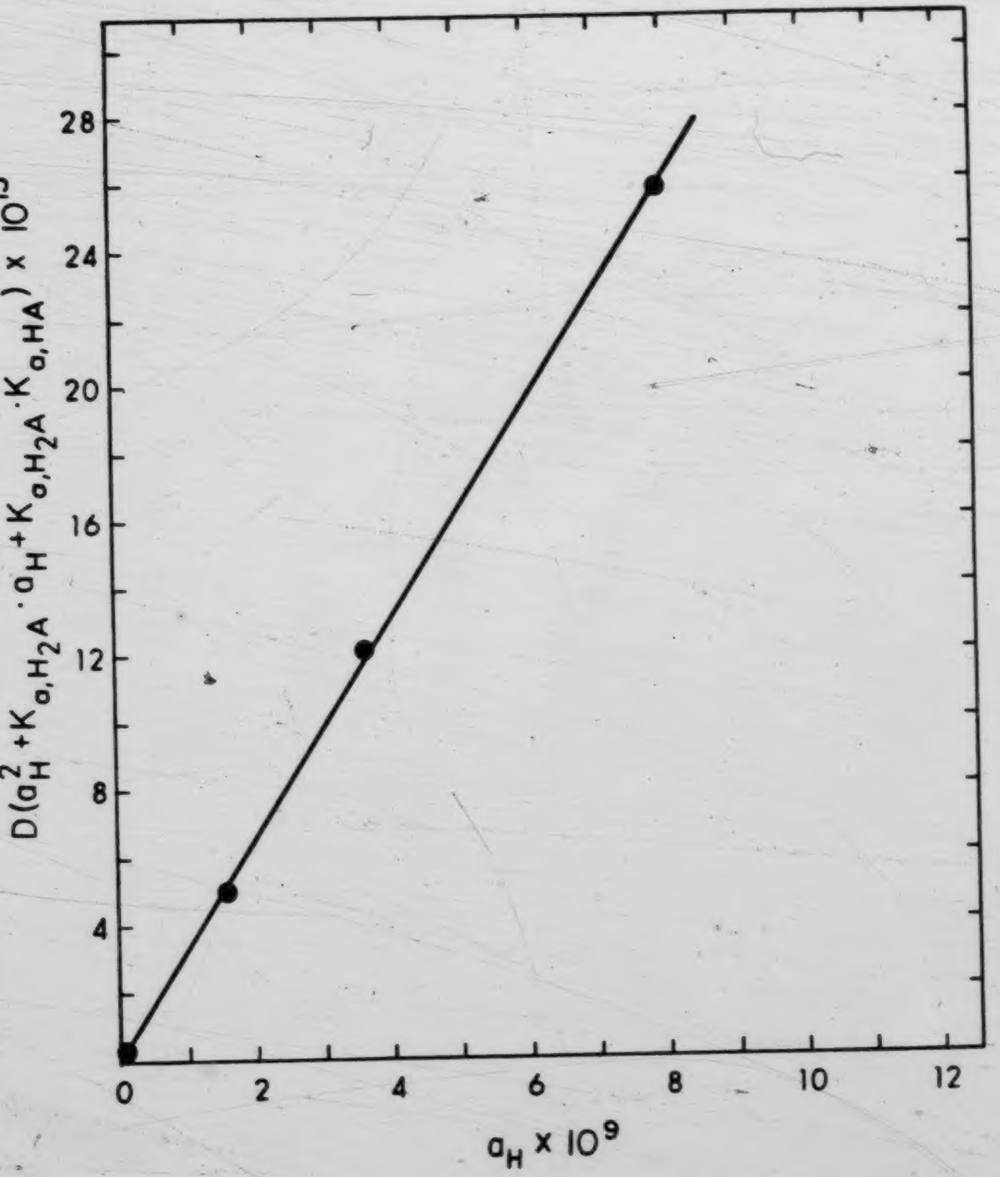

Figure 7. Plot of $D(a_H^2 + K_{a,H_2A} \cdot a_H + K_{a,H_2A} \cdot K_{a,HA})$ versus a_H used to evaluate K_{HA}. Data points calculated from Table 2, using $K_{a,H_2A} = 7.53 \times 10^{-9}$ and $K_{a,HA} = 5.87 \times 10^{-10}$. Line is a linear least-squares fit to data points.

other hand, the concentration of A^- is low in this pH range making it impossible to obtain a reasonable estimate of $K_{I,MA}$. The value of K_{HA} and its 95% confidence limits were found to be 433 ± 23.

A similar plot employing the four points at pH values between 11.1 and 13.1 provides a more accurate value of $K_{I,MA}$ ($K_{I,MA} = 0.14 \pm 0.32$) (Figure 8). The large uncertainty in $K_{I,MA}$ comes about because of the small value of $K_{a,HA}$ and the large value of K_{HA}. The constant $K_{I,MA}$ is indistinguishable from zero.

Neglect of $K_{I,H_2A \cdot A}$ in equation 30 is justified on the following grounds: The distribution isotherm measured for Naloxone between chloroform and an aqueous solution at the isoelectric pH of 8.68 over the range of Naloxone concentrations encountered during a titration, is linear [63]. From this linearity it can be concluded that $K_{I,H_2A \cdot A} < 10^7$, a value too small to influence the shape of the titration curve (see p. 19).

4.3 Quantitative Evaluation of Model

The titration curve theoretically predicted for Naloxone hydrochloride in the presence of chloroform was calculated using equations 13-18 using the measured values for all constants. The theoretically calculated titration curve (Figure 3, curve B) agrees well with the

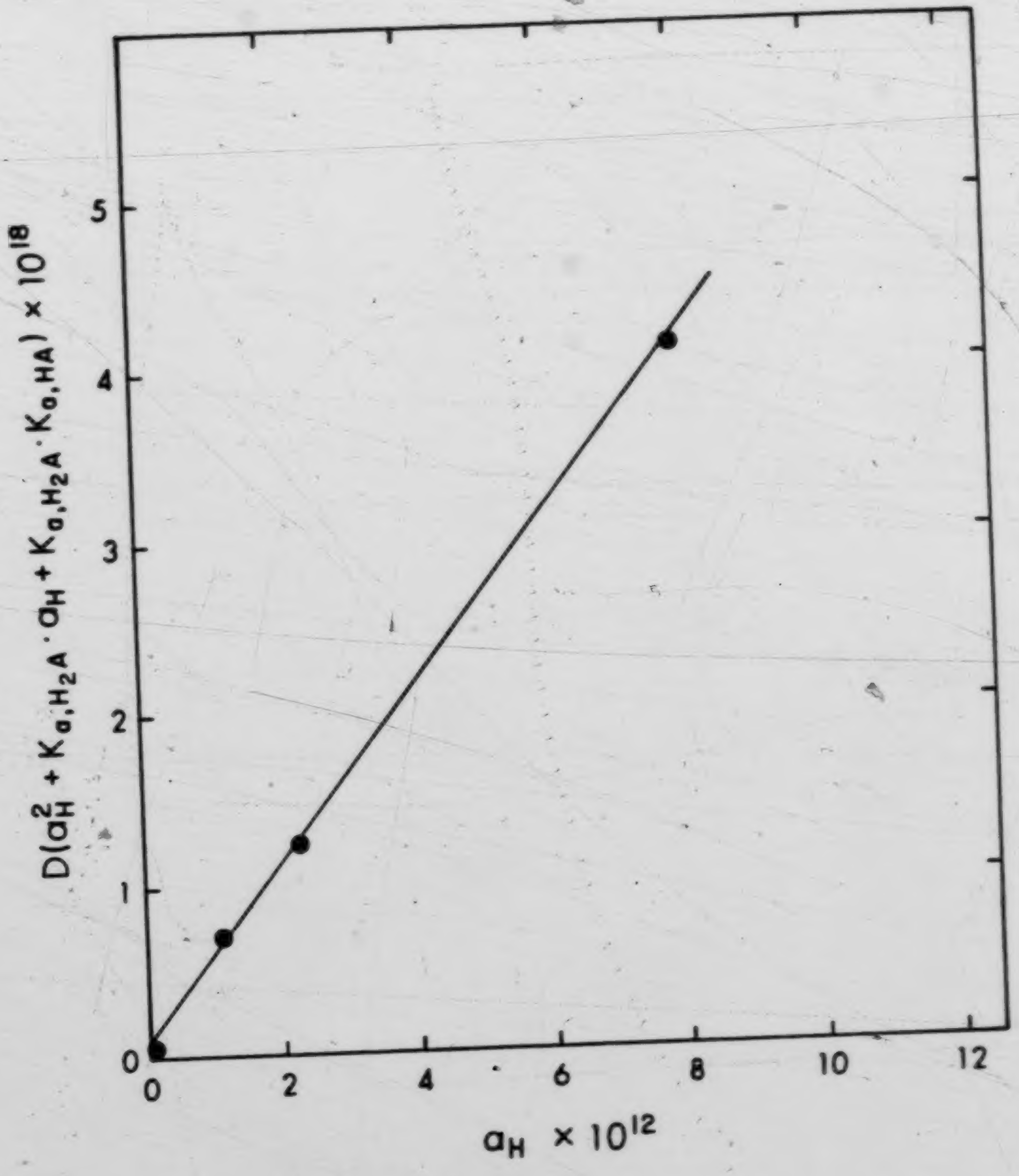

Figure 8. Plot of $D(a_H^2 + K_{a,H_2A} \cdot a_H + K_{a,H_2A} \cdot K_{a,HA})$ versus a_H used to evaluate $K_{I,MA}$.

experimental data points, suggesting the validity of the titration equations.

4.4 Applications to Quantitative Analysis

4.4.1 Naloxone Hydrochloride

The assay value of Naloxone Hydrochloride obtained from the first equivalence point in the two-phase titration is compared in Table 3 with results obtained by two other methods: the nonaqueous titration according to U.S.P. XIX [54] and an acid/base titration in n-propanol/water mixed solvent [8]. Results of all three methods agree within experimental error, yielding an average value of 90.7%. The remaining 9.3% is water.

4.4.2 Mixture of Molindone Hydrochloride and m-Nitrophenol

Two-phase titrations may be applied to assay mixtures of compounds having similar ionization constants but different charge types. Titration curves are presented in Figure 9 for a mixture of 3.00×10^{-4} mole of Molindone Hydrochloride (a protonated tertiary amine: BH^+) and 2.09×10^{-4} mole of m-nitrophenol (neutral HA acid). The ionization constants for Molindone Hydrochloride (pK_a = 7.3 [64]) and m-nitrophenol (pK_a = 8.4 [65]) are close so that the titration curve of the mixture in the absence of chloroform (curve A) shows only one "pH-break",

TABLE 3

Percent of Component by Three Titration Methods, Based on Weight Taken

Sample	Nonaqueous[c]	n-PrOH/H_2O[c]	Two-Phase[c]
Naloxone•HCl	90.5 ± 0.2	90.6 ± 0.3	90.9 ± 0.1
Naloxone•HCl (with NH_4Cl)[a]	-	-	91.2 ± 0.1
Molindone•HCl	99.2 ± 0.1	98.1 ± 0.2	98.1 ± 0.1
Molindone•HCl (with m-Nitrophenol)[b]	-	-	98.2 ± 0.2
m-Nitrophenol (with Molindone•HCl)[b]	-	-	100.6 ± 0.3

[a] Mole ratio Naloxone•HCl/NH_4Cl was 2.25:1.

[b] Mole ratio Molindone•HCl/m-Nitrophenol was 3:2.

[c] Uncertainties are standard deviations.

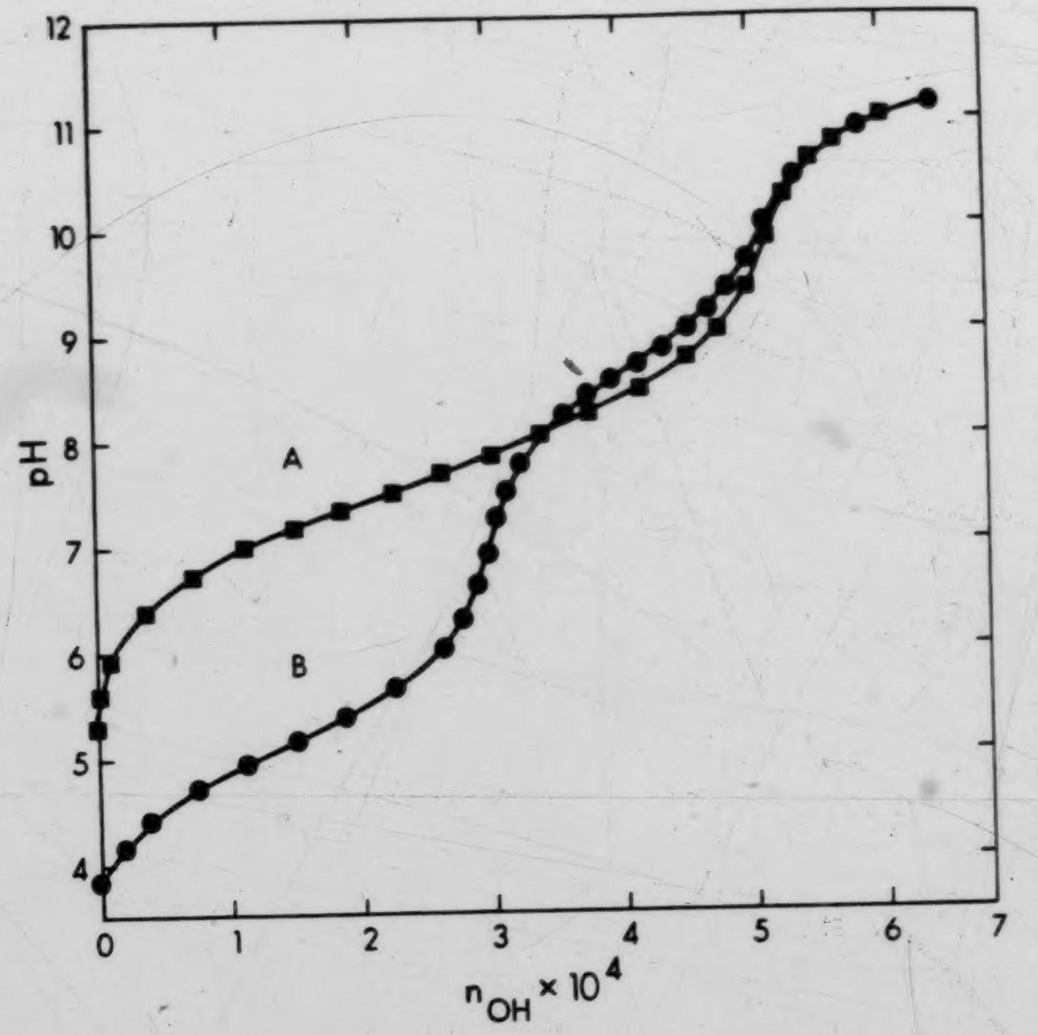

Figure 9. Titration of a mixture of Molindone·HCl and m-nitrophenol with NaOH. $K_{a,BH} = 5 \times 10^{-8}$; $K_{a,HA} = 4 \times 10^{-9}$; V = 0.060 L of 0.108 M NaCl; $n_{BH} = 3.00 \times 10^{-4}$ moles; $n_{HA} = 2.09 \times 10^{-4}$ moles; V_o = 0.0 L (Curve A), 0.020 L of chloroform (Curve B).

corresponding to the total moles of the two acids. However, in the presence of chloroform BH^+ appears to titrate as a stronger acid ($pH_{1/2} = 5.2$) while HA behaves as a slightly weaker acid ($pH_{1/2} = 8.6$). This is consistent with the expectation that the neutral Molindone species, B, will extract into chloroform with a large distribution coefficient. From the magnitude of the shift in the proton binding region for Molindone•HCl ($pK_{a,BH^+} - pK^{app}_{a,BH^+} = 2.00 \pm 0.04$) the distribution coefficient for the neutral species can be calculated (equation 27) to be $K_B = 297 \pm 28$. This assumes that extraction of the ion-pair BHX is small enough to be ignored. Similarly the shift in the proton-binding region for m-nitrophenol ($pK_{a,HA} = pK^{app}_{a,HA} - -0.26 \pm 0.04$) can be substituted into equation 24 and, with the assumption that $K_{I,MA}$ for m-nitrophenolate is negligibly small, the distribution coefficient K_{HA} is calculated to be 2.5 ± 0.5 at 25°C. This agrees with the value of 2.57 reported at 20°C for K_{HA} of m-nitrophenol between chloroform and phosphate buffer of ionic strength equal to 0.2 [66] and is lower than the value of 4.0 reported at 20°C for a measurement made at an unspecified ionic strength [67].

Table 3 presents the assay values obtained for Molindone•HCl titrated alone and admixed with m-nitrophenol. In the nonaqueous titration with perchloric acid in the presence of mercuric acetate it is actually the chloride ion in Molindone•HCl which is being titrated. This method is subject to interference from any other halide salts that might be present and therefore is relatively non-selective. It gives an assay value about one percent higher than found by the partially aqueous and the two-phase titrations. The two-phase assay values obtained for Molindone•HCl alone and mixed with m-nitrophenol agree well with one another and with the value obtained for Molindone•HCl alone in propanol/water.

4.4.3 Naloxone Hydrochloride and Ammonium Chloride

It is possible to use the two-phase titration medium to provide differential titrations of other acid mixtures than those in which the conjugate species have charges of opposite sign. Ammonium ion NH_4^+ has a K_{a,BH^+} value of 5.8×10^{-10} which falls between K_{a,H_2A} (7.5×10^{-9}) and $K_{a,HA}$ (5.9×10^{-10}) of Naloxone Hydrochloride. The titration of a mixture of ammonium chloride and Naloxone Hydrochloride in water shows only one end point "pH-break" corresponding to the sum of all three available acidic protons in the mixture (Figure 10, curve A). However the distribution coefficient of NH_3 is very small ($K_B = 0.04$) [68] so that the titration curve of NH_4^+ is hardly perturbed by the presence of chloroform. A mixture of Naloxone•HCl and NH_4Cl may therefore be accurately

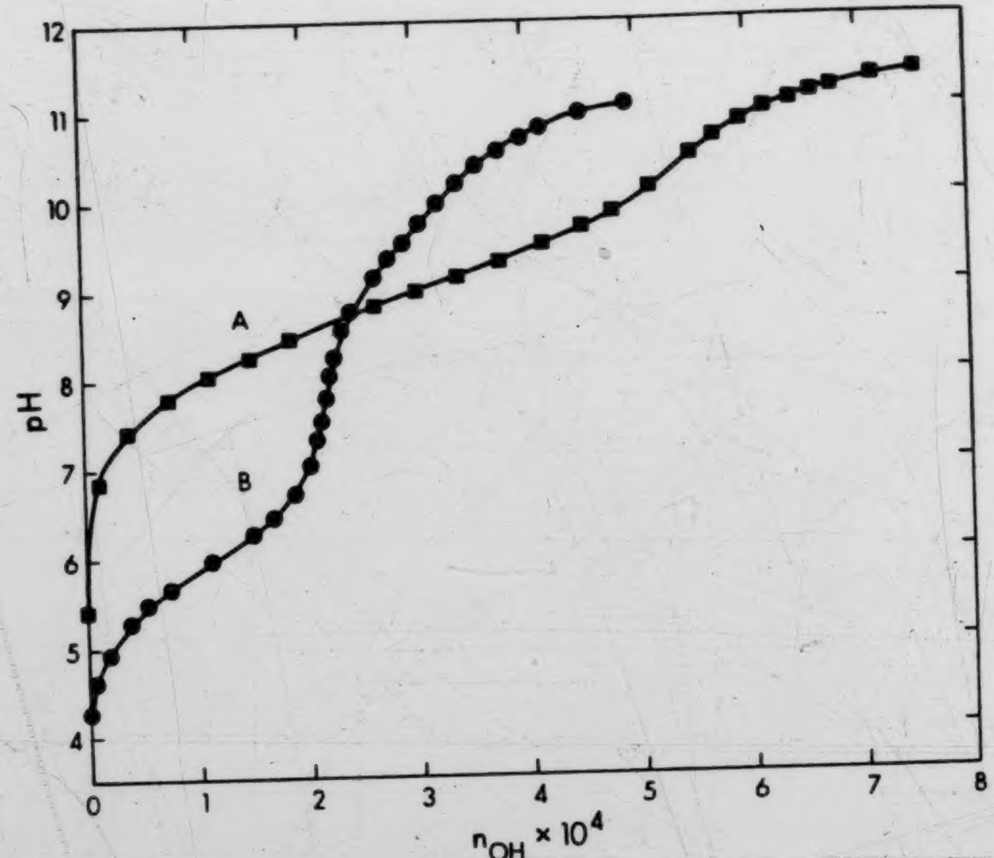

Figure 10. Titration of a mixture of Ammonium Chloride and Naloxone·HCl with NaOH. $K_{a,NH_4} = 5.8 \times 10^{-10}$; $K_{a,H_2A} = 7.53 \times 10^{-9}$; $K_{a,HA} = 5.87 \times 10^{-10}$, $V = 0.060$ L of 0.108 M NaCl; $n_{NH_4} = 1.06 \times 10^{-4}$ moles; $n_{H_2A} = 2.18 \times 10^{-4}$ moles; $V_o = 0.0$ L (Curve A), 0.020 L of chloroform (Curve B).

titrated to the first equivalence point of Naloxone•HCl in an aqueous-chloroform mixture (Figure 10, curve B). The results of such an assay for Naloxone•HCl in a mixture containing about a 2:1 mole ratio of Naloxone•HCl and NH_4Cl are given in Table 3. These results demonstrate the feasibility of using mixtures of immiscible solvents as a differentiating titration medium for acids which have the same charge type but which exhibit very different partition coefficients.

CHAPTER 5

CONCLUSIONS

The apparatus required to perform potentiometric titrations in the presence of two liquid phases is nearly as simple as that involved in a one phase titration and the equilibration time required after the addition of each increment of titrant is also comparable for the two systems. There is no need to shut off the magnetic stirrer while reading the pH. Consequently, it is feasible to use automatic titrators for two-phase titrations.

Compared with titrations performed in partially aqueous solvents such as ethanol-water, methanol-water and n-propanol-water [8], two-phase titrations have the advantages that, if the solubility of the immiscible organic solvent in the aqueous phase is low, then the latter is simply a dilute aqueous electrolyte solution and pH measurements with the glass electrode have the same significance as they do in any dilute aqueous electrolyte. It is unnecessary to employ "transfer activity coefficients" to correct pH meter readings and aqueous pK_a values as it is in mixed aqueous-organic solvents [69,70].

Titrations of the charge type acids discussed in this work have also been performed in the presence of a nonionic adsorbent as a second phase in place of an organic solvent [13,14]. Two problems were noted in the previous work [13,14]: slow attainment of equilibrium between the adsorbent and solution (i.e. up to 5 min/increment of titrant) and precipitation of the uncharged form of acidic or basic compounds. The use of a water-immiscible solvent for the second phase resolves both of these difficulties.

PART II

PRE-COLUMNS OF AMBERLITE XAD-2 FOR DIRECT INJECTION LIQUID CHROMATOGRAPHIC DETERMINATION OF METHAQUALONE IN BLOOD PLASMA

CHAPTER 1

INTRODUCTION

Determination of drugs in complex biological samples like blood plasma by gas or liquid chromatography frequently involves sample cleanup steps, such as solvent extraction and protein precipitation, prior to injection onto the chromatograph. This is not only because of the large number of potentially interfering chromatographic peaks obtained from the plasma but also because the high molecular weight components of plasma (some of them colloidal) seriously contaminate or even plug the chromatographic column. In addition, the determination of trace levels of a drug usually requires concentration of the drug in order to raise the signal-to-noise ratio for its chromatographic peak to a high enough value for accurate quantification.

Among the standard techniques used for concentration and cleanup when dealing with biological samples are solvent extraction and adsorption onto columns of nonpolar adsorbent [71-73]. For example, recent gas chromatographic methods reported for the determination of the sedative, hypnotic drug methaqualone (MTQ) in blood samples employ preliminary solvent extractions of the drug using butyl chloride [74], chloroform [75-76] or ether [77].

As an alternative to solvent extraction, the use of short columns of nonpolar adsorbent has grown in popularity in recent years. The most widely used such adsorbent is Amberlite XAD-2 (XAD), a macroporous copolymer of styrene and divinylbenzene. (Additional information on this resin may be found in the introduction to Part III of this thesis.) Gelbke et al [78] and Gudzinowicz and Gudzinowicz [72] have reviewed the applications of XAD to the isolation of drugs from blood and urine samples. Typically the pH of the blood or urine sample is adjusted with a suitable buffer to suppress the ionization of the drugs of interest, and the treated sample is loaded onto the XAD column. The relatively nonpolar drugs which are immobilized near the top of the resin column are then separated from the more polar blood or urine components (e.g. proteins, amino acids, saccharides, etc.) by washing the resin bed with the aqueous buffer. Finally, the drugs are eluted from the column with an organic solvent or mixture of solvents, prior to chromatographic analysis. Some of the more important pre-1976 solvent extraction and column adsorption cleanup techniques used in the gas chromatographic determination of MTQ have been reviewed

[72]. Solvent extraction and adsorption-column cleanup steps have also been used prior to high performance liquid chromatographic (HPLC) determinations of MTQ [79-80].

Alternative to using adsorbent columns "off-stream" is their "on stream" incorporation into the flow scheme of a liquid chromatograph as a "pre-column" in advance of the analytical column. In this way concentration and cleanup of complex samples become part of the chromatographic operation and are accomplished by switching valves. Preliminary sample handling can therefore be minimized. Frei [79] has recently reviewed the use of pre-columns in this way.

Applications of on-line pre-columns for pre-HPLC sample treatment include determinations of the cytostatic drug methotrexate [82], of antidepressants clovoxamine and fluvoxamine [83], of a metabolite of an antihypertensive drug, endralazine [84] of a cardiotonic agent and antiplatelet drug [85] and of secoverine [86] in blood plasma. Huber and coworkers [87] have used the technique to study the metabolism of aminopyrine. Mohammed, Veening and Dayton [88] have used the technique to monitor as a function of time the levels of riboflavin in hemodialysate fluid from uremic patients. The technique has also been used recently to monitor methanol extracts of medicated animal feed [89].

The pre-column packing materials used in the above examples [82-89] were chemically bonded alkyl-silica reverse-phase sorbents. Thus the pH of the aqueous solvents which can be pumped through the pre-column is limited to pH < 8, since the siloxane functionality (Si-O-Si-C) which binds the alkyl groups to the silica support is readily hydrolyzed in alkaline solution [90]. Consequently it is not possible to use the nonpolar silica bonded phases to adsorb BH^+ type drugs in the form of their strongly retained conjugate base, B, if their pK_a is greater than 8. One way to overcome this limitation would be to use an ion exchanger in the pre-column to enable moderately strong bases (e.g. amines) to be sorbed as the cationic species. This approach has been used by Adler, Margoshes, Snyder and Spitzer [91] to preconcentrate polyamines from urine samples. Koch and Kissinger [92] and Lankelma and Poppe [93] have also utilized on-line pre-columns of ion exchange packings for the respective analyses of serotonin and methotrexate in blood plasma samples.

Macroporous styrene-divinylbenzene copolymer resins such as Amberlite XAD-2 (XAD) have the advantage relative to the silica bonded phase sorbents of chemical stability over the entire pH range from 0 - 14. Cantwell [94] has used an on-stream pre-column of XAD for the determination of p-hydroxybenzoate preservatives in pharmaceutical cough syrups. Aldehyde flavoring agents which also strongly sorb on the pre-column were selectively eluted as bisulfite adducts. Determination of the pharmaceutically active components in these cough syrups was effected using on-line pre-columns containing both XAD and an anion exchanger [95]. Hitachi Gel 3010, a styrene-divinylbenzene copolymer similar to XAD, has been used in an off-stream "micro pre-column" for the determination of steroids in diluted blood serum [96]. Microparticulate XAD resin has also been used as a high efficiency column packing for liquid chromatography [97] and Amberlite XAD-7, a macroporous poly(methylmethacrylate) resin has been applied in on-line pre-columns for the HPLC analysis of multicomponent analgesic tablets [98-99].

With the exception of the work of Roth and coworkers [85] which appeared in the literature shortly before publication of the present study [100], no investigators had reported HPLC methods enabling the direct injection of large volumes of untreated blood plasma into a liquid chromatograph. In each of the HPLC methods using on-line pre-columns cited above [81-84,86], it was necessary to perform some preliminary sample treatment such as dilution of the sample [83,96], precipitation [82] or enzymatic degradation [86] of proteins, or solvent extraction [84] prior to injection into the chromatograph.

In the present study the factors affecting the use of XAD pre-columns for on-stream sample treatment are characterized for the HPLC determination of trace levels of methaqualone in blood plasma. The pre-column makes possible direct injection of relatively large volumes (0 - 4 mL) of undiluted blood plasma. Since MTQ is almost completely metabolized at therapeutic dosage levels, very little is excreted, making it desirable to measure plasma levels rather than urine levels [101]. Some important analytical and biological properties of MTQ have been summarized [102].

CHAPTER 2

EXPERIMENTAL

2.1 Chromatograph

A diagram of the liquid chromatograph is shown in Figure 11. Pump P_1 is a Chromatronix Model CMP-2VK (Laboratory Data Control, Riviera Beach, Fla.). With the Teflon rotary sampling valve V_1 (Laboratory Data Control, model R6031 SVP) in the position shown by the solid lines, the standard or sample liquid is drawn into the Teflon sample loop L_1 by pulling on a syringe attached to the outlet line. L_1 was 0.5 mL except where specified otherwise. During this time, solvent 1 is pumped through column C_1 to a tee-connector (part no. CJ3031, Laboratory Data Control) from which it passes through two parallel branches consisting on the one hand of a coil of Teflon tubing L_2 and on the other hand of sampling valve V_1. The split stream reunites at the second tee-connector and flows through filter F, sampling valve V_2 (stainless steel, part No. 7010, Rheodyne, Inc. Cotati, CA), the pre-column C_2 and then to waste.

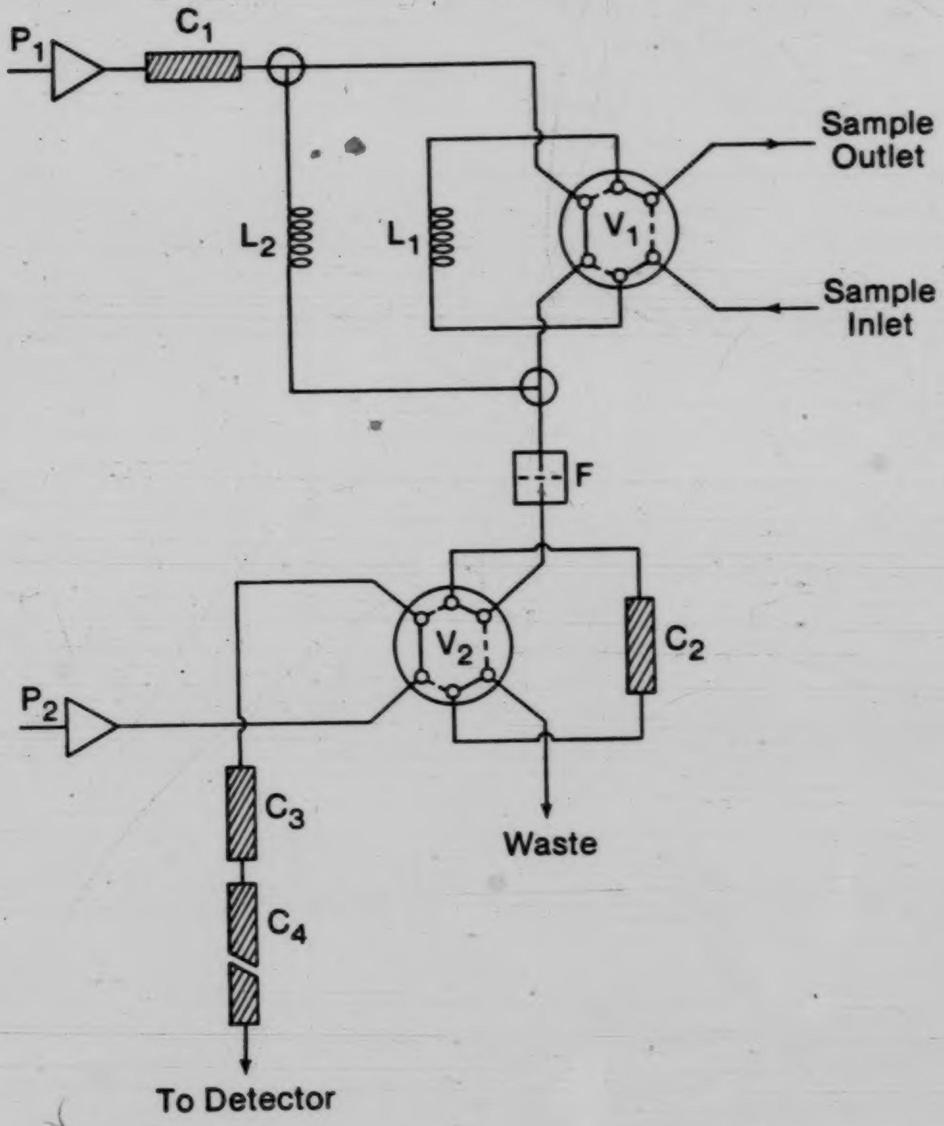
P1
C1
Sample Outlet
L2
L1
V1
Sample Inlet
F
V2
C2
P2
C3
Waste
C4
To Detector

Figure 11. Diagram of the liquid chromatograph used in the MTQ determination (see text for details).

Filter F is a low dead-volume, large surface area inline filter composed of a filter holder machined from Kel-F and two 1.0 cm diameter disks of Zitex porous Teflon, 2-5 µm pore size, 0.007 inch thick (No. E 606-223, Chemplast Inc., Wayne, N.J.). This filter removes larger particles which are occasionally present in plasma samples and which would tend to plug the 2 µm frits in the pre-column causing a gradual increase in pressure at pump P_1.

With valve V_2 in the position shown by solid lines, pump P_2 (model SP8000 liquid chromatograph, Spectra Physics, Santa Clara, CA) pumps solvent 2 through valve V_2, guard column C_3 and analytical column C_4 to the detector.

C_1 is a solvent purifier column which consists of a 5.0 cm × 0.46 cm i.d. stainless steel tube dry-packed with 125-149 µm XAD. This column removes an impurity from Solvent 1 which otherwise is concentrated on C_2 and gives an interfering peak when C_2 is subsequently eluted with Solvent 2. The pre-column C_2 is a 2 cm long × 0.20 cm i.d. stainless steel column dry-packed with 125-149 µm, 63-74 µm or 37-44 µm XAD. This column was constructed from a stainless steel column (part No. 84550, Waters Associates Inc., Milford, MA) by replacing the 2 cm × 0.40 cm i.d. column piece with a locally made one of 0.20 cm bore. Guard column C_3 is a 2 cm × 0.40 cm i.d. stainless steel column (part No. 84550, Waters Associates Inc.) dry-packed with 30-38 μm CO:PEL ODS (part No. 4102-010, Whatman Inc., Clifton, NJ). The analytical column C_4 is a 25 cm × 0.46 cm i.d. stainless steel column packed with 10 μm LiChrosorb RP-8 (part No. A1132-010, Spectra Physics).

The detector was either a Model 8200 Absorbance Detector (Spectra Physics) set at 254 nm or a Model 770 Spectroflow Monitor (Schoeffel Instrument Corp., Westwood, NJ) set at 265 nm. An Autolab Minigrator (Spectra Physics) and a Series 5000 Fisher Recordall potentiometric recorder (Fisher Scientific Co.) were used to record the chromatographic data.

All experiments were done at ambient temperature. However, in order to minimize the effect of short-term temperature fluctuations, column C_4 and the tube connecting it to the detector were wrapped with glass wool. This significantly reduced the noise level at the detector output.

2.2 Resins

Grinding of the Amberlite XAD-2 resin has been previously described [94]. "Cuts" of various particle size were obtained by sieving with standard wire mesh sieves; washed successively with 3 M hydrochloric acid, water and methanol; and the fine particles removed by repeatedly suspending the resin in methanol and decanting the supernatant. The cleaned resin was subsequently air dried.

2.3 Chemicals and Solutions

Double Distilled Water used to prepare sample solutions and mobile phases has been described in Part I of this thesis.

Acetonitrile (Caledon Laboratories Ltd. Georgetown, Ontario) was distilled before use.

Methaqualone Hydrochloride (MTQ), U.S.P. (Charles E. Frosst and Co., Pointe Claire, Quebec) was used as received. Its structure is:

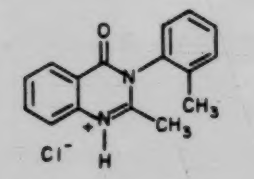

METHAQUALONE · HCl

Bovine Albumin (MW = 69,000 g/mole) was obtained from Sigma Chemical Company, St. Louis, MO (No. A-6003). A 2.8 × 10^{-3} M solution of bovine albumin was prepared by dissolving 4.88 g of the dry protein in 25 mL water and filtering the resulting solution through a 10 - 20 μm porous Teflon filter membrane (No. E249-122 Chemplast Inc., Wayne, NJ) contained in a Swinny Syringe Filtration unit (Cat No. 4310, Gelman Instrument Company, Ann Arbor, Michigan).

Mobile phase Solvent 1 was 0.1 M NH_4Cl/0.1 M NH_3 in water (pH = 9.3). Mobile phase Solvent 2 was prepared by diluting 680 mL of 0.029_4 M citric acid/sodium citrate aqueous buffer (pH 5.4_5) to 1 litre with acetonitrile.

2.4 Standards and Samples

An aqueous stock MTQ solution was prepared to contain 53.52 μg/mL. Standard solutions covering the concentration range 0.214 to 42.8 μg/mL were prepared by serial dilution.

Blood samples were collected from healthy volunteers in 7 mL Vacutainer tubes containing a small amount of K_3HEDTA (Becton, Dickinson & Co.). The red and white cells were removed by centrifugation for 20 min at 2600 rpm in a model HN-S centrifuge (International Equipment Co., Needham Hts., MA). The supernatant straw-yellow plasma was transferred to a stoppered 7 mL test tube. Spiked plasma samples containing 0.214, 0.652, 1.07 and 5.35 μg/mL of MTQ were prepared by transfering 1.00 mL aliquots of appropriate aqueous standards to 10 mL volumetric flasks and diluting to volume with blood plasma. A spiked plasma containing 10.7 μg/mL MTQ was prepared as above using a 2.00 mL aliquot of the MTQ stock solution.

An aqueous solution containing 10.7 μg/mL MTQ and 2.3 × 10^{-3} M bovine albumin was prepared by transfering a 2.00 mL aliquot of the MTQ stock solution to a 10 mL volumetric flask and diluting the contents to volume with 2.8 × 10^{-3} M bovine albumin solution.

2.5 Chromatographic Procedure

After filling the sample loop L_1, valve V_1 is rotated to the inject position (dashed lines). This allows Solvent 1 to flush the sample out of the loop to a tee-connector where Solvent 1 flowing in parallel branch L_2 dilutes the sample and raises its pH before it reaches the pre-column. The length of Teflon tubing used in L_2 is adjusted to obtain approximately equal flow rates in the two parallel branches, thus ensuring both rapid flushing of the sample loop and controlled adjustment of sample pH. In the present case it was a 50 cm × 0.05 cm i.d. Teflon tube.

Following injection of sample, Solvent 1 is pumped through C_2 for a specified time. For an injected volume of 500 μL the time is 5.0 min which corresponds to 10.0 mL of Solvent 1. During this time MTQ is strongly adsorbed (preconcentrated) near the top of C_2, while the bulk of the normal plasma components are washed through the XAD bed to waste. Valve V_2 is then switched to the inject position (dashed lines) allowing solvent 2 to backflush C_2. This strong solvent elutes MTQ from the XAD precolumn, through the analytical column C_4 to the detector. Immediately upon switching V_2 to the inject position, V_1 is switched back to its initial position (solid lines). Valve V_2 is returned to its initial position after 30 sec during which time MTQ has completely eluted from C_2. Following a 2 min delay to re-equilibrate C_2 with Solvent 1, the next sample is injected with V_1. Thus the total analysis time is about 7.5 min between injections. The flow rate of Solvent 1 was 2.0 mL/min except in a study of the effect of flow rate on recovery of MTQ from blood plasma. The flow rate of Solvent 2 was 3.00 mL/min in all experiments.

At the end of the day, both pumps P_1 and P_2 and the entire column and valve system are flushed first with water and then with distilled methanol. This treatment accomplishes, among other things, elution of the impurities that have adsorbed on the purifier column C_1 so that it is virtually never necessary to replace or repack this column.

2.6 System Characterization

Breakthrough studies of MTQ on the 37-44 μm pre-column were performed, using the chromatograph as shown in Figure 11, by injecting 500 μL of 10.7 μg/mL MTQ standard solution. Volumes of either 10, 20, 30 or 40 mL of Solvent 1 were then pumped through C_2 prior to elution with Solvent 2. Areas of the peaks eluted by Solvent 2 were compared to determine if recovery decreased with the volume of Solvent 1 used.

The effect of XAD particle size and flow rate of Solvent 1 on the recovery of MTQ from spiked plasma samples and bovine albumin solutions was evaluated by comparing the relative peak areas obtained for 500 μL injections of a spiked plasma and an aqueous standard, both containing 10.7 μg/mL. Following each injection, 10 mL of Solvent 1 was pumped through C_2 before the drug was eluted with Solvent 2.

Direct monitoring of plasma components as they elute from the XAD-2 pre-column was accomplished by connecting the outlet line of C_2 directly to the detector. The pre-column C_2 was packed with 37-44 μm XAD-2. The volume of the sample loop L_1 was adjusted by using appropriate lengths of 0.5 mm i.d. × 1/16" o.d. or 1.5 mm i.d. × 1/8" o.d. Teflon tubing, to achieve injection volumes of 40 μL, 500 μL and 4.0 mL.

CHAPTER 3

RESULTS AND DISCUSSION

Since it was desired to develop a technique for the determination of trace levels of drugs in blood plasma that would require no pretreatment of the plasma before injection into the chromatograph, it was necessary that Solvent 1 and the pre-column packing be chosen in such a way that the drug is completely retained while the interfering components of blood plasma are unretained on the pre-column. Amberlite XAD-2 is particularly suitable as a pre-column packing because of its inertness at all pH and its relatively strong adsorbent properties [95,97]. The choice of aqueous pH 9.3 NH_4Cl/NH_3 buffer for Solvent 1 was based on the following considerations: Most plasma proteins have their isoelectric pH below 7 [103] and thus have a large negative charge at pH 9.3 which contributes to a high water solubility. Similarly, at pH 9.3 many small molecules found in plasma are negatively charged. Consequently, the majority of plasma components should be relatively unretained on XAD in this solvent. On the other hand, the conjugate acid of MTQ has a pK_a of 2.5

[102]. Thus at pH 9.3 MTQ will be present as the free base which is strongly retained by XAD. This behavior is consistent with the findings of Evenson and Lensmeyer [76] who reported less "biological interference" in their gas chromatographic determination of MTQ in serum when the preliminary solvent extraction was performed at higher, rather than at lower, pH. The pH value of 9.3 was chosen in the present study also because a variety of basic amine drugs, including the amphoteric morphine derivatives, will be present primarily as the free base at this pH so that it can be expected to be a generally useful solvent for their determination in blood plasma.

The choice of an octyl-silica packing for the analytical column was based on the high efficiency, ready availability and popularity of such bonded-phase packings. Since this is a silica-based packing it is incompatable with pH > 8 and, consequently, could not be used in the pre-column. In fact, it was necessary to include a low pH buffer in Solvent 2 in order to lower the pH of the plug of Solvent 1 as it is washed from the pre-column through the analytical column when V_2 is switched. The lifetime of C_4 was well over six months under heavy use. The pre-column was generally re-packed with XAD every week or two.

3.1 Chromatography of Plasma

Curves 1-3 in Figure 12 are the elution profiles obtained by monitoring the absorbance of the pre-column effluent following injection of 40 μL, 500 μL and 4.0 mL of plasma. The eluent is Solvent 1. The rapid rise and fall in absorbance observed upon each injection indicates that the majority of UV absorbing plasma components elute from XAD essentially unretained, and it can be seen that 40 μL, 500 μL and 4.0 mL of plasma injected require respectively about 2, 10 and 40 mL of Solvent 1 to remove the bulk of plasma components from C_2 prior to switching to Solvent 2. Since the pre-column void volume, as calculated from the volume of the empty pre-column, the bulk density and the skeletal density of XAD [104], is about 0.04_3 mL, these volumes represent about 50, 250 and 1000 column volumes of Solvent 1.

The effectiveness of Solvent 1 in removing plasma components from the pre-column is shown in Figure 13A. The chromatogram was obtained by injecting 500 μL of untreated plasma, flushing 10 mL of Solvent 1 through the pre-column and then eluting with Solvent 2. The large, tailing, unretained peak results partly from the elution of plasma components which were not removed from the pre-column by Solvent 1. However, injection of 500 μL of distilled water yields a similar (but smaller) unretained

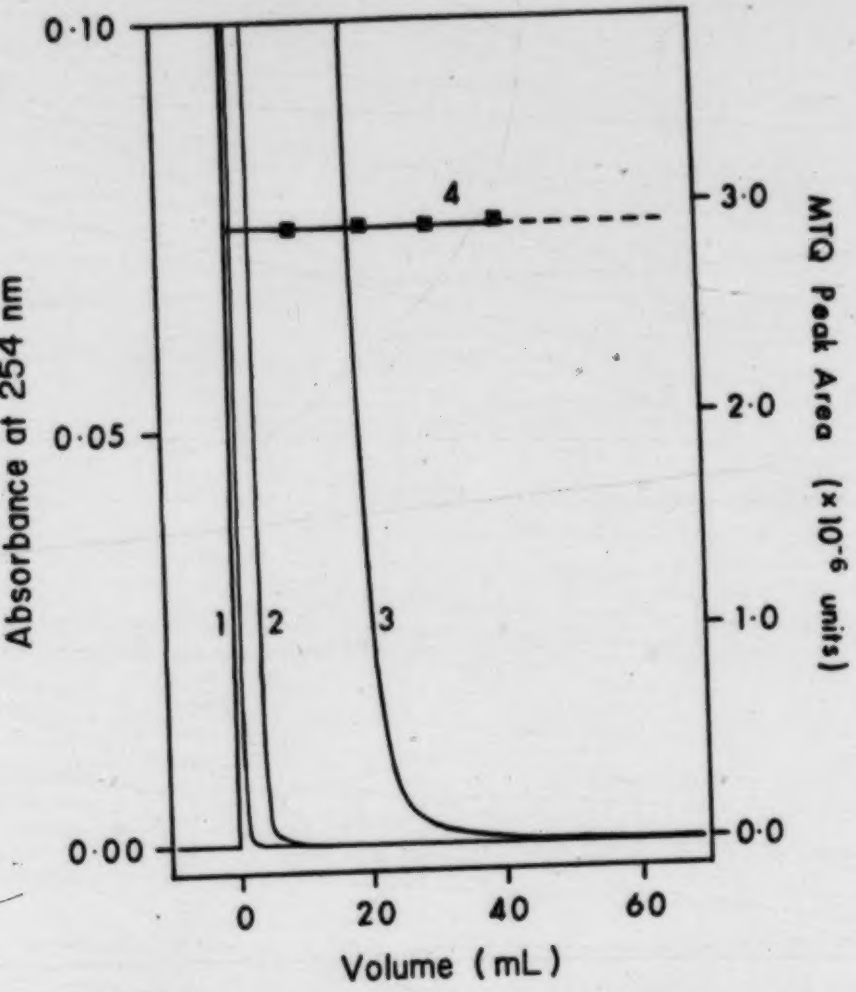

Figure 12. Elution of blood plasma from XAD (curves 1-3, left hand axis) and breakthrough study of MTQ (Curve 4, right hand axis) as a function of volume of Solvent 1 pumped through pre-column. Curve 1, 40 µL; Curve 2, 500 µL; Curve 3, 4.0 mL of plasma injected.

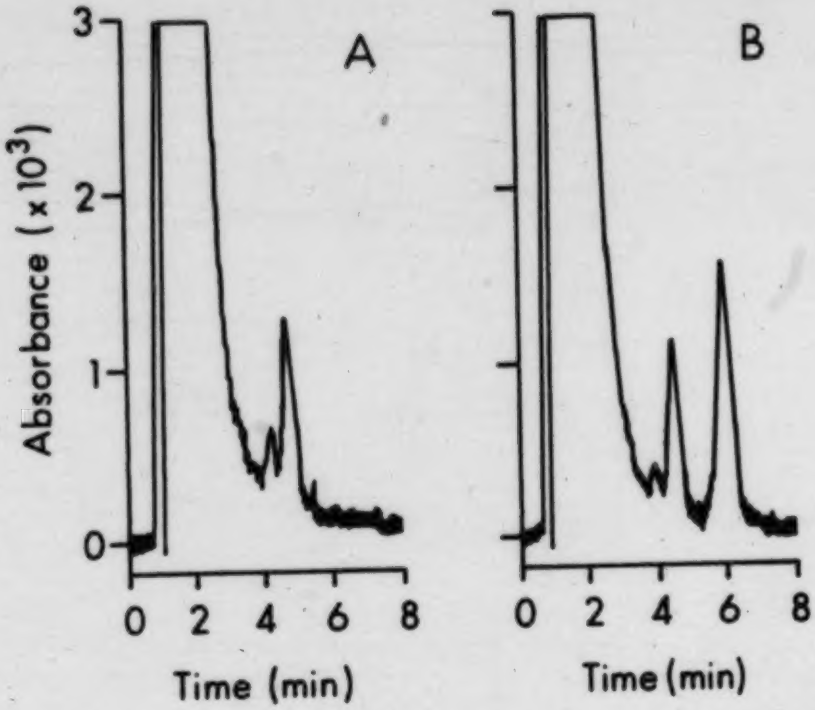

Figure 13. Chromatograms of 500 µL of blood plasma (A) and 500 µL of MTQ-spiked plasma (150 ng/mL) (B). See text for conditions. Wavelength 265 nm.

peak showing that refractive index effects associated with the plug of aqueous Solvent 1 flushed out of the pre-column by the acetonitrile-containing Solvent 2 are also responsible for a large part of the unretained peak. The two peaks eluting between 4 and 5 min are plasma components.

3.2 Chromatography of MTQ

In order to verify that MTQ is quantitatively retained on the XAD pre-column after washing with a volume of Solvent 1 that is sufficient to elute the plasma, a breakthrough study was performed on the 37-44 μm XAD column as described above. Curve 4 in Figure 12 shows that the peak area obtained upon elution of a fixed quantity of MTQ is independent of the volume of Solvent 1 passed through the column up to at least 40 mL. In addition, all of the eluted MTQ peaks exhibited the same width at half-height. Thus, it may be concluded that in Solvent 1 MTQ is strongly retained at the top of the XAD pre-column as a narrow band.

A typical chromatogram obtained for the injection of 500 μL of human blood plasma spiked with 150 ng/mL MTQ is presented in Figure 13B. The detector was a model 770 Spectroflow Monitor set at 265 nm. MTQ elutes in a clean region of the plasma chromatogram at about 6 min. The detection limit, defined as the concentration which gives a peak with height twice the standard deviation of the baseline noise, is 6 ng/mL (6 ppb). Although the molar absorptivity of MTQ is lower at 254 nm [102], the lower baseline noise exhibited by the Spectra Physics detector (254 nm interference filter) results in an even lower detection limit of 0.3-0.6 ng/mL.

3.3 Recovery from Plasma

The influence of blood plasma on the uptake of MTQ by the XAD pre-column was evaluated by comparing the relative peak areas obtained for a spiked blood plasma and an aqueous standard both containing 10.7 μg/mL MTQ. Two factors which were found to influence the recovery of MTQ from plasma: the flow rate of Solvent 1 through the pre-column and the XAD particle size are illustrated in Figure 14. A constant volume of 10 mL of Solvent 1 was pumped through the pre-column for all flow rates and particle sizes. The recovery of MTQ from plasma exhibits the greatest flow rate dependence for the relatively large 125-149 μm XAD. The flow rate dependence is less evident with the 63-74 μm XAD, and negligible for the smallest 37-44 μm particle size.

A similar experiment was performed to determine if the flow rate dependent recovery of MTQ could be

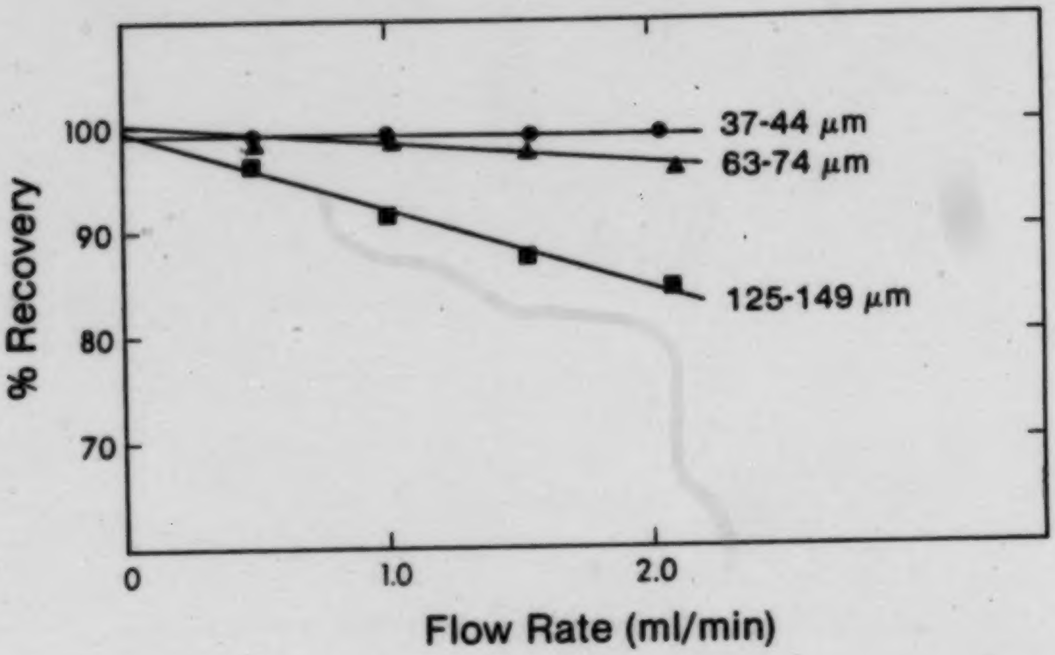

Figure 14. Effect of XAD particle size and Solvent 1 flow rate on recovery of MTQ from spiked plasma (10.7 μg/mL) by the pre-column.

attributed to the presence of proteins in the blood plasma. The influence of flow rate of Solvent 1 through the pre-column on the recovery of MTQ from an aqueous solution containing 2.3 mM of bovine albumin is shown in Figure 15. The recoveries of MTQ from blood plasma and from 2.3 mM bovine albumin using a precolumn with 63-74 μm XAD show essentially the same flow rate dependence (compare Figures 14 and 15).

The data of Figures 14 and 15 suggest that the adsorption of MTQ on XAD is kinetically slower in the presence of plasma proteins than in water alone. As the particle size is increased a longer residence time is required during the adsorption step to insure quantitative uptake. Other investigators [78], using gravity-flow columns of XAD resin have also reported that recovery of drugs from biological fluids is enhanced by loading the sample onto the resin bed at a low flow rate.

In order to explain this behavior two other observations should be noted: Christensen and Holfort [105] found that about 80% of MTQ is bound to serum protein in the concentration range 0.25 to 2.5 μg/mL. Also, the average pore diameter of XAD is 9 nm [104] which is small enough to exclude many plasma proteins [103]. The following two possible explanations of the slow uptake of MTQ seen in Figures 14 and 15 are consistent with the

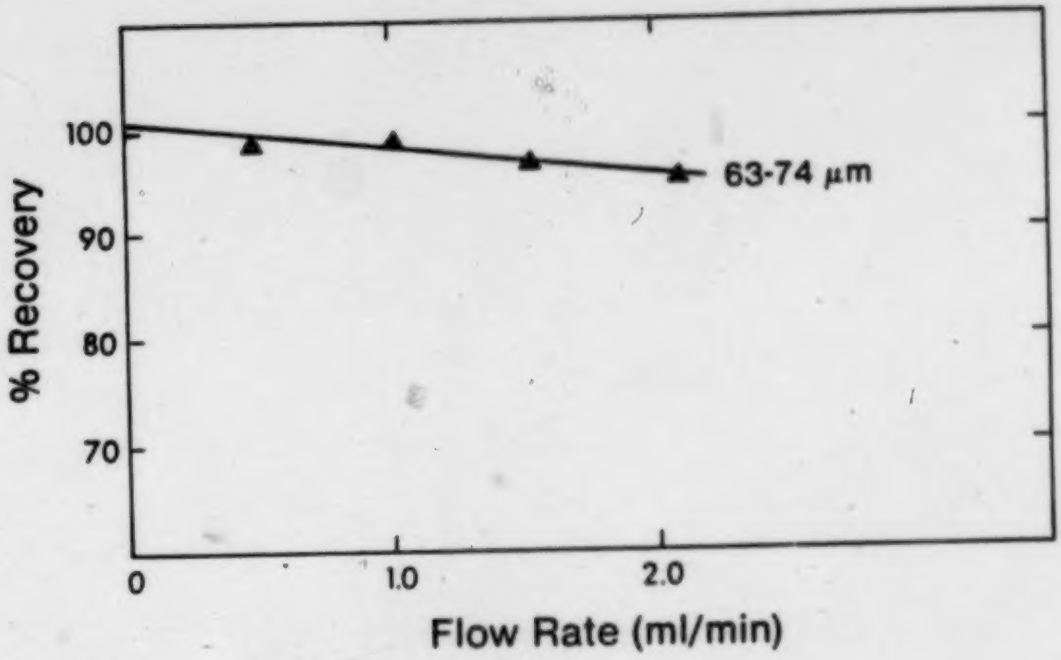

Figure 15. Effect of flow rate of Solvent 1 on recovery of MTQ from an aqueous 2.4 mM bovine albumin solution. XAD particle size 63-74 μm.

data: (i) Slow diffusion of dissociated MTQ or MTQ-protein complex to the resin surface and (ii) Slow dissociation of the protein-MTQ complex. While a decrease in solvent flow rate might yield more extensive adsorption of MTQ for either of the suggested mechanisms, the increased recovery with smaller particle size at a given flow rate seems to favor a diffusion controlled process [106], though of course it does not rule out the possibility that process (ii) could also be contributing to the overall rate control.

It is seen from the data in Figure 12 that quantitative recovery of MTQ, both that which is free and that which is initially protein-bound, is achieved by passage through the pre-column under the correct conditions. This illustrates an advantage of column adsorption (and solvent extraction) cleanup techniques over protein precipitation, in which strongly plasma-bound drugs are likely to precipitate along with the plasma [82].

It might seem that the use of even smaller particle size XAD [97] in the pre-column would be desirable, since it would allow even faster flow rates and a smaller pre-column. However, as the particle size is decreased the pre-column acts as an increasingly efficient filter and tends to become plugged with particulates suspended in the plasma. The use of 37-44 μm XAD represents a practical compromise. In another study [85] in which a relatively large volume of undiluted plasma was directly injected the pre-column packing was also relatively large (37-50 μm), while in cases where the plasma was diluted, deproteinized or in some other way cleaned up before injection, the use of smaller particle packings was possible [81-84,86,96]. The object of the present study, however, was to eliminate any pre-chromatographic sample handling except centrifugation of the whole blood, and the 37-44 μm XAD achieves this objective.

3.4 Column Efficiency

Although it has been found that pre-columns packed with particles of the same size as those in the analytical column produce very little extra-column band broadening [107], the use of particles significantly larger than 10 μm is necessary in the present study in order to avoid plugging the pre-column. It is therefore possible that the overall column efficiency will be degraded below that of the analytical column/guard column. (The pellicular packing in the short guard column would not be expected to degrade efficiency of the analytical column significantly [108].)

The loss in efficiency due to the pre-column can be minimized by using a backflush elution of the drug from the pre-column [82,85,89]. The results of a study of this effect are presented in Table 4 in terms of observed plate number N (tangent method) and asymmetry factor [108] for the MTQ peak eluting from the analytical column. The efficiency of the analytical/guard column combination without pre-column was N = 3101 ± 70 with an asymmetry factor of 1.07 ± 0.02. Comparison of N for the six combinations of particle size and elution pattern reveals two trends: (i) elution through the pre-column causes a severe loss in efficiency and (ii) in both elution modes efficiency is poorer for larger particle size. The first effect is much more pronounced and arises from the fact that in the "elute-through" mode the MTQ, initially adsorbed at the top of the column in a relatively narrow band, must pass through the full 2-cm of pre-column upon elution and experience all of the band dispersion effects of the column, while in the "backflush" mode it passes through a much shorter length of pre-column. The effect of particle size in either of the elution modes is consistent with a greater band dispersion for larger particle size [108]. The effect on tailing is not pronounced except for the largest particle size which yields a rather severe increase in tailing in both elution

TABLE 4

Effect of XAD Particle Size and Pre-Column Flow Direction on Overall Efficiency

	Backflush Mode[a,b]		Elute-through Mode[a,b]	
packing size µm	plate number	asymmetry factor	plate number	asymmetry factor
125-149	2462 ± 60	1.49 ± 0.05	1120 ± 55	1.55 ± 0.08
63- 74	2753 ± 61	1.21 ± 0.13	1408 ± 90	1.14 ± 0.07
37- 44	3010 ± 68	1.17 ± 0.05	1803 ± 65	1.19 ± 0.05

[a] Plate number = 3101 ± 70 and asymmetry factor = 1.07 ± 0.02 for analytical column/guard column alone.

[b] Errors are standard deviation for four injections.

modes. Use of the smallest particle size XAD with backflush results in nearly the same efficiency and tailing as the analytical column/guard column system alone.

3.5 Quantitative Analysis

The use of a pre-column on which the sample compound is preconcentrated before elution onto the analytical column provides a precise means of sample introduction and leads to high precision in quantitative determinations [92]. Consequently, it was possible to avoid the additional step of adding an internal standard when quantifying MTQ in plasma. Calibration plots of peak area vs concentration of aqueous standard injected were obtained in the concentration ranges: 0.2 to 1.0 µg/mL, 1.0 to 10.0 µg/mL and 10.0 to 50.0 µg/mL. All three plots were linear with correlation coefficients of 0.99999, 0.99998 and 0.99998, exhibiting identical slopes (within 1%) and ordinate intercepts equal to zero within the detection limits quoted above.

A series of five blood sample spiked with 0.2 to 11 µg/mL of MTQ were assayed by comparing peak areas with the aqueous MTQ calibration plots. Recovery of MTQ is quantitative (see Table 5) over the concentration range studied. Triplicate injections of spiked plasma yield

TABLE 5

Recovery of MTQ Added to Blood Plasma

Amount added µg/mL	Amount Found µg/mL	% Recovery
0.2141	0.2102 ± 0.0026	98.2
0.6422	0.6281 ± 0.0006	97.8
1.070	1.052 ± 0.0004	98.3
5.352	5.173 ± 0.0002	96.6
10.70	10.38 ± 0.04	97.0
		$\bar{x}$ = 97.8 ± 0.7

assay values with a relative standard deviation of 1% or less.

Plasma levels expected for doses of MTQ in the therapeutic range are typically from 2-4 µg/mL one hour after oral ingestion to about 0.2 µg/mL seven hours after [76,101]. Berry has studied the distribution of MTQ between plasma and red blood cells and finds the ratio to be about 94 to 6 [101]. Consequently, centrifugation of the red cells is an adequate sample preparation rather than prior hemolysis followed by centrifugation of red cell membranes. MTQ does not form glucuronide or sulfate conjugates since it possesses no hydroxyl group, making hydrolysis of plasma samples also unnecessary.

3.6 Other Compounds

MTQ is metabolized by liver microsomal oxidoreductases to a series of monohydroxy derivatives which can go on to form O-glucuronide and O-sulfate conjugates as well as O-methyl derivatives [109,110]. Three of the principal metabolites of MTQ (3'-hydroxy, 4'-hydroxy, and 7-hydroxy) were chromatographed under the conditions of the determination and all eluted well before MTQ. This is expected to be true for all metabolites as well as their conjugates since they are more polar than MTQ [111].

Other drugs, some of which are subject to abuse, are likely to be found in plasma samples being analyzed for MTQ. A number of these were chromatographed under the described conditions. The following drugs yielded no chromatographic peak near that of MTQ: amphetamine, morphine, codeine, cocaine, phenobarbital, secobarbital, butabarbital, amobarbital, barbital, barbituric acid, diazepam, oxazepam, chlordiazepoxide, anileridine, quinine, nicotine and caffeine. The drug methamphetamine yielded a very asymmetric (tailing) peak on the RP-8 column whose retention time decreased with sample loading, being located after that of the MTQ peak at low methamphetamine concentrations and before it at higher. If the ionic strength of Solvent 2 is raised by the addition of a salt such as sodium perchlorate the methamphetamine peak becomes sharper and elutes always ahead of the MTQ peak.

PART III

CHROMATOGRAPHIC RETENTION MECHANISM OF ORGANIC IONS ON A LOW CAPACITY CATION EXCHANGER

CHAPTER 1

INTRODUCTION

Amberlite XAD-2 is a styrene-divinylbenzene copolymer commercially produced as white, insoluble 20-50 mesh beads. Each bead consists of an agglomeration of a large number of microspheres. As a result the beads have a "macroporous" structure with a large surface area (330 m^2/g) [112] and a large average pore diameter (9 nm) [113]. Since the highly crosslinked copolymer matrix itself is essentially nonporous [114], sorption of sample species occurs at the interface between the surface of the microspheres and the solution. Small molecules have free access to all of the surface within the bead via diffusion through the pore liquid [113].

The retention of organic nonelectrolytes on nonpolar resins such as XAD from aqueous/organic solvent mixtures has been shown to occur by adsorption [114-120]. Generally speaking, adsorption of a sample molecule increases with the surface area of the resin [114,120], the size and number of nonpolar substituents in the molecule [114,115] and with increasing percentage of water in the solvent [120-123]. Addition of an inert electrolyte (e.g. NaCl) to the solvent, at concentrations below about 0.1 M, typically has a slight effect on the sorption of neutral species [123,124]. Enhanced adsorption of nonelectrolytes has been observed at ionic strengths above about 0.1 M, the effect being ascribed to "salting-out" [123-125].

Amberlite XAD-2 not only adsorbs neutral molecules, it also adsorbs organic ions. Several investigators [114,119,120,123] have reported that weak acids and bases are usually much less strongly retained on XAD as the anionic or cationic species than as the neutral form. The adsorption onto XAD of aliphatic and aromatic sulfonates [115,120,126], carboxylates [120,127,128], organic ammonium ions [120,123], amino acids and peptides [129] and metal complexes [130] has been studied. Generally, the extent of adsorption of the ionic species onto the XAD resin was found to increase with increasing concentration of inert electrolyte in the solution.

The sorption mechanism for organic cations on XAD has been studied by Cantwell and Puon [112] using sorption isotherms and microelectrophoresis. The results from both experimental techniques were quantitatively explained in terms of the Stern-Gouy-Chapman (SGC) model of the electrical double layer. The model has also been shown to describe the retention of organic anions on XAD [112]. According to the model, the distribution coefficient of an ion depends upon the electrical potential at the resin surface. Consequently, linear sorption isotherms and symmetrical chromatographic peaks are only obtained if the surface potential does not vary with the amount of sample ion adsorbed. This condition is achieved experimentally either by using very low sample concentrations so that the electrical surface potential is close to zero or by adding a sufficiently large excess of a second adsorbed organic ion (potential determining ion) to the mobile phase that the adsorbed sample ion makes a negligible contribution to the surface charge. By choosing either an organic cation or anion to control the surface potential, the chromatographic retention of the sample ion may be either enhanced or diminished.

In such a system, sorption of both the sample ion and the potential determining ion depends on the ionic strength in the mobile phase [131]. Consequently the surface charge density of the adsorbent varies with ionic strength. As an alternative to generating a variable surface charge density by adding a potential determining ion, a constant surface charge density can be produced on the adsorbent by covalently binding ionic functional groups to the resin surface, thus converting the XAD to a low capacity ion exchange resin.

Afrashtehfar and Cantwell [132,133] attached quaternary ammonium groups to about 5% of the surface phenyl rings of XAD resin to create a low capacity (45 μeq/g) surface quaternized ion exchanger. Using the SGC model of the double layer, chromatographic retention data for an organic counterion was shown to be quantitatively accounted for by two processes: ion exchange of the sample ion for other counterions in the diffuse part of the double layer, and adsorption on the resin surface. Surface adsorption is strongly influenced by the surface potential [112] while ion exchange is independent of potential.

In the present work the mechanism of retention of organic cations on a low capacity cation exchanger (SXAD), synthesized by surface sulfonation of XAD, has been investigated by studying sorption isotherms of sample ions. In order to facilitate these measurements a precolumn equilibration technique has been developed. Chapter 2 presents the theoretical foundation, in terms of the SGC model and double layer ion exchange, for understanding the ionic retention mechanism. Chapter 4 gives the experimental results, which serve to validate the use of the ion exchange/surface adsorption model to explain the retention of cations on a low capacity cation exchanger.

CHAPTER 2

THEORY

Chromatographic retention of ionic species on low capacity macroporous ion exchange resins such as SXAD can be viewed as a phenomenon occurring in the electrical double layer at the sorbent/solution interface. Two mechanisms are proposed to account for the sorption of ionic species: ion exchange in the "diffuse part (vide infra) of the double layer and adsorption onto the surface of the resin. The necessary concepts from electrical double layer theory are presented in Section 2.1.1 and subsequently applied in Sections 2.1.2 and 2.1.3 to develop the chromatographic retention equations.

To test the proposed sorption mechanism, it was necessary to develop an experimental technique capable of measuring the distribution coefficient for strongly sorbed sample ions. The theoretical basis of this technique will be discussed in the second part of this chapter (Section 2.2).

2.1 Proposed Model

2.1.1 Electrical Double Layer Theory

The most widely used quantitative treatment of the electrical double layer is Stern's modification [134] to the model proposed by Gouy [135] and Chapman [136]. The Stern-Gouy-Chapman (SGC) model has been reviewed in several places [137-141] and a concise summary may be found in Shaw's book [142]. The essential features of the SGC model will be presented in the following discussion of the SXAD/solution interface.

The SGC model provides the following description of the interface between the SXAD surface and an electrolyte solution (Figure 16). The surface of the resin is taken to be a flat, impenetrable wall. The electrical charge of the covalently bound sulfonate groups is assumed to be uniformly distributed (smeared) over a mathematical plane denoted as the "charge surface".

The SXAD particle and solution taken together are electrically neutral, consequently the negative charge on the particle surface must be neutralized by an excess of positive charge resulting from a redistribution of ions in the adjacent solution phase. The surface electrostatically attracts ions of opposite charge ("counterions", e.g. Na^+), causing their concentration near the surface to be greater than that in bulk

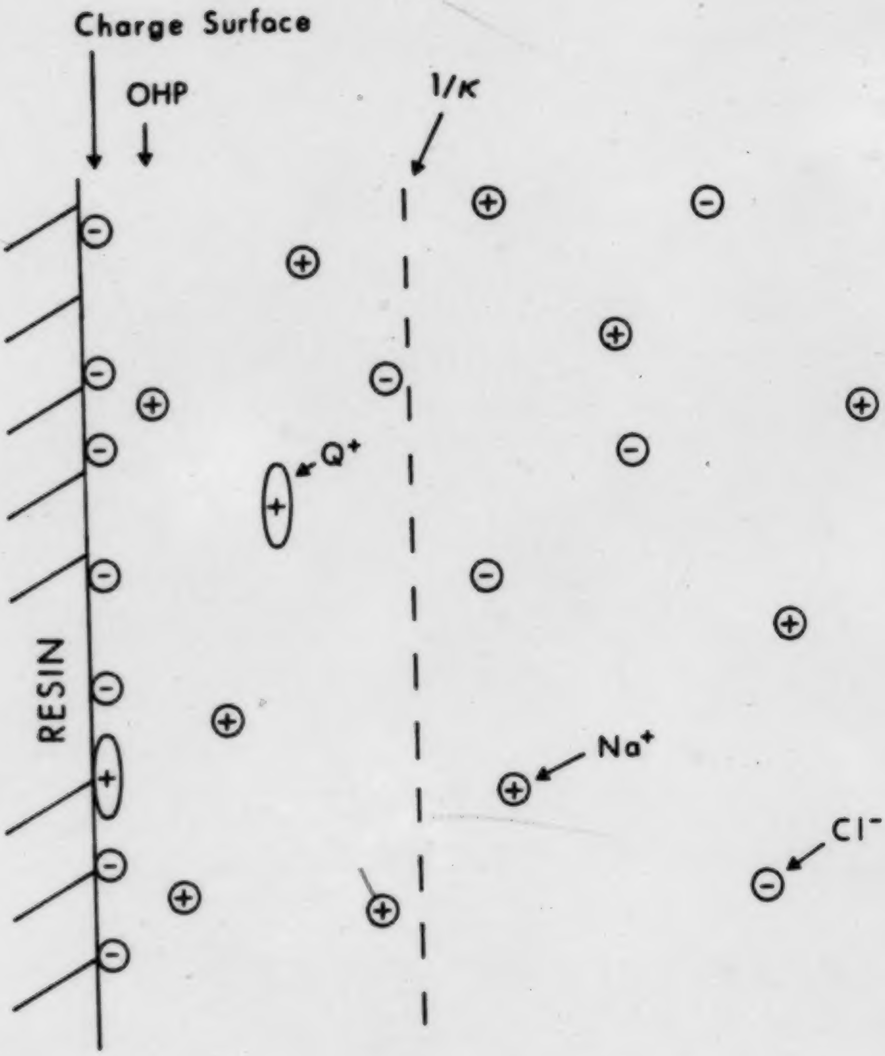
Charge Surface
OHP
1/κ
Q⁺
RESIN
Na⁺
Cl⁻

Figure 16. Diagram of the interfacial region between a sulfonated Amberlite XAD-2 (SXAD) bead and an aqueous electrolyte solution.

solution.* At the same time, the surface repels ions of like charge ("coions", e.g. Cl^-) so that their concentration is depleted near the surface. Superimposed on these processes are random thermal motions which tend to cause counterions to diffuse back into bulk solution and coions to diffuse towards the surface. This causes the region of excess positive charge in the solution adjacent to the surface to be thicker than it would be in the absence of thermal agitation. Hence it is referred to as the "diffuse" part of the double layer.

Assuming they are nonadsorbed, ionic species can approach the charge surface only to within about a hydrated ionic radius. This plane of closest approach of hydrated ions is called the "Outer Helmholtz Plane" OHP [137]. The OHP thus divides the electrical double layer into two parts: the "compact" part which extends from the charge surface to the OHP and the "diffuse" part which includes the OHP and extends from it into bulk solution.

Counterions may become specifically adsorbed onto the resin surface, losing part of their hydration shell in the process. The driving forces for adsorption onto the surface may include some or all of the following: coulombic attraction, van der Waals forces, hydrogen bonding and water structure effects [143,144]. For the purposes of this study, the centers of the specifically adsorbed ions are considered to be in the same plane as the charge surface.

---

*The "bulk solution" is a region in solution sufficiently far away from the charge surface that electroneutrality prevails throughout it at the microscopic level.

Two contributions to the electrical charge density of the surface, σ_o, must be considered: covalently bound charge sites (i.e. $-SO_3^-$) and specifically adsorbed ions. In the present work, the number of specifically adsorbed ions is kept much lower than the number of fixed charge sites on the resin. Consequently for the purpose of this work the surface charge density (coulombs/cm^2) may be calculated from the equation:

$$\sigma_o = \frac{Z_R . F . Q_{wgt}}{A_{sp} . 10^3} \qquad (32)$$

where Z_R is the valence (including sign) of the fixed charge sites ($Z_R = -1$ for $-SO_3^-$), F is the Faraday constant, Q_{wgt} is the ion exchange capacity of the resin (meq/g) and A_{sp} is the specific surface area of the resin ($A_{sp} = 3.3 \times 10^6$ cm^2/g) for SXAD [112]).

The electrical potential $\psi(x)$ at a distance x from the charge surface is defined in such a way that $e\psi(x)$ is the reversible electrical work required to transport an elementary charge e from bulk solution to the point x. Consequently the electrical potential of bulk solution is taken as zero, and the electrical potential at the surface ψ_o may be expressed as the sum of the potential across the compact layer, $\psi_o - \psi_{OHP}$, and the potential across the diffuse layer ψ_{OHP}. By treating the two parts of the double layer separately (see below), ψ_o may be related both to the surface charge density and to the distribution of ions in the interfacial region.

The compact part of the double layer may be treated as a parallel plate capacitor with one "plate" at the charge surface and the second plate at the OHP. The potential in volts across this "capacitor" is given by:

$$\psi_o - \psi_{OHP} = \frac{\sigma_o}{C_1} \tag{33}$$

where the surface charge density σ_o is calculated from equation 32 and the specific capacitance C_1 (Farads/cm^2) is given by:

$$C_1 = \frac{\varepsilon\varepsilon^\circ}{4\pi d} \tag{34}$$

The permittivity of the compact layer $\varepsilon\varepsilon^\circ$ is equal to the product of the unitless dielectric constant for the pure bulk solvent ε (78.52 for water at 25°C, ignoring dielectric saturation effects (141)), and the permittivity of a vacuum ε° (1.112×10^{-12} Farad/cm). The thickness of the compact layer, d, is taken to be equal to the hydrated radius of the principal counterion (e.g. Na^+). This thickness d, and consequently the capacitance C_1 are assumed to be invariant with changes in electrolyte concentration [112,145,146].

Quantitative treatment of the diffuse part of the double layer involves considering the manner in which charge (counterions and coions) and electrical potential are distributed as a function of distance from the OHP. These two factors are interdependent as the following discussion shows.

The concentration of an ion i in the diffuse layer at a distance x from the OHP is given by the Boltzmann distribution equation [137]:

$$C_i(x) = C_i \exp\left(\frac{-Z_\pm F\psi(x)}{RT}\right) \qquad (35)$$

where C_i is the concentration of i in moles/liter in bulk solution and $Z_\pm$ is the valence (including sign) of i. The numerator of equation 35 is the reversible electrical work (Joule/mole) required to transport i from bulk solution to point x. Equation 35 indicates that the highest concentrations of counterions ($Z_\pm = 1$) and the lowest concentrations of coions ($Z_\pm = -1$) are found in regions of the diffuse layer where $\psi(x)$ has its maximum negative value.

In order to determine the actual distribution of counterions and coions as a function of distance from the OHP, it is necessary to consider the electrical "screening effect" of electrolyte ions on the potential which is seen by a given ion in solution. This screening effect may be quantitatively expressed by the Poisson equation [137]:

$$\frac{d^2\psi(x)}{dx^2} = -\left(\frac{4\pi}{\varepsilon\varepsilon^\circ}\right) \sum_i Z_\pm F C_i(x) \qquad (36)$$

which indicates that the rate of change of the potential gradient $d^2\psi(x)/dx^2$ at a distance x from the OHP is proportional to the excess positive charge at that point, $\sum_i Z_\pm F C_i(x)$. Consequently the potential varies linearly with distance in regions of the double layer where the excess charge is zero (i.e. the compact layer). On the other hand, in the diffuse layer the potential versus distance plot is curved, the curvature increasing with the excess positive charge in a given region.

Combination of equations 35 and 36 gives rise to a second order differential equation which can be solved for $\psi(x)$. The resulting equations (Equations 7.4-7.6,7.8 of reference 143) have been used along with equations 32 and

35 to calculate the data for Figure 17, in which the concentration of counterions (labelled C_+) and coions (labelled C_-) are plotted as a function of distance from the OHP. Concentration profiles were calculated for two different electrolyte concentrations (c = 0.1 and 0.5 mol/l) assuming $Q_{wgt} = 0.050$ meq/g, $Z_R = -1$ and $A_{sp} = 3.3 \times 10^6$ cm^2/g. The horizontal dashed lines in Figure 17 represent the concentration of counterions and coions in the bulk solution. Consequently the total area between the dashed line of curve 1 and the curve labelled C_+ represents a positive "surface excess" of counterions in the diffuse layer, $\Gamma_{+,DL}$. On the other hand, the area between the dashed line and the C_- curve represents a negative "surface excess" (or absence) of coions in the diffuse layer $\Gamma_{-,DL}$. Here the "surface excess" $\Gamma_{i,DL}$ is defined as the number of moles of i in the diffuse layer adjacent to one square centimeter of surface, which are in excess of the number of moles of i which would be in the same volume of solution if there were no interactions between species i and the surface.

In the absence of specific adsorption, the electrical charge due to the fixed charge sites of the surface (i.e. $-SO_3^-$) must be balanced by an equivalent excess of counterions relative to coions in the diffuse layer:

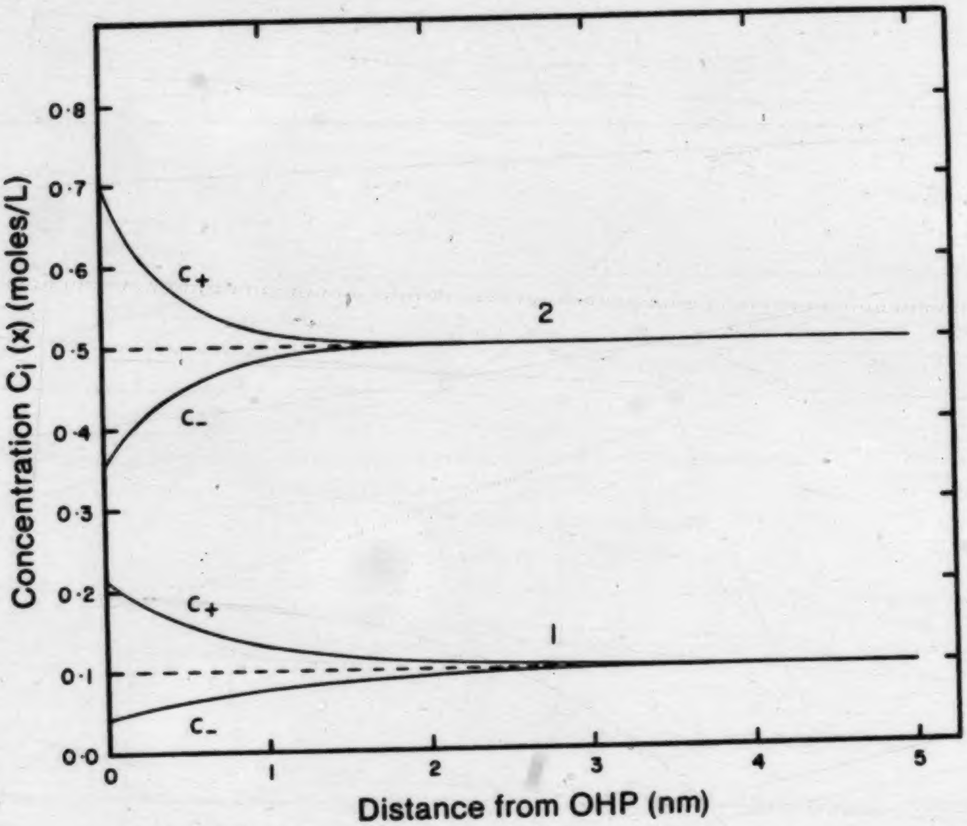

Figure 17. Concentration of counterions (C_+) and coions (C_-) as a function of distance from the Outer Helmholtz Plane. Data for a SXAD resin with Q_{wgt} = 0.050 meq/g and aqueous NaCl electrolyte ($d = 4.7 \times 10^{-8}$ cm). c = 0.100 M (curve 1) and c = 0.500 M (curve 2).

$$\sigma_o = ZF(\Gamma_{+,DL} - \Gamma_{-,DL}) \tag{37}$$

Here Z, the valence (without sign) of the counterions and coions is equal to 1. The term $(\Gamma_{+,DL} - \Gamma_{-,DL})$ is represented by the total area between the C_+ and C_- curves in Figure 17.

Reeves [147] has given $\Gamma_{+,DL}$ and $\Gamma_{-,DL}$ as explicit functions of ψ_{OHP}. Substituting these expressions into equation 37 and solving for ψ_{OHP} yields:

$$\psi_{OHP} = \left(\frac{2RT}{ZF}\right) \sinh^{-1}\left[\left(\frac{4\pi\sigma_o}{\varepsilon\varepsilon^\circ\ \kappa}\right) \cdot \left(\frac{ZF}{2RT}\right)\right] \tag{38}$$

where R is the universal gas constant (Joule K^{-1}mole^{-1}), T is the absolute temperature, $\sinh^{-1}$ is the inverse hyperbolic sine function [148] and κ is given by:

$$\kappa = \left(\frac{8\pi Z^2F^2c}{1000\ \varepsilon\varepsilon^\circ\ RT}\right)^{1/2} \tag{39}$$

with c being the electrolyte concentration (ionic strength) (mole/L) in bulk solution. When $Z\psi_{OHP}$ is much smaller than about 0.025 V at 25°C, the Debye-Huckel approximation [142] may be applied to equation 38 giving:

$$\psi_{OHP} = \frac{4\pi\sigma_o}{\varepsilon\varepsilon^\circ\ \kappa} = \frac{\sigma_o}{C_2} \tag{40}$$

from which it is seen that, at low potentials, the diffuse part of the double layer has the same capacitance, C_2, as a parallel plate condenser with distance $1/\kappa$ between the plates. Physically, $1/\kappa$ is also the distance from the OHP at which $\psi(x)$ has the value ψ_{OHP}/e [142].

When the ionic strength c is constant, the "thickness" of the diffuse layer, $1/\kappa$ is also constant (equation 39) and ψ_{OHP} increases linearly with σ_o. On the other hand, since $1/\kappa$ is proportional to $c^{-1/2}$, increasing the ionic strength causes the thickness of the diffuse part of the double layer to decrease (compare curves 1 and 2, Figure 17). In these studies where σ_o is maintained at a constant value by the ion exchange capacity of the resin Q_{wgt} (equation 32), with specific adsorption of sample ion making a negligible contribution (i.e. at "trace conditions", see below), this compression of the diffuse part of the double layer results in a proportional decrease in ψ_{OHP} (equation 40).

The electrical potential at the charge surface, ψ_o, can now be given as the sum of the potentials across the compact layer (equations 33 and 34) and the diffuse layer (equations 38 and 39):

$$\psi_o = \frac{\sigma_o}{C_1} + \frac{2RT}{ZF} \sinh^{-1} \left[\left(\frac{500\pi}{\varepsilon\varepsilon^\circ\ RT}\right)^{1/2} \cdot \sigma_o \cdot c^{-1/2} \right] \qquad (41)$$

This expression, valid for all values of ψ_{OHP}, has been plotted in Figure 18 for several values of σ_o (calculated from Q_{wgt} using equation 32) with $C_1 = 1.48 \times 10^{-4}$ Farad/cm^2 (calculated from equation 34, using $d = 4.7 \times 10^{-8}$ cm as the hydrated radius of Na^+ [57]). The first term on the right side of equation 41 can be restated as $\psi_o - \psi_{OHP}$ and is a constant for a given batch of resin, while the second term is equal to ψ_{OHP} and approaches zero with increasing electrolyte concentration c. The rate of decrease in ψ_o with increasing c, seen in Figure 18, is gradual at values of c above 0.1 M with ψ_o approaching a value of σ_o/C_1 at large c.

2.1.2 Sorption on a Low Capacity Cation Exchanger

2.1.2.1 Ion Exchange of a Counterion

On surface sulfonated cation exchange resins such as SXAD, ion exchange may be viewed as a competition between sample counterions Q^+ and electrolyte counterions M^+ (e.g. Na^+) for a position in the diffuse part of the electrical double layer. The exchange reaction may be represented by the equilibrium:

$$Q^+ + (M^+)_{DL} \rightleftarrows M^+ + (Q^+)_{DL} \qquad (42)$$

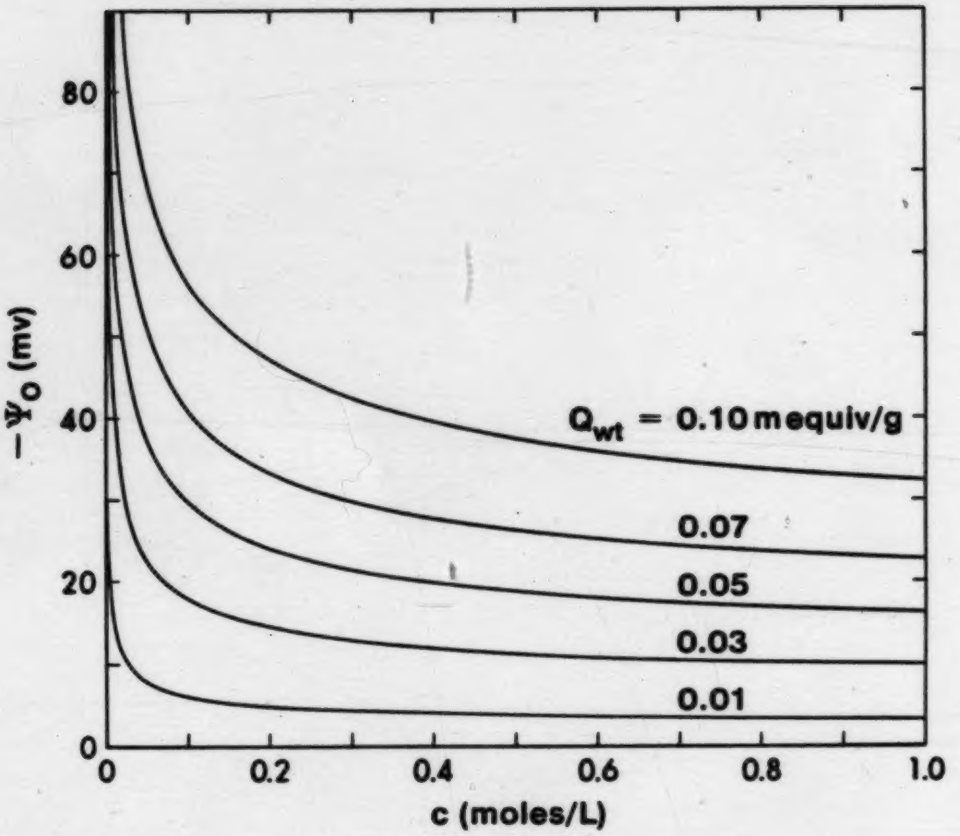

Figure 18. Dependence of electrical potential at the charge surface, ψ_O, on ionic strength c. NaCl electrolyte ($d = 4.7 \times 10^{-8}$ cm). Numbers on curves give Q_{wgt} in meq/g.

in which counterions in the diffuse part of the double layer are indicated by a subscript DL and counterions in the bulk solution have no subscript. The equilibrum constant or "selectivity coefficient" [149] for the above ion exchange reaction may be written [133]:

$$K_{Q^+/M^+} = \frac{\Gamma_{Q^+,DL}\cdot[M^+]}{[Q^+]\cdot\Gamma_{M^+,DL}} = \exp\left(-\frac{\overset{\circ}{\mu}_{Q^+,DL} - \overset{\circ}{\mu}_{M^+,DL}}{RT}\right) \qquad (43)$$

Here $\Gamma_{Q^+,DL}$ and $\Gamma_{M^+,DL}$ are the respective surface excesses (moles/cm^2) of Q^+ and M^+ in the diffuse part of the double layer, $[Q^+]$ and $[M^+]$ are the respective bulk solution concentrations (moles/L) and $\overset{\circ}{\mu}_{Q^+,DL}$ and $\overset{\circ}{\mu}_{M^+,DL}$ are the standard chemical potentials for the transfer of Q^+ and M^+ from bulk solution into the diffuse layer. Since both ions involved are univalent, ionic activity coefficients are assumed to have cancelled out of equation 43 [150].

The ion exchange contribution to chromatographic retention of a sample counterion Q^+ may be expressed as a distribution coefficient, which is the ratio of the concentration of Q^+ in the diffuse layer, $\Gamma_{Q^+,DL}$, to that in the bulk solution, $[Q^+]$. For symmetrical chromatographic peaks it is necessary that the distribution coefficient of Q^+ be invariant with changes in $[Q^+]$ [151]. It is apparent from equation 43 that this will occur if the number of moles of Q^+ added to the system is much smaller than: (a) the moles of ion exchange sites on the resin and (b) the number of moles of M^+, so that $\Gamma_{M^+,DL}$ and $[M^+]$ do not change significantly with sorption of small amounts of Q^+ (equation 43). Under these "trace conditions" of ion exchange [152], the total counterion surface excess, $\Gamma_{+,DL}$, and the total coion surface excess $\Gamma_{-,DL}$, can be approximated by $\Gamma_{M^+,DL}$ and $\Gamma_{Cl^-,DL}$, respectively. Introducing these approximations into the electroneutrality condition (equation 37) and letting α be the fraction of the surface charge density σ_o which is neutralized by a positive surface excess of counterions (see below), allows $\Gamma_{M^+,DL}$ to be expressed as:

$$\Gamma_{M^+,DL} = \frac{-\alpha.\sigma_o}{Z.F} \qquad (44)$$

Substituting for $\Gamma_{M^+,DL}$ in equation 43 from equation 44; noting that under trace conditions $[M^+]$ is equal to the ionic strength c; and multiplying $\Gamma_{Q^+,DL}$ by the specific surface area of the resin in cm^2/kg, $10^3 \cdot A_{sp}$, to give the concentration of sorbed Q^+ in units of moles per kilogram of resin, gives rise to the equation for the distribution coefficient of Q^+:

$$K_{Q^+,IEX} = \frac{10^3 \cdot A_{sp} \cdot \Gamma_{Q^+,DL}}{[Q^+]} = - \frac{10^3 \cdot A_{sp} \cdot \alpha \cdot \sigma_o \cdot K_{Q^+/M^+}}{Z \cdot F \cdot c} \qquad (45)$$

Equation 45 shows that the ion exchange distribution coefficient for Q^+ varies inversely with ionic strength c, is constant if c is kept constant, and increases linearly as the ion exchange equilibrium constant, K_{Q^+/M^+}, increases. Since $Z = 1$, and σ_o is negative for a cation exchanger, the distribution coefficient, $K_{Q^+,IEX}$ is always positive. This is in agreement with the behaviour predicted and observed for ion exchangers under trace conditions [149].

The quantity α in equation 45 was introduced because only this fraction of the surface charge density σ_o is neutralized by a positive excess of counterions in the diffuse layer, $\Gamma_{+,DL}$, the remaining fraction $(1-\alpha)$, of σ_o is neutralized by the absence of coions (negative surface excess), $\Gamma_{-,DL}$. If the ratio of these two surface excesses is denoted by β, then according to Grahame [137]:

$$\beta = \frac{-\Gamma_{+,DL}}{\Gamma_{-,DL}} = - \frac{\exp(-ZF\psi_{OHP}/2RT) - 1}{\exp(ZF\psi_{OHP}/2RT) - 1} \qquad (46)$$

and α can be calculated from:

$$\alpha = \frac{\Gamma_{+,DL}}{\Gamma_{+,DL} - \Gamma_{-,DL}} = \frac{\beta}{1 + \beta} \qquad (47)$$

When $Z\psi_{OHP} << 0.025$ V at 25°C, the Debye-Huckel approximation (i.e. $\exp(ZF\psi_{OHP}/2RT) \sim 1 + ZF\psi_{OHP}/2RT$) [142] may be used to simplify equation 46. Under these conditions, the surface charge density σ_O is balanced by equal contributions from $\Gamma_{+,DL}$ and $\Gamma_{-,DL}$, thus β=1 and α=0.5. On the other hand when $Z\psi_{OHP}$ becomes large (i.e. several tenths of a volt) the exclusion of coions from the diffuse layer is negligible compared to the surface excess of counterions. In this case β becomes a very large number with increasing ψ_{OHP} and the fraction α approaches unity. Since the Debye-Huckel approximation results in a considerably simpler treatment of the electrical double layer, it is often extended to the range $Z\psi_{OHP} < 0.025$ V, where it is still accurate to within 10% [112,132]. This condition (i.e. $Z\psi_{OHP} < 0.025$ V) is fulfilled for all experiments which have been performed, consequently for this work the value of α in equation 45 can be assumed to be equal to 0.5.

2.1.2.2 Surface Adsorption of a Counterion

The adsorption of a counterion Q^+ onto the charge surface of SXAD may be represented by the equilibrium:

$$Q^+ \rightleftarrows (Q^+)_{ADS} \qquad (48)$$

Since the electrical double layer, taken as a unit, must have a zero net electrical charge, this process must be accompanied by either the expulsion of a counterion from the diffuse layer or by the transfer of a coion into the diffuse layer from bulk solution:

$$(M^+)_{DL} \rightleftarrows M^+ \tag{49}$$

$$Cl^- \rightleftarrows (Cl^-)_{DL} \tag{50}$$

When Q^+ is a moderately large organic ion and M^+ is a well hydrated inorganic ion such as Na^+, reactions 49 and 50 can be assumed to be energetically equivalent [133]. Under these conditions the distribution coefficient for adsorption of Q^+ may be written in the form [133,137,150,153]:

$$K_{Q^+,ADS} = \frac{10^3 \cdot A_{sp} \cdot \Gamma_{Q^+,ADS}}{[Q^+]}$$

$$= \frac{A_{sp} \cdot \gamma_{Q^+} \cdot d}{\gamma_{Q^+,ADS}} \exp\left(- \frac{Z_+ F \psi_o + \mu^{\circ}_{Q^+,ADS}}{RT}\right) \tag{51}$$

where d is the thickness of the compact layer (cm), and $10^3 \cdot A_{sp} \cdot \Gamma_{Q^+,ADS}$ is concentration of Q^+ adsorbed onto the charge surface of SXAD in moles per kilogram of resin.

The numerator in the exponential term is the free energy (Joule/mole) required to transport Q^+ from bulk solution to the charge surface. Two contributions to this sorption energy are apparent: the electrical work required to transport Q^+ to the charge surface, $Z_+F\psi_O$, and the standard chemical potential for adsorption $\mu^{\circ}_{Q^+,ADS}$.

The value of the adsorption distribution coefficient for Q^+ is affected by $\gamma_{Q^+,ADS}$ and γ_{Q^+}, the respective activity coefficients for Q^+ on the surface of the resin and in bulk solution. The reference state for Q^+ in bulk solution is taken to be infinite dilution in pure water. This allows γ_{Q^+} to be calculated from the Debye-Huckel or some similar equation.

Initially, the logical choice for reference state for adsorbed Q^+ ions would appear to be infinite dilution of adsorbed Q^+ on the surface of the neutral (unsulfonated) XAD resin. With this choice of reference state, and using the treatment of Lucassen-Reynders [154], Stranahan and Deming [155] have given the following expression for the activity coefficient of Q^+ ion adsorbed on a surface bearing a mole fraction X_j of ionic charge sites:

$$\gamma_{Q^+,ADS} = \exp\left(\frac{\omega X_j}{RT}\right) \qquad (52)$$

where ω is the energy of interaction between the adsorbed Q^+ ion and the surrounding charge sites (both those on the surface and those in the adjacent solution phase). This expression is not applicable to the presently reported studies, for two reasons. First, the interaction energy term ω, includes all of the electrostatic contributions to the free energy of adsorption. However part of ω, the electrostatic energy required to transport a Q^+ ion from bulk solution to the charge surface, is explicitly treated in SGC theory. Consequently use of equation 52 in the present studies would result in the same electrostatic term being counted twice. Even if ω was redefined to include only those electrostatic effects not treated by SGC theory, the second problem of a lack of a satisfactory way of estimating the redefined ω term would remain. Therefore, in the present studies the reference state for adsorbed Q^+ ion was taken to be infinite dilution on the particular batch of SXAD resin being used, rather than on the surface of uncharged XAD. Then, by definition, at low $\Gamma_{Q^+,ADS}$ values, $\gamma_{Q^+,ADS} \equiv 1$. This definition of $\gamma_{Q^+,ADS}$ is equivalent to incorporating the ωX_j term of equation 52 into the chemical potential for adsorption $\mu^{\circ}_{Q^+,ADS}$. Since this additional term ωX_j will vary with the ion exchange capacity of the resin (i.e. X_j), values of $\mu^{\circ}_{Q^+,ADS}$ obtained on different capacity SXAD resins are not strictly comparable.

Evaluation of the adsorption contribution to the retention of a sample ion is greatly facilitated if the experiments can be performed under trace conditions. The criteria for trace conditions for adsorption are the same as those given for ion exchange: moles of Q^+ << moles of ion exchange sites on resin and moles of Q^+ << moles of M^+. Under these conditions $\gamma_{Q^+,ADS} = 1$, the surface charge density σ_o and the electrical potentials ψ_o and ψ_{OHP} are all independent of the small amount of Q^+ adsorbed.

2.1.2.3 Surface Adsorption of a Coion

An expression analogous to equation 51 can be written for the adsorption of a sample coion S^-:

$$K_{S^-,ADS} = \frac{10^3 \cdot A_{sp} \cdot \Gamma_{S^-,ADS}}{[S^-]}$$

$$= \frac{A_{sp} \cdot \gamma_{S^-} \cdot d}{\gamma_{S^-,ADS}} \exp\left(- \frac{Z_- F\psi_o + \overset{\circ}{\mu}_{S^-,ADS}}{RT}\right) \qquad (53)$$

In this case $Z_- = -1$, consequently the distribution coefficient $K_{S^-,ADS}$ decreases as the surface potential ψ_o becomes increasingly negative.

2.1.2.4 Exclusion of a Coion

Electroneutrality requires that the surface charge density σ_o be balanced by both a positive surface excess of counterions, $\Gamma_{+,DL}$, and a negative surface excess of coions $\Gamma_{-,DL}$. When a sample coion S^- is present in solution in addition to the electrolyte coion Cl^-, both S^- and Cl^- will make a contribution to $\Gamma_{-,DL}$. As in the case of ion exchange of counterions, we can speak of S^- and Cl^- competing for a position in the diffuse layer. The situation may be represented by the following "ion exchange" reaction:

$$S^- + (Cl^-)_{DL} \rightleftarrows (S^-)_{DL} + Cl^- \qquad (54)$$

The equilibrium constant for this reaction is given by:

$$K_{S^-/Cl^-} = \frac{\Gamma_{S^-,DL}\cdot[Cl^-]}{[S^-].\Gamma_{Cl^-,DL}} = \exp\left(-\frac{\overset{\circ}{\mu}_{S^-,DL} - \overset{\circ}{\mu}_{Cl^-,DL}}{RT}\right) \qquad (55)$$

Both $\Gamma_{S^-,DL}$ and $\Gamma_{Cl^-,DL}$ are negative, thus the equilibrium constant K_{S^-/Cl^-} is positive.

The distribution coefficient for S^- due to this process may be derived in a manner analogous to that used in the derivation of $K_{Q^+,IEX}$. The final equation, which applies under trace conditions (i.e. $\Gamma_{S^-,DL} << \Gamma_{Cl^-,DL}$ and $[S^-] << [Cl^-]$) is:

$$K_{S^-,EXC} = \frac{10^3 \cdot A_{sp} \cdot \Gamma_{S^-,DL}}{[S^-]} = \frac{10^3 \cdot A_{sp} \cdot (1-\alpha) \cdot \sigma_o \cdot K_{S^-/Cl^-}}{Z.F.c} \quad (56)$$

Here $(1-\alpha)$ is the fraction of the surface charge density σ_o which is neutralized by the exclusion of coions from the diffuse layer. For this work, the low potential approximation of $(1-\alpha) = 0.5$ is used (see p. 114). Since σ_o is negative for a cation exchanger, while K_{S^-/Cl^-} is positive and $Z = 1$, the distribution coefficient is less than or equal to zero. In other words, $10^3 \cdot A_{sp} \cdot \Gamma_{S^-,DL}/[S^-]$ is the distribution coefficient for the negative sorption of S^-. Since this process corresponds to the process of "coion exclusion" or "Donnan exclusion" in gel type ion exchangers [149], the distribution coefficient has been denoted by $K_{S^-,EXC}$.

2.1.3 Dependence of Sorption on Ionic Strength

2.1.3.1 Sorption of a Counterion

The distribution coefficient for sorption of a sample counterion, Q^+, on SXAD is equal to the sum of the distribution coefficients for the ion exchange and adsorption contributions:

$$K_{Q^+} = K_{Q^+,IEX} + K_{Q^+,ADS} \quad (57)$$

Substituting equations 45 and 51 into equation 57, incorporating the Debye-Huckel approximation for α (which is valid for $\psi_{OHP} < 0.025$ V; see p. 114) and noting that $\gamma_{Q^+,ADS} \equiv 1$ at trace conditions gives:

$$K_{Q^+} = -\frac{10^3 \cdot A_{sp} \cdot \sigma_o \cdot K_{Q^+/M^+}}{2.Z.F.c} + A_{sp} \cdot \gamma_{Q^+} \cdot d \cdot \exp\left(-\frac{Z_+ \cdot F \cdot \psi_o + \mathring{\mu}_{Q^+,ADS}}{R.T}\right) \qquad (58)$$

The ion exchange contribution to the retention of Q^+, given by the first term on the right side of equation 58, is proportional to c^{-1} and therefore decreases with increasing ionic strength. Since the surface potential ψ_o is a decreasing function of ionic strength (Figure 18, equation 41), the adsorption contribution to K_{Q^+} also diminishes as c increases. However, the functional dependence of the adsorption term on ionic strength is different from the c^{-1} dependence of the ion exchange term.

2.1.3.2 Sorption of a Coion

Retention of a sample coion S^- on SXAD is also described in terms of two processes: ion exclusion and surface adsorption. In this case the overall distribution coefficient for sorption of S^- is given by:

$$K_{S^-} = K_{S^-,EXC} + K_{S^-,ADS} \tag{59}$$

Substituting equations 53 and 56 into equation 59, using $\alpha = 0.5$ and $\gamma_{S^-,ADS} = 1$ as done previously for the sorption of a counterion, gives:

$$K_{S^-} = \frac{10^3 \cdot A_{sp} \cdot \sigma_o \cdot K_{S^-/Cl^-}}{2 \cdot Z \cdot F \cdot c}$$

$$+ A_{sp} \cdot \gamma_{S^-} \cdot d \cdot \exp\left(- \frac{Z_- \cdot F \cdot \psi_o + \mu^\circ_{S^-,ADS}}{R \cdot T}\right) \tag{60}$$

This equation is very similar in form to equation 58 for retention of a counterion on SXAD. However there are two important differences which arise because counterions are positively charged ($Z_+ = 1$) while coions are negatively charged ($Z_- = -1$). For a counterion, the ion exchange contribution to K_{Q^+} is always positive, and both the ion exchange and adsorption contributions to K_{Q^+} decrease with increasing ionic strength. In contrast, the ion exclusion contribution to the retention of a coion S^- (first term on right side of equation 60) is negative, and increasing the ionic strength leads to an increased sorption of S^- due to both the ion exclusion and surface adsorption terms.

2.2 Sorption Isotherms

In fundamental studies of the retention of chemical compounds on chromatographic sorbents, the experimental data are often presented in the form of a sorption isotherm (Figure 19), in which the concentration of the compound on the sorbent, C_s, is plotted versus its concentration in the mobile phase solution, C_m. At any point on the isotherm, the distribution coefficient K, is equal to the slope of the straight line which joins that point to the origin. Consequently, the sorption isotherm indicates the manner in which the distribution coefficient of a compound varies with its concentration in solution.

Sorption isotherms may have widely differing shapes depending upon the physiochemical mechanism responsible for retention [156], however in all cases the isotherms approach linearity when C_s and C_m become sufficiently small (Figure 19). The requirements for linear sorption isotherms are: (i) the concentration of the sample on/in the sorbent, C_s, is small compared to the concentration of "sorption sites" and (ii) the concentration of sample in the mobile phase, C_m, is small relative to the concentrations of all other components in the mobile phase. These, it will be recognized, are a more general statement of what was defined above as "trace

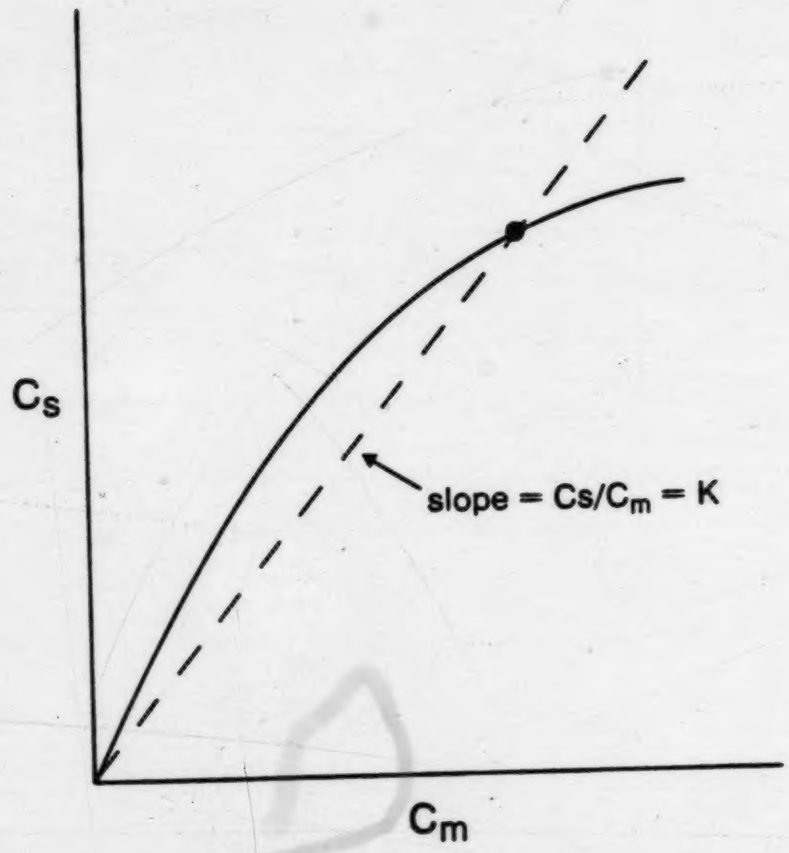

Figure 19. Hypothetical sorption isotherm (solid curve). Slope of dashed line is equal to the distribution coefficient, K, at a given point on the isotherm (see text).

conditions". Hence, under trace conditions the isotherm is linear and thus the distribution coefficient is a constant, unaffected by changes in C_m.

Techniques used for measuring sorption isotherms for gas chromatography have been extensively discussed by Huber and Gerritse [157] and by Conder and Young [158], and their extension to liquid chromatographic systems have been discussed by Dondi et al [159] and by de Jong et al [160]. Although terminology differs with different authors, these techniques may be broadly divided into two categories: equilibrium techniques and non-equilibrium techniques.

Among the non-equilibrium methods are those employing the maxima of eluted peaks (i.e. elution chromatography) [159-162] and those using the breakthrough profile [159]. Equilibrium methods include batch (static) equilibration [159-162], a column-recycle technique which is a type of batch equilibration [160,163], and column equilibration [159]. Only the most widely used of these techniques will be discussed here, namely: elution chromatography, batch equilibration and column equilibration.

In elution chromatography, the sample compound is introduced to the inlet of the sorbent-packed column as a narrow zone, which migrates along the column at a rate dependent on its distribution coefficient and the velocity of the mobile phase. Provided the concentration of the injected sample solution is low enough to ensure that the linear region of the sorption isotherm is involved, the distribution coefficient is given by the equation [164]:

$$K = \frac{V_R - V_m}{W_s} \tag{61}$$

where the "chromatographic retention volume", V_R, is the volume (L) of mobile phase required to transport the midpoint of the sample zone the length of the sorbent bed, V_m is the volume (L) of mobile phase contained within the packed column, and W_s is the weight (kg) of sorbent in the column.

When, as in the present investigation, it is necessary to measure distribution coefficients for strongly sorbed species at low concentrations, the elution method discussed above is unsuitable. The two principal problems are long retention times and finite detection limit. As the distribution coefficient increases, the migration velocity of the sample zone on the column decreases, resulting in a larger retention volume V_R and longer retention time. More strongly retained peaks are broader and shorter, and tend to become buried in the baseline detector noise. Use of higher sample concentrations to produce detectable peaks places the sample on the nonlinear portion of the isotherm.

The second commonly used technique for measuring isotherms is batch equilibration. In this technique a known weight of sorbent is added to a solution of the sample compound and the mixture is agitated at constant temperature until phase distribution equilibrium is achieved. The number of moles of sample compound sorbed, and thus the distribution coefficient, may be calculated from the concentration of the sample compound in solution before and after addition of the sorbent. Alternatively, the concentration of sample compound on the sorbent may be determined directly after filtering the solution from the sorbent and eluting the sample compound with an appropriate solvent. In contrast to elution chromatography, batch methods are not limited to measurement of relatively small (i.e. $K \lesssim 10^2$ L/kg) distribution coefficients in the linear region of the sorption isotherm.

A third technique for measuring sorption isotherms is the column equilibration method, which will be discussed now. Consider a chromatographic column containing a known weight of sorbent, W_s, through which a mobile phase solvent is being pumped. At a specified time, a second portion of the mobile phase solvent containing a known concentration of the sample compound, C_m, is directed through the column by switching a valve. If the compound is not retained on the sorbent, this step-change in sample concentration (referred to as the "front" of the sample zone) migrates through the column at the same speed as the solvent, emerging from the outlet after one column volume, V_m, of solution has been pumped through the column. However, if the compound is retained the sample molecules spend part of their time immobilized on the sorbent and the front of the sample zone emerges from the column outlet as a more or less diffuse, sigmoidal or distorted sigmoidal concentration step at some retention volume V_R (equation 61). A suitable detector monitoring the concentration of sample in the column effluent would display the "breakthrough curve" indicated diagrammatically by the solid curve in Figure 20. When the plateau of the breakthrough curve has been reached (e.g. point X, Figure 20) the concentration of sample entering the column (dashed line) is equal to the concentration of sample leaving the column. At this point, a known weight of sorbent, W_s, is at equilibrium with a solution containing a known concentration, C_m, of sample.

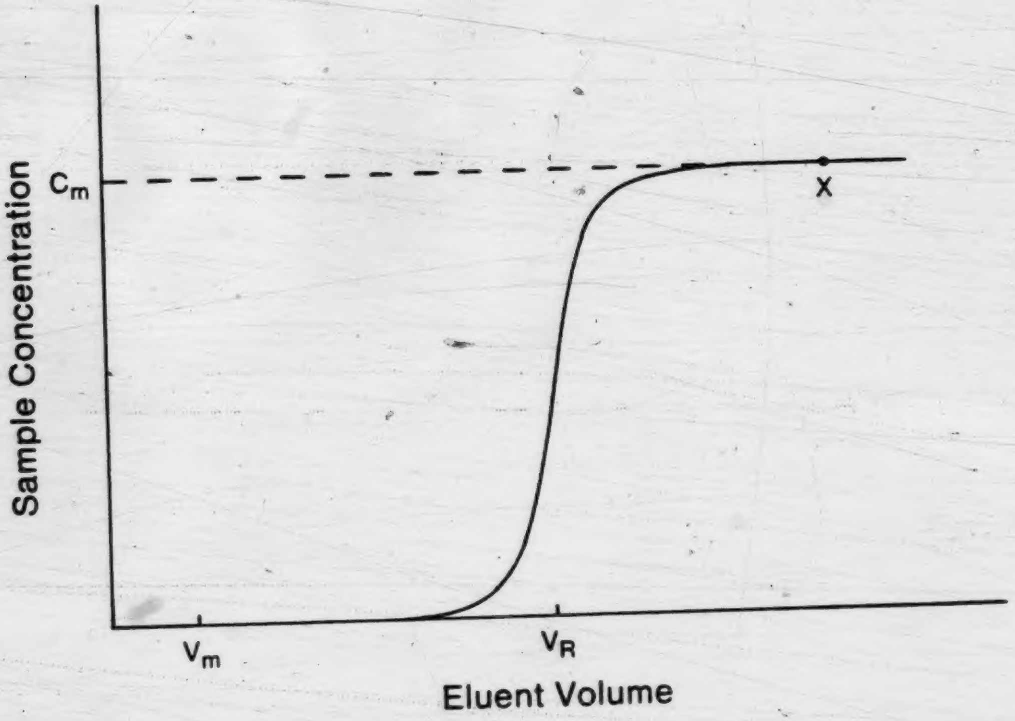

Figure 20. Breakthrough profile for sample component (solid curve), assuming the sorption isotherm is linear. Dashed line: concentration of sample component, C_m, entering column. See text for details.

Once the sorbent has been equilibrated with sample solution, the distribution coefficient may be determined as follows: The number of moles of sample retained on the sorbent is measured. This is equal to the total number of moles of sample contained in the column, n_T, minus the number of moles of sample in solution contained in the void spaces of the column, $C_m \cdot V_m$. Dividing this difference by the weight of sorbent in the column, W_s, gives the concentration of sample retained on the sorbent:

$$C_S = \frac{n_T - C_m \cdot V_m}{W_s} \tag{62}$$

The distribution coefficient can then be calculated as:

$$K = \frac{C_s}{C_m} \tag{63}$$

Determination of distribution coefficients using equations 62 and 63 requires measurement of the total number of moles of sample contained in the equilibrated column, n_T. Two ways of obtaining this information will be noted here. When the concentration of the sample component in the mobile phase is high enough, and the detection limit of the detector is low enough, then it is possible to accurately monitor the breakthrough profile of the eluting sample zone (Figure 20). In this case, the value of n_T can be determined from the total area between the breakthrough profile and the horizontal dashed line. This area may be calculated by multiplying the retention volume of the sample, V_R, by its mobile phase concentration, C_m [165]. Alternately, as in these studies, n_T may be determined by eluting the sample compound from the equilibrated column for subsequent quantitation. When it is necessary to measure distribution coefficients of strongly sorbed sample components at very low concentrations, this second approach has the advantage, in that compounds with large distribution coefficients are preconcentrated on the column prior to their elution and subsequent quantitative determination.

In Part II of this thesis a small pre-column was used in place of the loop of a sample injection valve in order to preconcentrate and purify trace amounts of sample component prior to chromatographic analysis. In the present work, a small pre-column packed with the sorbent of interest (i.e. SXAD) is used in a related chromatographic apparatus to measure sorption isotherms by the column equilibration method discussed in the preceeding paragraph. After the pre-column packing has been equilibrated with the sample solution, switching a valve allows the sorbed component to be eluted from the pre-column for on-line quantitation by high performance liquid chromatography. The value of n_T which is determined in this manner can be used to calculate the distribution coefficient for the sample component by using equations 62 and 63.

CHAPTER 3

EXPERIMENTAL

3.1 Procedure

Sorption isotherm and distribution coefficient data for three sample compounds (m-nitrobenzyltrimethylammonium chloride, acetaminophen and sodium p-nitrobenzenesulfonate), were obtained by the precolumn equilibration method described in Section 2.2. A schematic diagram of the chromatograph is given in Figure 21. The pre-column C_1 contains the sorbent (i.e. XAD or SXAD) to be characterized.

With the sample injection valve V_1 in the "load" position (solid lines connecting valve ports in Figure 21), an aqueous solution containing a known concentration, C_m, of the sample compound is pumped through column C_1 to waste using pump P_1. This process is continued until the sorbent is totally equilibrated with the aqueous sample solution (i.e. on the horizontal plateau after the breakthrough curve in Figure 20). During this time, pump P_2 delivers eluent through valve V_1, through a similar injection valve V_2 fitted with a 20 μL sample loop L, and

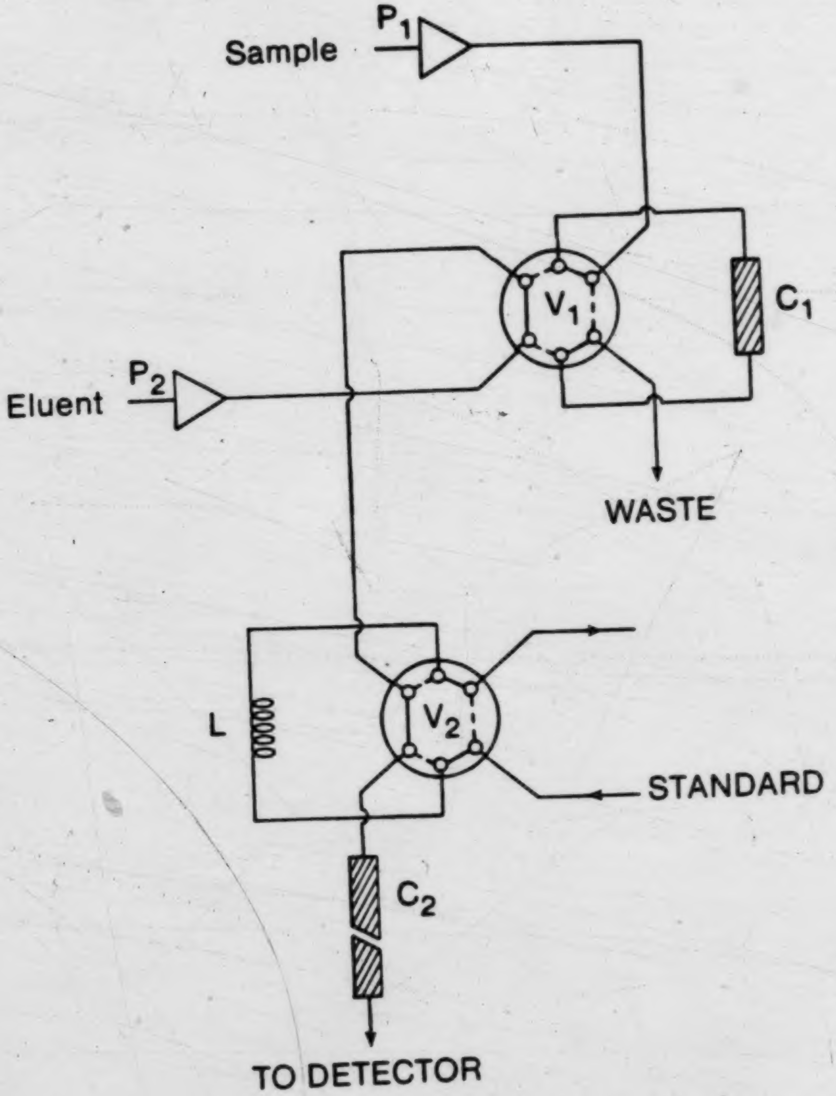

Sample
P1
V1
C1
P2
Eluent
WASTE
L
V2
STANDARD
C2
TO DETECTOR

Figure 21. Liquid chromatograph used to measure distribution coefficients by the column equilibration method.

then through the analytical column C_2 to a UV spectrophotometric detector.

Sometime after equilibration of the resin in C_1 with the sample solution, valve V_1 is switched to the "inject" position (dashed lines, Figure 21). This allows the eluent to backflush C_1, eluting the sorbed compound off the resin, through V_1 and V_2, onto the analytical column C_2 where it is separated from interfering peaks before reaching the detector. The number of moles of the sample compound eluted from C_1 (including that in sample solution contained in the tubing, in valve V_1 and in the column void spaces) is found by comparison of the area of the peak eluting from C_2 with a calibration plot of peak area vs moles of sample compound. The calibration plot is obtained in a separate experiment by injecting a series of standard solutions of the sample compound using the loop L of valve V_2.

The distribution coefficient of the sample compound between the sorbent and the mobile phase solution can be calculated from equations 62 and 63, once V_m (the sum of the void volume and extra column volume of resin-packed column C_1) has been measured (see below). The sorption isotherm is obtained by measuring the distribution coefficient at several different concentrations, C_m, of sample compound.

3.2 Apparatus

Two different designs for pre-column C_1 were used, according to the weight of resin required. In the first design, the 2.0 cm long × 0.40 cm i.d. column piece from a commercially available stainless steel guard column (part No. 84550, Waters Associates Inc., Milford, MA) was replaced with a locally machined part of either 0.20 or 0.30 cm bore. The resulting columns held either about 30 or 50 mg of resin. A second pre-column C_1, designed to hold up to 5 mg of resin, was made by a simple modification to a stainless steel inline filter assembly (part No. 7302, Rheodyne Inc., Cotati, CA). A schematic diagram of this pre-column is given in Figure 22. The resin was packed in a 0.35 cm long × 0.30 cm i.d. Teflon tube and held in place by two 0.10 cm thick frits. These frits were made by cutting the centre out of the 0.35 cm long × 0.30 cm i.d. porous stainless steel filter plug supplied with the filter assembly. In both cases, the pre-columns were dry-packed with the sorbent of interest.

Several different analytical columns were used for column C_2 depending on the sample compound studied (see Section 3.7).

Valves V_1 and V_2 were stainless steel sample injection valves (part No. 7010, Rheodyne Inc., Cotati,

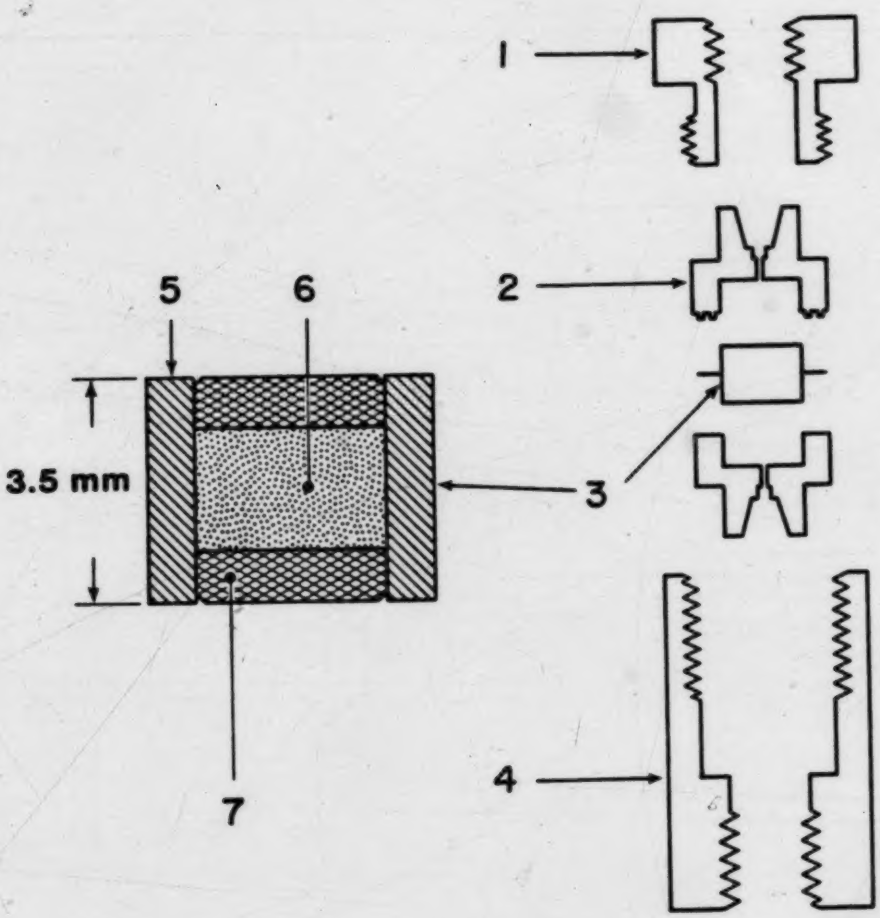

Figure 22. Pre-column for small weights of sorbent.

1. Cap
2. Filter end piece
3. Pre-column
4. Body of inline filter assembly
5. Teflon tube
6. Sorbent
7. Frit

CA). The standard rotor seals normally supplied with these valves are composed of Vespel, a polyimide polymer which can be hydrolyzed at alkaline pH. The carboxylate groups resulting from such hydrolysis may cause cationic sample compounds to sorb onto the surface of the rotor seals resulting in systematic errors in the measured distribution coeficient. Since part of this work (Section 3.9) required the injection of aqueous sodium hydroxide solutions from one of these valves, the Vespel rotor seals were replaced with chemically inert ones (part No. 7010-039-T) composed of Tefzel, a Teflon-graphite composite.

Pump P_1 was a Chromatronix Model CMP-2VK glass/Teflon reciprocating piston pump (Laboratory Data Control, Riviera Beach, FL). The high pressure chromatography pump of a Spectra Physics SP8000 liquid chromatograph (Spectra Physics, Santa Clara, CA) was used for P_2.

For distribution coefficient measurements, the sample peaks eluting from column C_2 were detected with a UV spectrophotometric detector (Model SF770, Schoeffel Instrument Corp., Westwood, NJ). The areas of the eluted peaks were measured with either an Autolab Minigrator (Spectra Physics) or a Vista 401 (Varian Instruments, Palo Alto, CA) electronic digital integrator. In both cases the chromatograms were recorded on a series 5000 Recordall potentiometric recorder (Fisher Scientific Co.). Sample valves V_1 and V_2 and the columns C_1 and C_2 were thermostatted at 25.0 ± 0.5°C for all studies.

3.3 Chemicals

m-Nitrobenzyltrimethylammonium chloride was used as received from Aldrich Chemical Co., Milwaukee, Wisconsin.

Acetaminophen (p-hydroxyacetanilide) was supplied by Matheson, Coleman and Bell (Norwood, Ohio) and was used without further purification. Its structure is:

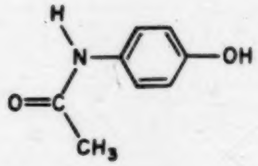

Sodium p-nitrobenzene sulfonate was prepared by neutralizing an aqueous solution of p-nitrobenzenesulfonic acid (practical grade, Eastman Kodak Co., Rochester, New York) with sodium hydroxide, followed by recrystallization from water.

Other chemicals used were all reagent grade.

3.4 Reagents and Solvents

Deuterium Oxide (D_2O; 99.8% D, Stohler Isotope Chemicals, Waltham, MA) used for void volume measurements was supplied by D.L. Rabenstein.

Double Distilled Water used to prepare all aqueous solutions has been described in Part I of this thesis.

Acetonitrile was supplied by Caledon Laboratories, Georgetown, Ontario and was distilled before use.

Sodium Hydroxide (2.2 Molar) was prepared by diluting $12._0$ mL of 1:1 (w/w) aqueous sodium hydroxide to 100 mL with freshly boiled and cooled double distilled water. This stock solution was standardized, following a 25-fold dilution, by titration of 0.6 g portions of primary standard potassium acid phthalate to a phenolphthalein end point, using a 50 mL buret. Standard sodium hydroxide solutions covering the concentration range 0.002 to 0.2 M were prepared from the stock solution by serial dilution. These solutions were used to calibrate the conductivity detector in the measurement of ion exchange capacity.

Perchloric Acid (0.5 Molar) used in the ion exchange capacity measurements to convert the ion exchange resin to the H^+-form, was prepared by diluting 42 mL of 70% perchloric acid to one liter with double distilled water.

3.5 Sample Solutions

Acetaminophen solutions covering the concentration range 1×10^{-2} M to 1×10^{-5} M, which were used in the sorption isotherm measurements were prepared by serial dilution of an aqueous 1.003×10^{-2} M stock solution. The final solutions which were used both as calibration standards (injected from sample loop L in Figure 21) and as sample solutions (pumped through the pre-column C_1) also contained 1.00×10^{-3} M sodium chloride.

m-Nitrobenzyltrimethylammonium chloride (NBTACl) solutions used in the sorption isotherm measurements were prepared by serial dilution of an aqueous 1.002×10^{-2} M stock solution. The calibration standards covered the concentration range 4×10^{-6} to 1×10^{-3} M. Sample solutions which were pumped through the pre-column C_1, on the otherhand, had NBTACl concentrations in the range 2×10^{-8} M to 4×10^{-6} M and contained in addition 0.100 M to 1.00 M of an inert electrolyte (LiCl, NaCl or KCl).

Sodium p-Nitrobenzenesulfonate (NBSNa) calibration standards were prepared by serial dilution from a 1.022×10^{-2} M stock solution to give solutions with concentrations in the range 2×10^{-5} M to 2×10^{-4} M. The sample solutions contained 1.022×10^{-5} M NBSNa and 0.100 M to 1.00 M sodium chloride.

3.6 Sorbent Preparation

The grinding, sieving and purification of the parent, nonionic resin Amberlite XAD-2 (XAD) has been described in Part II of this thesis. For the present studies, XAD resin of 44-63 μm particle size was used, both as a sorbent to characterize the pre-column equilibration technique and as the starting material for the preparation of SXAD. The unsulfonated, parent resin will subsequently be referred to as resin #1.

The surface sulfonated Amberlite XAD-2 resins (SXAD) used in this work had been previously prepared by May [166], using the following procedure. A slurry containing 5 g of 44-63 μm XAD resin in 30 mL of methanol was added with stirring to 200 mL of an aqueous sulfuric acid solution. The reaction time, temperature and concentration of sulfuric acid were varied to control the degree of sulfonation of the resin. For the three SXAD resins used in the present study, these parameters had the following values: resin #2; 10 min, 90°C and 70 vol % H_2SO_4; resin #3; 1.5 min, -10°C and 90 Vol % H_2SO_4; resin #4; 2.0 min, -10°C and 95 vol % H_2SO_4. The reaction mixture was poured into 2.5 L of water to quench the reaction, and the resin recovered by suction filtration. After washing with 5 L of water and 500 mL of methanol, the resin was dried at 60°C in a vacuum oven overnight. The resulting ion exchanger, SXAD, was weighed as the oven-dried resin in the H^+-form prior to packing into the pre-column C_1.

3.7 Mobile Phases and Columns

The type of analytical column C_2 that was used and the composition and flowrate of the eluent delivered by pump P_2 (Figure 21) depended on which sample compound (Acetaminophen, NBTACl, or NBSNa) was being studied.

In the measurement of the isotherm for the sorption of acetaminophen on XAD from aqueous solution, C_2 was a 25 cm × 0.46 cm i.d. stainless steel column commercially packed with 10 µm LiChrosorb RP-8 (part No. A1132-010, Spectra Physics). The eluent was $10._0$ vol% acetonitrile/$90._0$ vol % aqueous 0.011 M sodium perchlorate, mixed in situ by the three-way proportioning valve of the SP8000 chromatograph and delivered at a flowrate of 3.0 mL/min. For distribution coefficient measurements made at low acetaminophen concentrations (i.e. 1×10^{-5} M $< C_m < 1 \times 10^{-3}$ M) the UV spectrophotometric detector was set to 250 nm, the wavelength corresponding to an absorbance maximum for acetaminophen. At higher acetaminophen concentrations (i.e. 1×10^{-3} M $< C_m < 1 \times 10^{-2}$ M) it was necessary to change the detector wavelength to 280 nm so that the absorbances of the eluted peaks were low enough to give a linear calibration plot.

For the second sample compound studied, NBTACl, the initial work, using SXAD resin #3 and NaCl electrolyte, was conducted using for C_2 a 50 cm × 0.21 cm i.d. glass column dry-packed with a silica based pellicular strong cation exchanger (Vydac CX, cat. no. 401 SC, The Separations Group, Hesperia, CA). The eluent, $70._0$ vol % acetonitrile in aqueous 0.10 M acetic acid/0.10 M sodium acetate, was used at a flowrate (pump P_2) of 0.70 mL/min. The UV spectrophotometric detector was set at 258 nm.

In subsequent studies with NBTACl, using SXAD resin #3 with KCl and LiCl and SXAD resin #2 with NaCl electrolyte, column C_2 was changed to a 25 cm × 0.46 cm i.d. stainless steel column commercially packed with 10 μm Partisil SCX (cat. no. 4227-104, Whatman Chemical Separation Inc., Clifton, NJ), a silica based strong cation exchanger of much higher efficiency. Consequently the sample peaks eluted from C_2 were narrower and had higher maximum absorbances, allowing distribution coefficient measurements at low values of C_m to be more easily made. Three different eluents were used with this column: $60._0$ vol% acetonitrile in aqueous 0.075 M acetic acid/0.075 M sodium acetate; $60._0$ vol% acetonitrile in aqueous 0.120 M acetic acid/0.120 M lithium acetate; and $60._0$ vol% acetonitrile in aqueous 0.0875 M acetic acid/0.0875 M potassium acetate. The flowrate in each case was 3.0 mL/min.

Chromatographic retention data for the third compound, NBSNa, on SXAD was obtained using for C_2 a 50 cm × 0.21 cm i.d. glass column dry-packed with a pellicular strong anion exchanger (Vydac AX, cat no. 301, The Separations Group). The eluent, $35._0$ vol % acetonitrile in aqueous 0.050 M acetic acid/0.050 M sodium acetate was used at a flowrate of 0.80 mL/min. The detector wavelength was set to 271 nm.

3.8 Equipment Calibration

Calculation of distribution coefficients from equations 62 and 63 requires, in addition to C_m and W_s which are easily measured, accurate values for n_T and V_m. The total number of moles of sample eluted from the pre-column, n_T, is determined from a calibration plot constructed by injecting calibration standards from sample loop L. Consequently, it is necessary to accurately measure the internal volume of loop L. It is also necessary to determine V_m, the void volume of C_1, which includes both the column and extra column void volumes.

Measurement of the volume of the sample injection loop L was performed by first disconnecting the tubing from V_2 to C_2 at the column inlet (see Figure 21) and switching valves V_1 and V_2 to the "load" position (solid lines). With water being pumped by P_2 through V_1 and V_2, loop L was filled with an aqueous 3×10^{-2} $\underline{M}$ acetaminophen standard solution. Valve V_2 was then rotated to the "inject" position causing the contents of the sample loop to be flushed by the water eluent into a 10 mL volumetric flask which was subsequently diluted to volume with water. The absorbance of this solution at 243 nm was compared to a Beer's law plot of absorbance versus acetaminophen concentration, to yield the concentration and, hence, the moles of acetaminophen injected. The volume of the sample loop, calculated as moles of acetaminophen injected divided by the concentration of the solution used to fill the loop, along with its standard deviation [167] is 23.88 ± 0.02 μL. A Cary 118 spectrophotometer (Varian Instruments, Palo Alto, CA) was used for absorbance measurements.

The value of V_m for the XAD packed column C_1 was obtained by a somewhat different procedure. In this case, the LiChrosorb RP-8 analytical column used for C_2 was reconnected to valve V_2 and double distilled water, used as the eluent, was pumped by P_2 at a flowrate of 1.0

mL/min. Sodium nitrate was used as the sample compound in this case, because it is expected to be unretained (not sorbed) on XAD. An aqueous sodium nitrate solution of known concentration was pumped by P_1 through C_1 until the effluent and influent were of identical composition. Valve V_1 was switched to "inject" and the area of the nitrate peak was measured with the detector set at 250 nm. Moles of nitrate eluted from C_1 were obtained by comparison of peak area with a calibration curve prepared by injecting a series of aqueous sodium nitrate solutions of known concentration using the previously calibrated injection loop L. The void volume V_m was then calculated as moles of nitrate eluted divided by concentration of nitrate in the solution pumped by P_1. In order to determine whether sodium nitrate is, indeed, unretained on XAD (see below), the procedure was repeated by pumping through C_1 a series of sodium nitrate solutions covering the concentration range 0.001 - 0.1 M. The same value of void plus extra column volume of C_1 was obtained regardless of sodium nitrate concentration. The value and its standard deviation are 73.3 ± 1.5 μL.

When column C_1 was packed with SXAD resin, deuterium oxide (D_2O) was used as an unretained sample compound in place of sodium nitrate for the determination of V_m. Since D_2O does not absorb in the ultraviolet region of the spectrum, the spectrophotometric detector was replaced by a differential refractive index detector (Model R401, Waters Associates Inc., Milford, MA). The analytical column C_2, the eluent (double distilled water) and the eluent flowrate were as described previously for the determination of V_m of the XAD packed pre-column. A calibration plot of area of the eluted D_2O peak versus moles of D_2O was constructed by injecting, from the previously calibrated sample loop L, a series of aqueous standard solutions of D_2O having concentrations in the range 2.0 to 4.0 vol %. After equilibration of column C_1 with an aqueous D_2O solution of known concentration and elution with water, the value of V_m was determined with the help of the calibration plot in a manner similar to that described above for sodium nitrate with the XAD column.

3.9 Ion Exchange Capacity Measurements

The ion exchange capacities of the SXAD resins packed in column C_1 were determined by an on-line method using the chromatograph shown in Figure 23. A sufficient volume of 0.5 M aqueous perchloric acid was pumped (P_2, Figure 23) through column C_1 to convert the SXAD resin to the H^+-form. During this time pump P_1 directed water through valves V_1 and V_2 to an electrical conductivity monitor

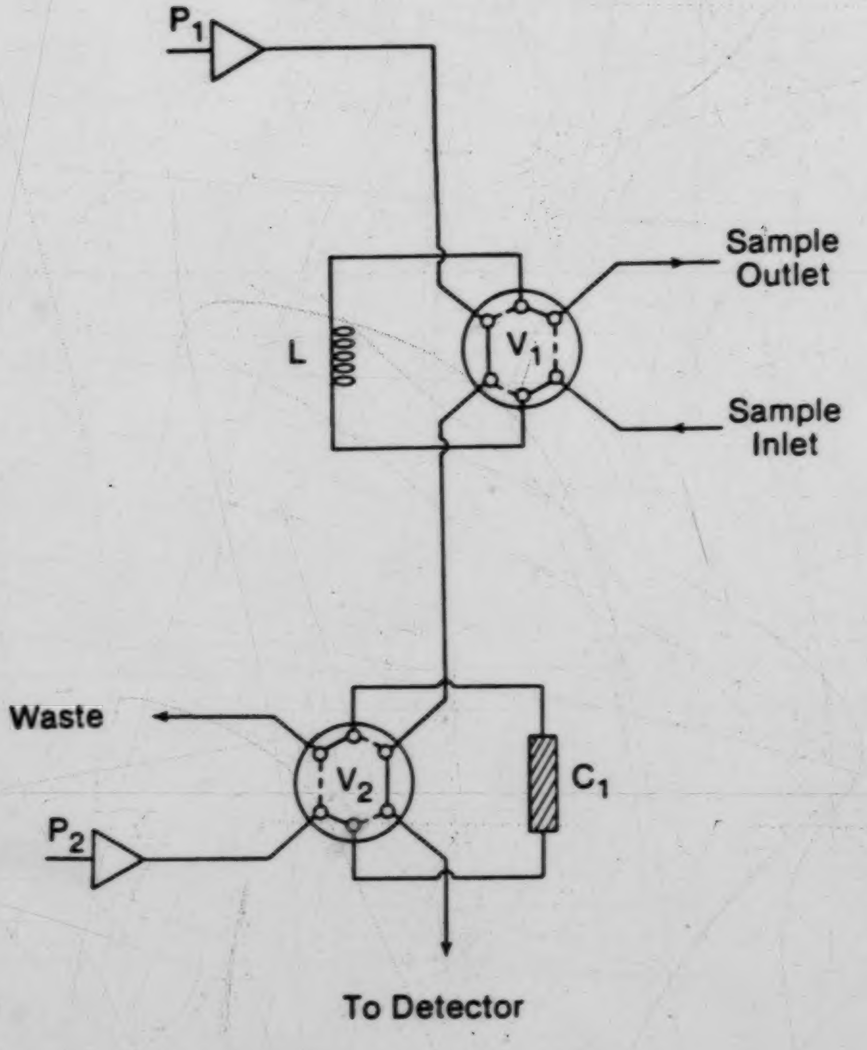
P_1
Sample Outlet
L
V_1
Sample Inlet
Waste
V_2
C_1
P_2
To Detector

Figure 23. Liquid chromatograph used to measure ion exchange capacities.

(Model 701, Laboratory Data Control) at a flowrate of 0.50 µL/min. When valve V_2 was switched to the "elute" mode (dotted lines, Figure 23), the perchloric acid in the void spaces of the column and connecting tubing was flushed through the detector to waste. Next, injection of an excess of a standard sodium hydroxide solution using valve V_1, caused quantitative conversion of the resin to the Na^+ form. The excess sodium hydroxide which eluted through the ion exchange bed in C_1 was measured by the conductivity detector.

The number of moles of excess sodium hydroxide was determined from a calibration plot constructed by injecting standard sodium hydroxide solutions of concentration in the range 0.003 M to 0.1 M, via the calibrated sample loop L of valve V_1. The ion exchange capacity of the resin is equal to the difference between the number of moles of sodium hydroxide injected onto the resin column and the moles of excess sodium hydroxide eluted, divided by the resin weight. The measurement was repeated for several concentrations of sodium hydroxide injected onto C_1.

CHAPTER 4

RESULTS AND DISCUSSION

The pre-column equilibration method described in Section 2.2 has been used to collect distribution coefficient data to test the proposed retention mechanism for counterions and coions on SXAD. Sections 4.1 and 4.2 of this Chapter describe the results of measurements of void volume and of ion exchange capacity for the SXAD resin packed column C_1. Section 4.3 gives the sorption isotherms that were measured to obtain the distribution coefficients under trace conditions. In Section 4.4 the experimental results are compared with the theoretical model of the sorption mechanism. Finally the relevance of these studies to "ion-pair" chromatography will be discussed in Section 4.5.

4.1 Void Volume Measurements

4.1.1 XAD Resin

Preliminary experiments to characterize the pre-column equilibration technique were performed using column C_1 packed with 0.0277 g of the unsulfonated, parent resin

XAD. The solute chosen for measurement of the void volume V_m, in this case, was sodium nitrate.

It is evident from equations 62 and 63 that the accuracy of the distribution coefficients measured by the pre-column equilibration technique is dependent upon the accuracy of the measured void volume, V_m. Therefore it is important to verify that sodium nitrate is, in fact, an unretained component. If NO_3^- ion experiences a slight retention or a slight exclusion due to low concentrations of ionic impurity sites on the XAD surface which give it a slight ion exchange capacity [131], then the distribution coefficient for NO_3^- and, consequently, the amount of it sorbed and the apparent V_m would vary with concentration. Such small amounts of impurity sites, if present, would be expected to vary from batch to batch of XAD, with resin treatment and with mobile phase pH.

The determination of V_m requires, as an initial step, that a sodium nitrate solution be pumped through pre-column C_1 until the concentration of nitrate in the pre-column effluent equals that entering the pre-column. Verification that breakthrough had occurred was obtained by pumping increasing volumes (i.e. $2._0$ mL, $5._0$ mL and $10._0$ mL) of the sodium nitrate solution through the XAD packed pre-column at a flowrate of 2 mL/min, before switching valve V_1 (Figure 21) to the inject position.

The area of the nitrate peak eluted from the analytical column C_2 was identical for all three volumes, indicating that less than 2 mL of sodium nitrate solution (or 1 minute) was needed to equilibrate the pre-column. To account for the possibility that sodium nitrate may have a non-zero distribution coefficient which could vary with sample concentration (i.e. a nonlinear sorption isotherm), this test was performed, with the same results, for the lowest concentration (1×10^{-3} $\underline{M}$) and the highest concentration (0.1 $\underline{M}$) sodium nitrate solutions used in the measurement of V_m. Since 2 mL of sodium nitrate solution was found to be sufficient to equilibrate the pre-column, 4 mL was used routinely to be on the safe side.

Values of V_m were measured using eleven sodium nitrate standard solutions, with concentrations in the range 1×10^{-3} $\underline{M}$ to 0.1 $\underline{M}$, to equilibrate the pre-column (see Table 6). The first question to be asked, whether or not sodium nitrate is a valid unretained solute, can be answered by determining if a significant correlation exists between the measured values of V_m and the sodium nitrate concentration. Linear regression analysis [168] of the data given in Table 6 gives a correlation coefficient, r, of 0.392. In order for the correlation coefficient to be statistically significant, the following condition [168] must be met:

TABLE 6

Measured Values of V_m for XAD Column[a] as a Function of Sodium Nitrate Concentration

$[NaNO_3]$ (moles/L)	V_m (µL)
1.00×10^{-3}	56.4[b]
2.00×10^{-3}	71.9
4.00×10^{-3}	73.1
6.00×10^{-3}	75.0
8.00×10^{-3}	72.1
1.00×10^{-2}	70.7
2.00×10^{-2}	72.8
4.00×10^{-2}	75.1
6.00×10^{-2}	74.4
8.00×10^{-2}	74.4
1.00×10^{-1}	73.9
	mean = 73.3 ± 1.5[c]

[a] Weight of XAD resin is 27.7 mg.

[b] Value rejected by Dixon's Q test.

[c] Standard deviation from mean of ten values.

$$\frac{r^2(n-2)}{1-r^2} > F_{\alpha,1,n-2} \qquad (63)$$

where n is the number of data values and $F_{\alpha,1,n-2}$ is the critical value of the F distribution for 1 and n-2 degrees of freedom at the confidence level α. Since the left hand side of inequality 63 is equal to 1.63 and $F_{0.95,1,9}$ is 5.12 there is no significant correlation between V_m and sodium nitrate concentration, at the 95% confidence level. Consequently sodium nitrate is a valid unretained solute to use in determining V_m for the XAD packed pre-column. The mean of the ten values of V_m obtained with sodium nitrate concentrations in the range 2×10^{-3} M to 0.1 M is the best estimate for V_m. The value at the lowest concentration, 1×10^{-3} M, was rejected on the basis of Dixon's Q test [169].

4.1.2 Low Capacity Cation Exchanger (SXAD)

Nitrate ion will be at least partially excluded from the intraparticle pores of SXAD resins with a significant electrical surface charge density σ_o (equation 56). Consequently it is necessary to use an alternate solute for measuring the value of V_m for SXAD packed pre-columns. Evidence from several investigators [170-172] has indicated that, for the hydrophobic alkyl-bonded-silica sorbents and for mobile phases containing a high percentage of water, deuterium oxide (D_2O) provides an accurate estimate of the column void volume. Since sulfonation of a small fraction of the surface phenyl groups of the styrene divinylbenzene copolymer does not significantly alter the hydrophobic character of the XAD surface (as evidenced by the nonwetting character of the SXAD resins in water), D_2O should also provide an accurate estimate of V_m for SXAD packed columns.

Values of V_m measured for pre-columns packed with two different SXAD resins are indicated in Table 7. For the SXAD resin of high ion exchange capacity (resin 3, Table 7) the value given is the mean of measurements obtained at four D_2O concentrations in the range 2.4-4.0 vol % D_2O. The value given for the lower capacity resin (resin 2, Table 7) is the mean of measurements obtained using D_2O concentrations of 0.5 vol % and 1.0 vol %. In neither case did the values obtained for V_m show a significant dependence on D_2O.

4.2 Ion Exchange Capacity Measurements on SXAD

Fritz and Story [173] have indicated that the methods presently used to prepare partially sulfonated ion exchange resins typically result in a heterogeneous distribution of ion exchange sites among individual resin beads. However in the studies described in this thesis,

TABLE 7

Characteristics of Resin-Packed Pre-Columns[a]

Resin Number	Weight of Resin (mg)	Void Volume (μL)	Ion Exchange Capacity (μeq/g)
1	27.7±0.1	73.3±1.5	--
2	49.93±0.02	135.0±0.5	9.7±0.2
3	3.44±0.02	26.07±0.05	54.5±1.2
4	4.27±0.02	--	>68.7±1.5[c]

[a] Uncertainties are standard deviations.

[b] Unsulfonated XAD resin.

[c] Value obtained at only one NaOH concentration. Resin not used in subsequent studies.

where the distributiion coefficients for strongly sorbed counterions are to be measured, it is desirable to use small quantities (i.e. 1-50 mg) of resin, in order to minimize the time required to equilibrate column C_1. Thus the possibility is introduced that, due to sampling errors [174], the small quantity of resin in the pre-column may have a significantly different ion exchange capacity than the entire batch of SXAD resin. Consequently it is desirable to measure the ion exchange capacity of the portion of SXAD resin in the pre-column used for the chromatographic retention measurements.

The procedure used for ion exchange capacity measurements (Section 3.9) involves four steps; conversion of the SXAD resin to the H^+-form; flushing the excess acid from the resin bed; injecting a known excess of sodium hydroxide into the resin column; and determination of the residual sodium hydroxide in the column effluent. A typical recorder tracing of conductivity detector response (i.e. specific conductance in units of reciprocal ohms per centimeter) during this sequence of events is shown in Figure 24. In this case, column C_1 contained 49.93 mg of SXAD (resin 2, Table 7). During the first two and a half minutes, five milliliters of 0.5 M perchloric acid is pumped through the pre-column to convert the SXAD resin to the H^+-form, while doubly distilled water is pumped

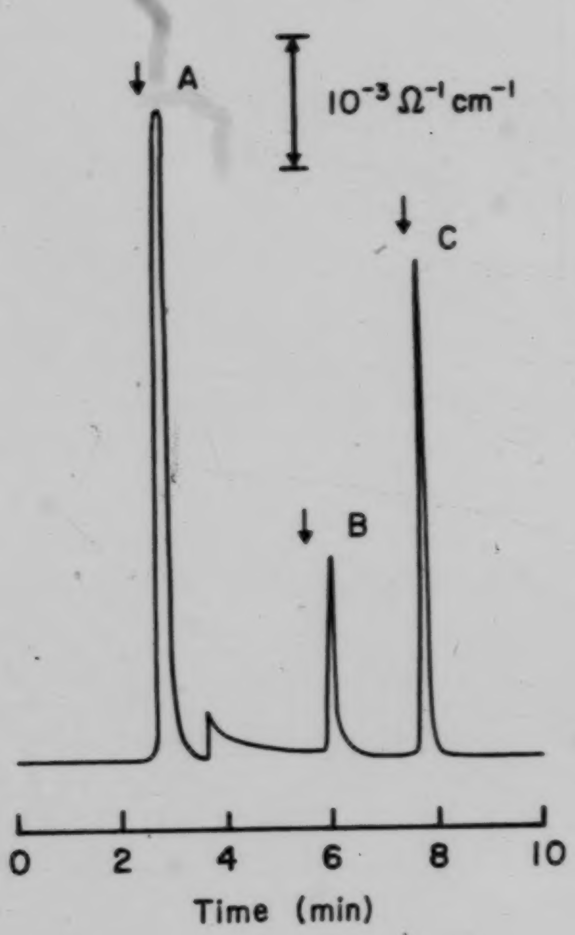

Figure 24. Specific conductance versus time profile observed during measurement of ion exchange capacity of SXAD resin. SXAD resin 2 (49.93 mg) in 2.0 cm × 0.30 cm i.d. column C_1. Excess $HClO_4$ (peak A), 3.962×10^{-4} M NaOH injected through C_1 (peak B) and 3.962×10^{-4} M NaOH standard (peak C).

through the conductivity detector. When valve V_2 (Figure 23) is switched to the "elute" position (dashed lines), the water eluent flushes the excess perchloric acid out of the pre-column and its associated tubing to the detector, giving rise to peak A of Figure 24. The discontinuity in the elution profile at about 3.5 minutes is due to a change in detector sensitivity. After about 5.5 minutes, when the excess perchloric acid has eluted from the pre-column, an aqueous NaOH standard solution is injected via loop L of valve V_1. As the injected plug of sodium hydroxide solution passes through the SXAD resin in C_1, provided sufficient time is allowed (see below), the exchange of hydronium ions in the resin for sodium ions in solution is driven quantitatively to completion by the subsequent neutralization of hydronium ions by hydroxide. The excess sodium hydroxide in the pre-column effluent passes through the detector, resulting in peak B of Figure 24. Calibration of the detector response is achieved by switching valve V_2 back to the "load" position and injecting aqueous sodium hydroxide standard solutions (e.g. peak C in Figure 24).

Several factors which affect the reliability of the measured ion exchange capacities were studied. First, it is important to verify that the 5 mL of 0.5 M perchloric acid pumped through column C_1 is sufficient to quantitatively convert the SXAD resin to the H^+-form. This was demonstrated by using $2._0$ mL, $5._0$ mL and $10._0$ mL of 0.5 M perchloric acid at a flowrate of $2._0$ mL/min to regenerate column C_1. For each of the SXAD resins studied, the measured ion exchange capacity was independent of the volume of acid used. The second factor, the volume of water required to flush the excess acid from C_1, was assumed to be sufficient when the conductivity detector response returned to baseline (e.g. at about 5.5 minutes in Figure 24).

The ion exchange capacities measured by this technique will be accurate only if the injected plug of sodium hydroxide solution has sufficient time, as it migrates through the pre-column, to reach equilibrium with the ion exchange resin. Two factors which can be expected to influence the attainment of ion exchange equilibrium are: (i) the flowrate of water, which determines the residence time of NaOH in the ion exchange bed and (ii) the concentration of injected sodium hydroxide solution which influences the rate of diffusion of sodium ions into and hydrogen ions out of the resin beads.

Table 8 illustrates the effects which these latter two experimental parameters have on the apparent ion exchange capacity (i.e. the capacity calculated assuming ion exchange equilibrium has been achieved). These data

TABLE 8

Effect of Flowrate of Water Eluent and Sodium Hydroxide Concentration on the Apparent Ion Exchange Capacity[a]

Flowrate (mL/min)	Concentration NaOH Injected (moles/L)	Ion Exchange Capacity (μeq/g)
0.20_0	0.0180	63.4±0.5[b]
0.50_0		62.4±0.2
1.0_0		61.7±0.2
		mean = 62.5±0.3[c]
0.20_0	0.0300	68.6±1.7
0.50_0		68.4±1.1
1.0_0		69.0±1.8
		mean = 68.7±1.5[c]

[a] Data for 4.27 mg of SXAD (resin 4) in pre-column.

[b] Uncertainties are standard deviations for three replicates.

[c] Pooled standard deviation.

were obtained using pre-column C_1 packed with 4.27 mg of the highest capacity SXAD resin prepared (resin 4, Table 7). Two points may be noted. First, as a larger excess of sodium hydroxide is injected onto the H^+-form SXAD resin in column C_1, the apparent ion exchange capacity of the resin increases, indicating a closer approach to ion exchange equilibrium. Second, provided a sufficiently large excess of sodium hydroxide has been injected, the value obtained for the ion exchange capacity does not show a significant dependence on the flowrate of water through C_1, at least for flowrates in the range 0.2-1.0 mL/min.

In measurements of the ion exchange capacity for SXAD resins 2 and 3 (Table 7) several concentrations of sodium hydroxide were injected onto C_1 using a water flowrate of 0.5 mL/min. Ion exchange equilibrium between the injected plug of NaOH and the H^+-form SXAD resin was assumed to have been attained provided the measured ion exchange capacity was invariant with increasing excess of injected sodium hydroxide solution.

Calculation of the ion exchange capacities for the two SXAD resins used in the chromatographic retention studies are given in Tables 9 and 10. The second and third columns on the left give the concentration and number of moles of sodium hydroxide injected onto the SXAD packed column C_1. The standard deviations given for the

TABLE 9

Calculation of Ion Exchange Capacity[a] for SXAD-packed Column C_1. SXAD Resin #2

Resin Number	Concentration NaOH Injected (moles/L)	Moles NaOH Injected × 10^6	Moles NaOH Eluted[b] × 10^6	Weight Resin (mg)	Ion Exchange Capacity (μeq/g)
2	3.962×10^{-2}	0.9461 ± 0.0015	0.439 ± 0.009	49.93 ± 0.02	10.2 ± 0.2
	5.924×10^{-2}	1.415 ± 0.002	0.940 ± 0.008	49.93 ± 0.02	9.5 ± 0.2
	7.924×10^{-2}	1.892 ± 0.003	1.416 ± 0.011	49.93 ± 0.02	9.5 ± 0.2
				mean	9.7 ± 0.2[c]

[a] Uncertainties are standard deviations.

[b] Uncertainties are standard deviations evaluated from calibration plot.

[c] Pooled Standard deviation (N = 12).

TABLE 10

Calculation of Ion Exchange Capacity for SXAD-packed Column C_1. SXAD Resin #3

Resin Number	Concentration NaOH Injected (moles/L)	Moles NaOH Injected × 10^6	Moles NaOH Eluted[b] × 10^6	Weight Resin (mg)	Ion Exchange Capacity (µeq/g)
3	1.210×10^{-2}	0.2889 ± 0.0005	0.1025 ± 0.0014	3.44 ± 0.02	54.2 ± 0.5
	1.814×10^{-2}	0.4332 ± 0.0007	0.2432 ± 0.0012	3.44 ± 0.02	55.2 ± 0.5
	2.419×10^{-2}	0.5776 ± 0.0009	0.3923 ± 0.0013	3.44 ± 0.02	53.9 ± 0.6
	4.108×10^{-2}	0.9810 ± 0.0016	0.796 ± 0.005	3.44 ± 0.02	53.8 ± 1.6
	6.162×10^{-2}	1.471 ± 0.0024	1.281 ± 0.006	3.44 ± 0.02	55.2 ± 1.9
				mean	54.5 ± 1.2[c]

[a] Uncertainties are standard deviations for 4 replicates.

[b] Uncertainties are standard deviations evaluated from calibration plot.

[c] Pooled standard deviation (N = 20).

moles NaOH injected were calculated from the relative uncertainties in the volume of loop L (0.9 ppt) and the concentration of NaOH (1.3 ppt). The number of moles of excess sodium hydroxide (fourth column, Tables 9 and 10) was determined by comparison of the area of the NaOH peak eluted from C_1 to a linear calibration plot constructed by switching valve V_2 to the "load" position (solid lines, Figure 23) and injecting a series of four sodium hydroxide standards via calibrated sample loop L. The standard deviations in moles NaOH eluted from C_1 were evaluated from the linear least squares fit to the calibration data [168]. Since the measured ion exchange capacities (sixth column, Tables 9 and 10) showed no significant dependence on the concentration of injected sodium hydroxide solution, the measurements can be assumed to have been made under equilibrium conditions. The mean and pooled standard deviation [62] of the ion exchange capacities of the two SXAD resins are given in Tables 9 and 10.

4.3 Sorption Isotherm Measurements

4.3.1 Acetaminophen on XAD Resin

An initial test to characterize the pre-column equilibration technique involved measuring the sorption isotherm of the neutral compound, acetaminophen, on the nonionic, parent resin XAD.

The first step in measuring the sorption isotherm of acetaminophen involves equilibration of the XAD resin contained in column C_1 with an aqueous acetaminophen standard solution. For both the lowest concentration (1 × 10^{-6} M) and the highest concentration (4 × 10^{-4} M) of acetaminophen standards pumped through C_1 at a flowrate of 2 mL/min, a volume of $2._0$ mL was found sufficient to reach this equilibrium state. Thus, a volume of 4 mL was used to equilibrate C_1 in the sorption isotherm measurements.

The sorption isotherm for acetaminophen on XAD resin in aqueous 1 × 10^{-3} M sodium chloride solution is given in Figure 25. Six data points were collected in the linear region of the sorption isotherm (i.e. $C_m < 1 \times 10^{-5}$ M, see Figure 25A). The least squares regression line drawn through these data points has a slope of 32.1 ± 0.6 L/kg and an ordinate intercept of $(-1.7 \pm 3.5) \times 10^{-6}$ moles/kg, where uncertainties are 95% confidence limits. The slope of this plot is equal to the distribution coefficient for acetaminophen at trace conditions. Figure 25B gives the portion of the sorption isotherm for acetaminophen at higher concentrations, where deviations from trace conditions for the sorption process become significant. The dashed line in Figure 25B is extrapolated from the data obtained in the linear region of the isotherm.

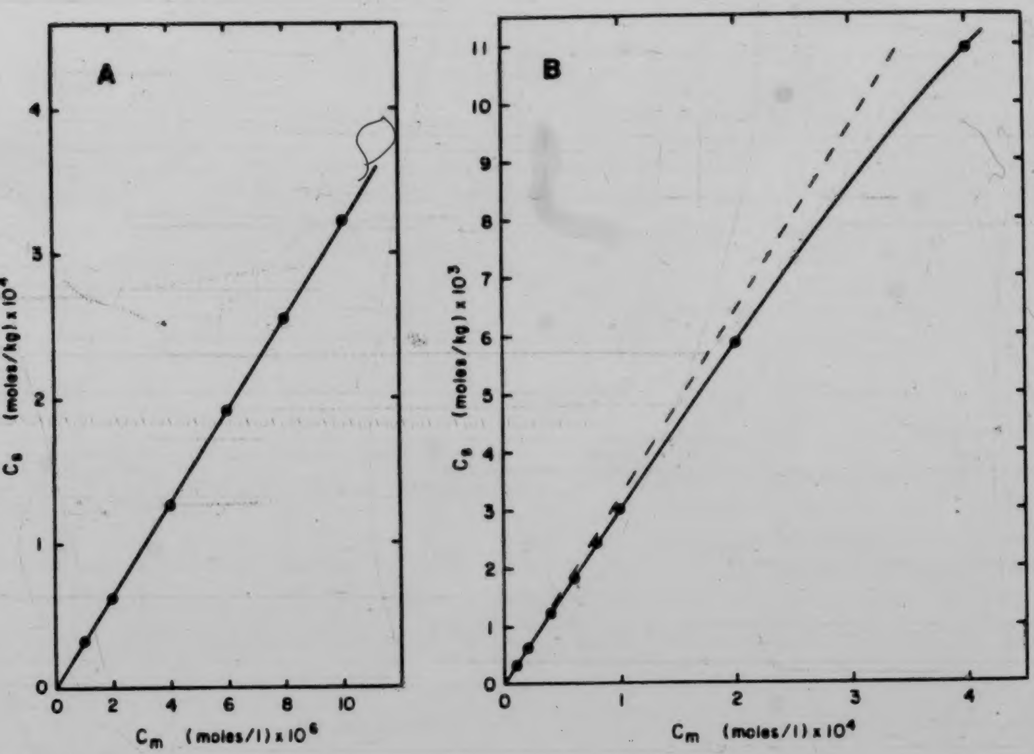

Figure 25. Isotherm for sorption of acetaminophen from aqueous 1.0×10^{-3} $\underline{M}$ sodium chloride onto XAD at 25.5°C. Curve A, low concentration region; Curve B, high concentration region.

The pre-column equilibration technique is evidently capable of yielding high precision distribution coefficient measurements at low sample concentrations with a 2 minute equilibration time and a 3 minute retention time for acetaminophen on the analytical column C_2, the time required to collect each point on the isotherm is about 3 minutes when replicates of the same sample solution are involved, since V_1 is switched back to the load position after only a few seconds and C_1 is equilibrating with one replicate while the previous one is migrating through C_2. When it is desired to change to a new sample solution with a different concentration, the clearance time for the CMP-2VK pump (about 7 minutes) must be added, to give a turn-around-time of about 10 minutes between different points on the isotherm.

4.3.2 Counterion on SXAD Resin

Most of the chromatographic retention data for the sample counterion, $NBTA^+$, were collected using column C_1 packed with 3.44 mg of the 0.0545 meq/g SXAD resin. Prior to measuring the sorption isotherms, experiments to determine the volume of $NBTA^+$ solution required to equilibrate column C_1 were performed as described previously (see p. 152) using 25 mL, 50 mL, 100 mL and 250 mL of 1×10^{-7} $\underline{M}$ $NBTA^+Cl^-$ solutions containing 0.1 $\underline{M}$ and 1.0 $\underline{M}$ sodium chloride. In the case of $NBTA^+$ solutions containing 0.1 and 1.0 M sodium chloride, the respective volumes used to equilibrate the SXAD column were 100 mL and 50 mL. The corresponding equilibration times for a flowrate of $2._0$ mL/min are 50 and 25 minutes.

Figure 26 presents isotherms for the sorption of $NBTA^+$ on the 54.5 µeq/g SXAD resin from aqueous 0.1 M and 1.0 M sodium chloride solutions. Deviations from sorption isotherm linearity can be expected to occur when the concentration of sorbed $NBTA^+$, C_s, becomes significant relative to the ion exchange capacity of the resin (see p. 123). For the sorption isotherm of $NBTA^+$ at ionic strength 0.1 M, this appears to occur when the sorbed $NBTA^+$ concentration increases above about one percent of the ion exchange capacity of the resin (indicated by the arrows on the ordinate axis at about 5×10^{-4} moles/kg). The isotherm for $NBTA^+$ in 1.0 M sodium chloride shows deviations from linearity at somewhat lower sample loadings.

Sorption data for $NBTA^+$ on this resin were collected at several ionic strengths (NaCl) in the range 0.1 to 1.0 M, using sample loadings (C_s) less than about one percent of the ion exchange capacity (Figure 27). The three data points on the $NBTA^+$ sorption isotherm at $C_s < 5 \times 10^{-4}$ moles/kg and ionic strength 0.1 M, show a good fit to the least squares regression line through the origin [168],

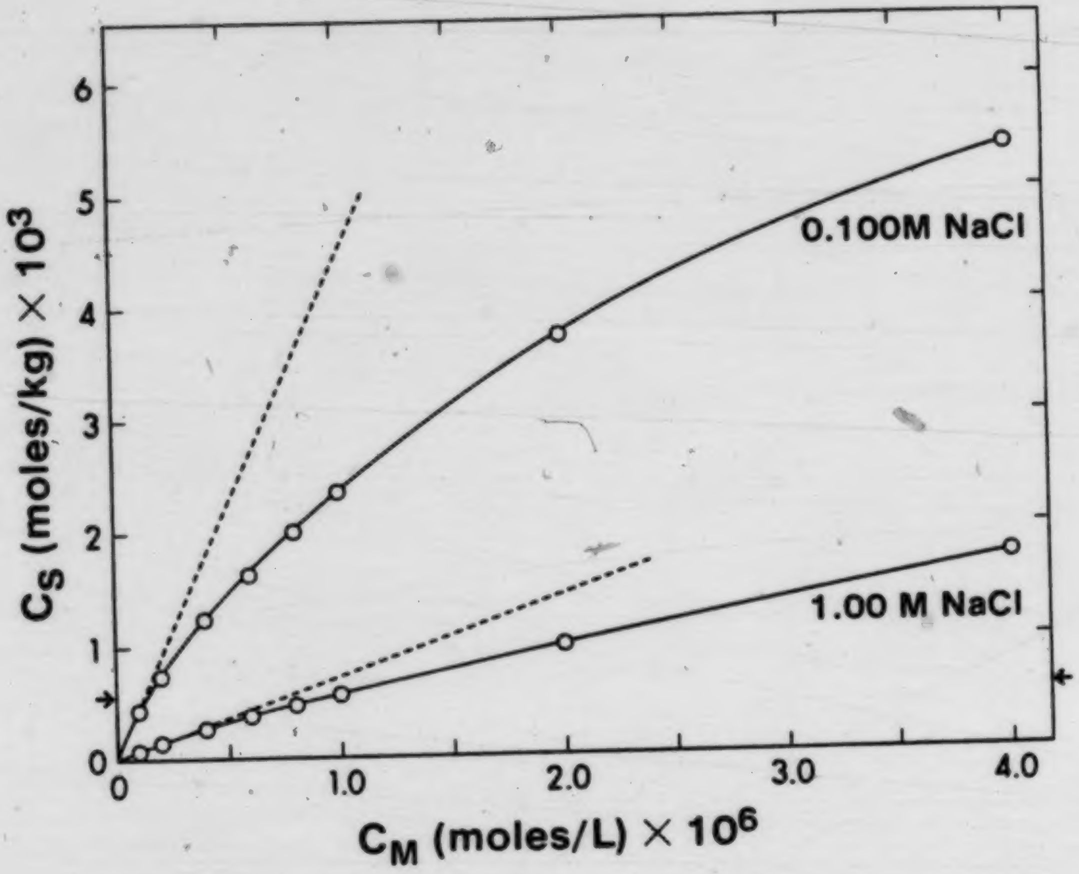

Figure 26. Isotherms for the sorption of $NBTA^+$ from aqueous NaCl solution onto 54.5 μeq/g SXAD resin (25.0°C). Dashed lines are extrapolated from linear region of isotherm.

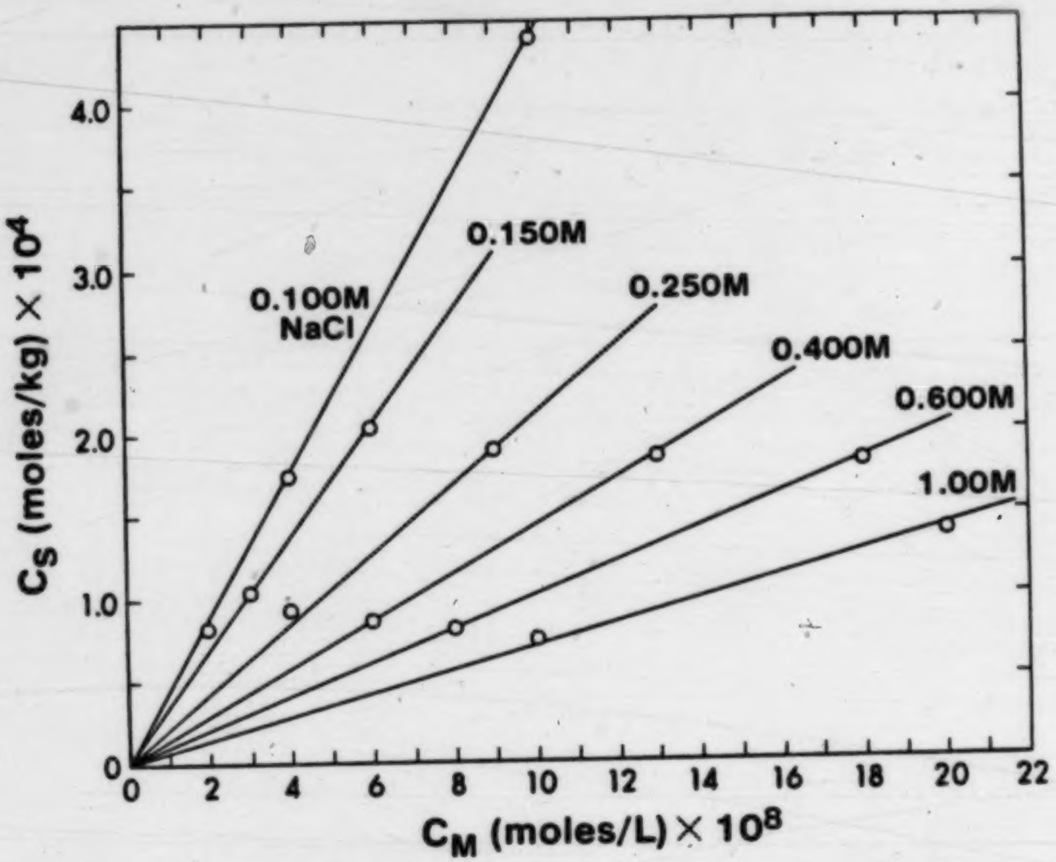

Figure 27. Linear region of isotherms for sorption of $NBTA^+$ from aqueous NaCl solutions onto 54.5 μeq/g SXAD resin (25.0°C). Numbers near lines give concentration of sodium chloride in the aqueous solution.

suggesting that trace conditions have been achieved. Sorption data for $NBTA^+$ at higher ionic strengths were collected at two sample loadings. In each case the distribution coefficient for $NBTA^+$ at trace conditions was evaluated from the slope of the least squares regression line through the origin.

In subsequent studies of the sorption of $NBTA^+$ on either the 54.5 μeq/g SXAD resin or the 9.7 μeq/g SXAD resin, sorption isotherms were not measured. Based upon the sorption data shown in Figures 26 and 27, the sorption isotherms were assumed to be linear below a sample loading of 1% of the ion exchange capacity. Thus the distribution coefficient data were obtained from measurements at a single sample loading such that $C_s < 0.01\ Q_{wgt}$. The volume of $NBTA^+Cl^-$ solution used to equilibrate the SXAD packed column was 100 mL for all the studies mentioned above.

4.3.3 Coion on SXAD Resin

The isotherm for the sorption of the coion NBS^- on SXAD resins will also approach linearity at a sufficiently low mobile phase sample concentration (see p. 123). As in the case of the sample counterion $NBTA^+$, a sample loading of one percent of the ion exchange capacity was taken to be sufficient to achieve trace conditions (i.e. linear region of isotherm). Equilibration of the 54.5 μeq/g SXAD resin in column C_1 required 10 mL of NBS^- solution.

4.4 Dependence of Sorption on Ionic Strength

4.4.1 Sorption of a Counterion on SXAD Resin

According to the physiochemical model proposed in Sections 2.1 and 2.2, the sorption of counterions on a low capacity cation exchanger such as SXAD, should be described by equation 58. In order to test this prediction, the ionic strength dependence of the distribution coefficient for sorption of the counterion $NBTA^+$ was measured (Section 4.3.2) using SXAD resins of two different ion exchange capacities (9.7 μeq/g and 54.5 μeq/g) and three different inert electrolytes (LiCl, NaCl and KCl). For each set of data (given in Figures 28-31 and Appendix II), the nonlinear least squares curve fitting program "KINET" [55] was used to calculate from equation 24 the values of the ion exchange equilibrium constant, K_{Q^+/M^+}, and the chemical potential for adsorption, $\mu^{\circ}_{Q^+,ADS}$, which best fit the experimentally observed distribution coefficient versus ionic strength data. The molar activity coefficient for $NBTA^+$, γ_{Q^+}, required in equation 58 was assumed to be equal to that for benzyltrimethylammonium ion and was calculated from the experimentally determined molal activity coefficients for this ion [175]. The value of d, the distance of closest approach of nonadsorbed counterions to the

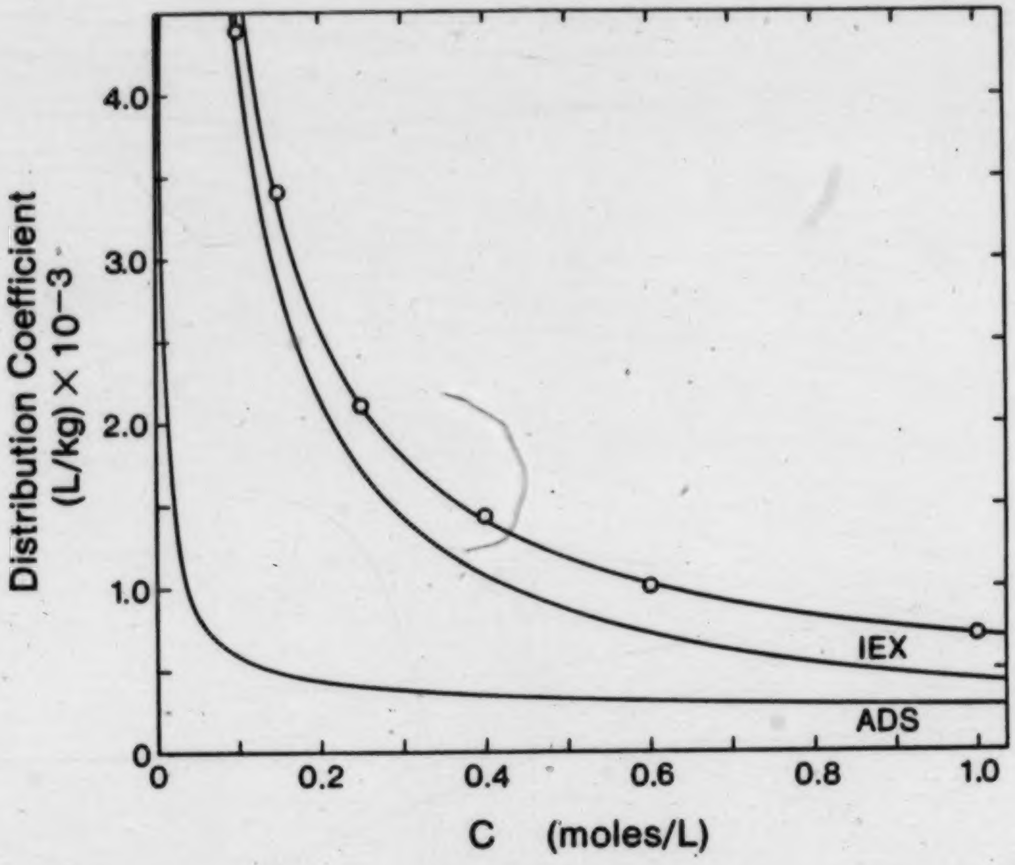

Figure 28. Distribution coefficient for the sorption of $NBTA^+$ on 54.5 µeq/g SXAD resin as a function of NaCl concentration.

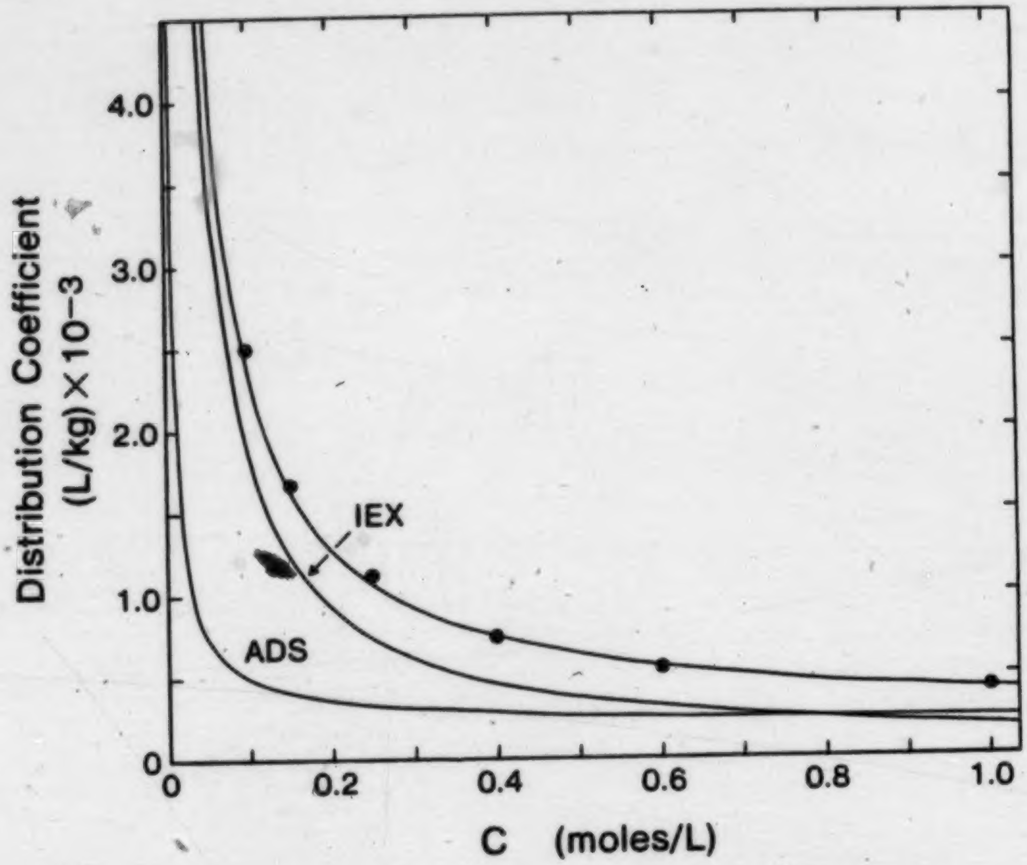

Figure 29. Distribution coefficient for the sorption of NBTA$^+$ on 54.5 μeq/g SXAD resin as a function of KCl concentration.

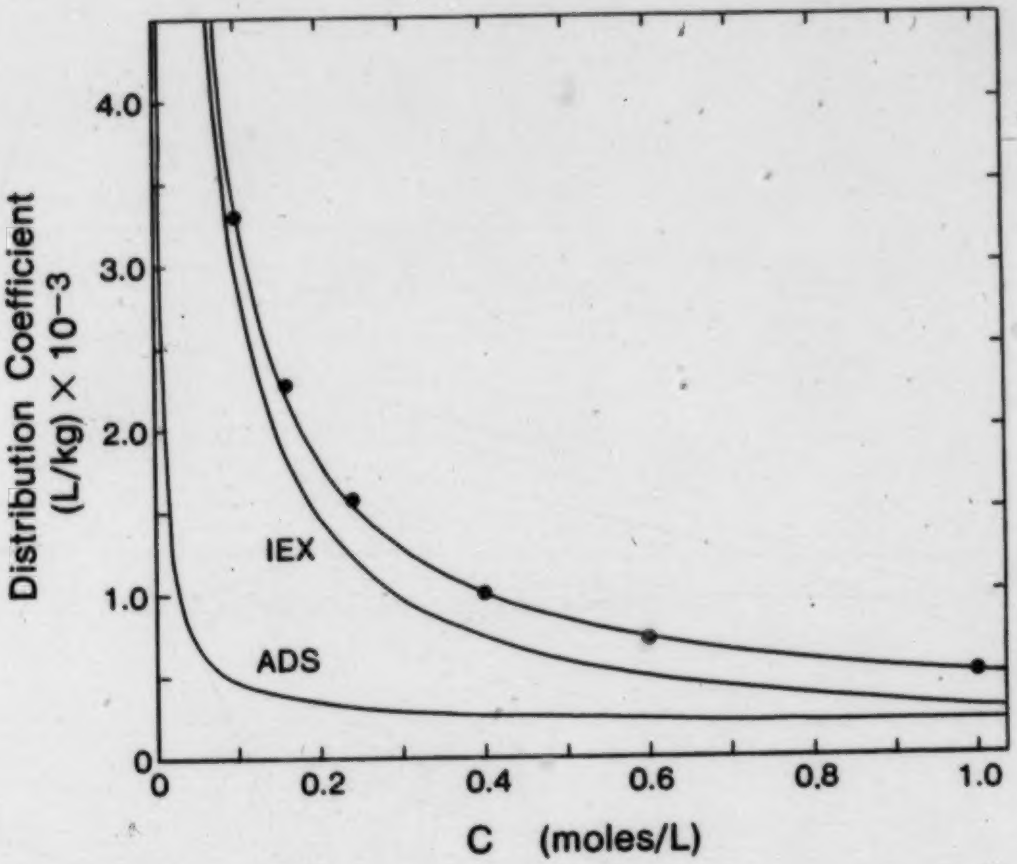

Figure 30. Distribution coefficient for the sorption of NBTA$^+$ on 54.5 μeq/g SXAD resin as a function of LiCl concentration.

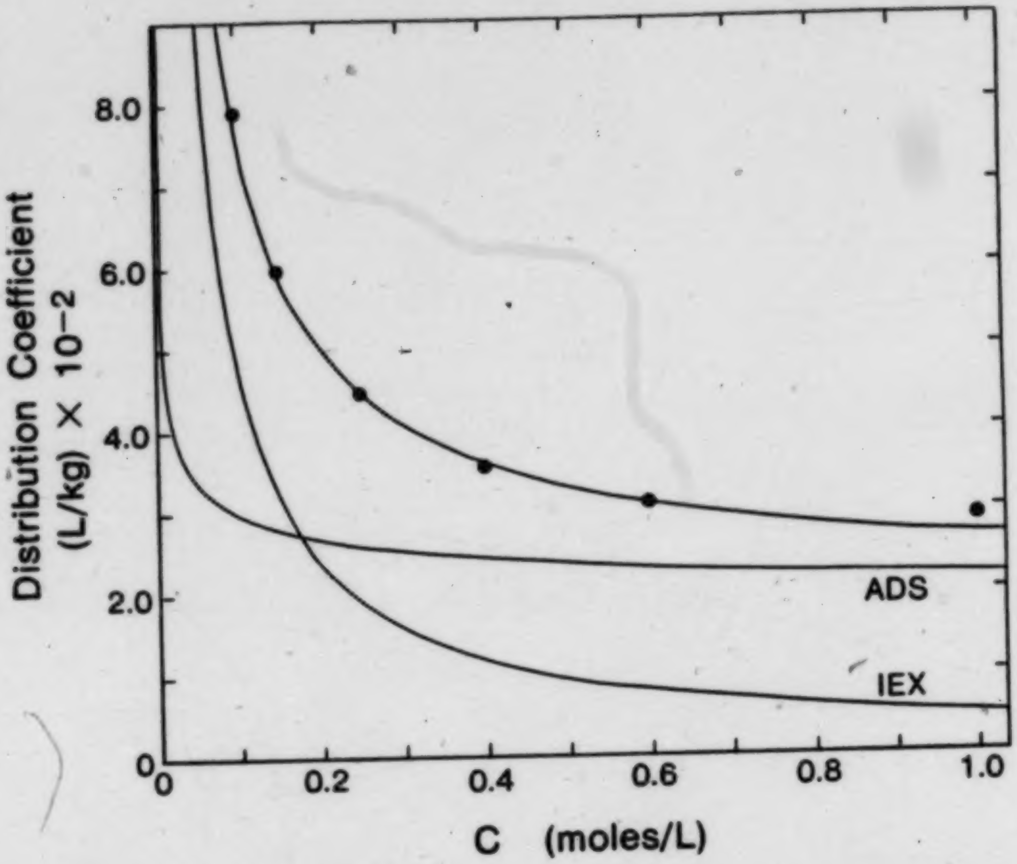

Figure 31. Distribution coefficient for the sorption of NBTA$^+$ on 9.7 μeq/g SXAD resin as a function of NaCl concentration.

hydrated ionic radius of the electrolyte counterion (d = 5.3×10^{-8} cm (Li^+), d = 4.7×10^{-8} cm (Na^+) or d = 3.9×10^{-8} cm (K^+)) [57].

A plot of the distribution coefficient for the sorption of $NBTA^+$ on the 54.5 μeq/g SXAD resin versus ionic strength (NaCl), is given in Figure 28. The upper curve is the least squares fit of equation 58 to the five experimental data points measured at ionic strengths from 0.15 M to 1.0 M. The point at c = 0.1 M, on the steeply rising part of the curve, was omitted in the curve fitting because its inclusion yielded poorer precision in the evaluated constants. The calculated values and standard deviations of K_{Q^+/Na^+} and $\overset{\circ}{\mu}_{Q^+,ADS}$ were $(1.58 \pm 0.04) \times 10^4$ and $(-1.88 \pm 0.04) \times 10^4$ Joule/mole. The ion exchange contribution to the retention of $NBTA^+$, given by the curve labelled "IEX", was calculated from equation 58 by substituting the measured value for K_{Q^+/Na^+} and setting the second term on the right side of equation 58 equal to zero. The curve labelled "ADS" which gives the adsorption contribution to K_{Q^+}, was calculated by inserting -1.88×10^4 Joule/mole for $\overset{\circ}{\mu}_{Q^+,ADS}$ in the second term on the right side of equation 58 and setting the first term to zero. The upper curve in Figure 28, which is equal to the sum of the curves for sorption of $NBTA^+$ due to adsorption and ion exchange, shows a close agreement with experimental data, lending support to the proposed retention model.

It is evident from Figure 28 that ion exchange is the principal mechanism responsible for the sorption of $NBTA^+$ on the 54.5 μeq/g SXAD resin from aqueous NaCl solutions. The adsorption contribution to K_{Q^+} becomes increasingly significant as the ionic strength is raised. Since the distribution coefficient for ion exchange of Q^+, $K_{Q^+,IEX}$, approaches zero at high ionic strength (equation 45) while the adsorption contribution, $K_{Q^+,ADS}$, approaches a finite limiting value (equation 51), the two curves will cross at a sufficiently high ionic strength. For a given counterion Q^+, the magnitude of $K_{Q^+,IEX}$ and $K_{Q^+,ADS}$ and hence, the location of the crossing point of the curves, is determined by four factors: (i) the ion exchange capacity of the SXAD resin (which determines σ_o (equation 32) and ψ_o (equation 41)); (ii) the type of electrolyte counterion (determines value of d in equation 58 and affects the magnitude of K_{Q^+/M^+}); (iii) the magnitudes of the ion exchange selectivity coefficient K_{Q^+/M^+} and (iv) the chemical potential $\overset{o}{\mu}_{Q^+,ADS}$.

Experiments similar to those summarized in Figure 28 were performed using K^+ and Li^+ in place of Na^+ and also using a lower capacity ion exchanger. These will be discussed below. The values obtained for K_{Q^+/M^+} and $\overset{o}{\mu}_{Q^+,ADS}$ are summarized in Table 11.

TABLE 11

Ion Exchange Equilibrium Constants and Standard Chemical Potentials of Adsorption for Q^+ on SXAD Resins[a]

Q^0_{wgt} (μeq/g)	M^+	K_{Q^+/M^+} $\times 10^{-3}$	$\mu^\circ_{Q^+,ADS}$ (Joule/mole) $\times 10^{-4}$
9.7 ± 0.2	Na^+	9.6 ± 0.4	-1.88 ± 0.04
54.5 ± 1.2	Na^+	15.8 ± 0.4	-1.79 ± 0.01
54.5 ± 1.2	Li^+	10.7 ± 0.2	-1.68 ± 0.01
54.5 ± 1.2	K^+	6.7 ± 0.2	-1.81 ± 0.01

[a] Uncertainties are standard deviations.

Figure 29 is a plot of the distribution coefficient for the sorption of NBTA$^+$ on the same SXAD resin from aqueous KCl solution. Comparison of the data points in Figures 28 and 29 indicates a significant decrease in the sorption of NBTA$^+$ from KCl solution relative to that observed from NaCl solution. The nonlinear least squares fit of equation 58 to the data points in Figure 29 (upper curve) resulted in the values of K_{Q^+/M^+} and $\mu^{\circ}_{Q^+,ADS}$ shown in Table 11. Note that the value of $\mu^{\circ}_{Q^+,ADS}$ obtained for adsorption of NBTA$^+$ from KCl solution is essentially identical to that observed using NaCl electrolyte. Consequently, the decreased sorption of Q^+ may be attributed to a decrease in $\mu^{\circ}_{M^+,DL}$ (equation 43), resulting presumably from the lower hydration energy of K^+ relative to Na^+.

The values of K_{Q^+/M^+} and $\mu^{\circ}_{Q^+,ADS}$ were substituted into equation 58 as described previously to calculate the ion exchange (curve labelled "IEX", Figure 29) and adsorption (curve "ADS") contributions to the sorption of NBTA$^+$. Although the values of $\mu^{\circ}_{Q^+,ADS}$ for NBTA$^+$ are identical in KCl and NaCl solution, at a given ionic strength, the distribution coefficient for adsorption of NBTA$^+$ from KCl solution is slightly lower than that observed using NaCl solution (compare the "ADS" curve in Figures 28 and 29). This results from the smaller hydrated ionic radius of K^+ ($d = 3.9 \times 10^{-8}$ cm) relative to that for Na^+ ($d = 4.7 \times 10^{-8}$ cm) (second term in equation 58).

The measurement of the ionic strength dependence of the sorption of $NBTA^+$ on the 54.5 μeq/g SXAD resin was repeated using aqueous LiCl electrolyte (Figure 30). In this case, the $NBTA^+$ ion was found to be less strongly sorbed by the SXAD resin from aqueous LiCl solution than it was from NaCl solution (Figure 28). The chemical potential for adsorption of $NBTA^+$ from LiCl solution is observed to have nearly the same value as that obtained using NaCl electrolyte (Table 11). Consequently, the decreased sorption of $NBTA^+$ in LiCl solution compared to NaCl solution can be attributed to the decrease in K_{Q^+/M^+}.

The lower selectivity coefficient observed for the exchange of $NBTA^+$ for Li^+ relative to that observed for the exchange of $NBTA^+$ for Na^+ (see Table 11), constitutes a reversal in the "normal" ion exchange selectivity sequence (i.e. the ion with the lower hydration energy (smallest hydrated radius) preferred by the ion exchanger) [149]. Selectivity reversals in ion exchange equilibria are not at all uncommon [176-178]. The work of previous investigators on microporous (gel type) ion exchangers has led to several hypotheses to explain selectivity reversals. Eisenman [176-177] and Reichenberg [178] have pointed to different relative contributions of hydration energies and electrostatic attractions for different types of exchange sites. Diamond and others [179-181] have noted the influence of counterions and fixed charge sites on the hydrogen bonded structure of water in the exchanger. Elucidation of the reasons for the observed "reversed" selectivity sequence in the present case would require further work which is beyond the scope of the present thesis. However, one point to consider in this connection is the fact that SXAD has a largely hydrophobic surface which tends to promote the formation of hydrogen-bonded water structure in its vicinity [144,182]. Consequently it is not unreasonable to suspect that the selectivity sequence observed on SXAD for the exchange of a large poorly-hydrated organic ion for an alkali metal ion might differ from that observed on highly sulfonated gel type exchangers.

The salient point concerning the studies summarized in Figures 28 through 30, and in Figure 31, is the fact that there is good agreement between the experimental data points and the theoretical curve predicted by equation 58. This stands as evidence in support of the ion exchange/surface adsorption model for the sorption of counterions on a low capacity cation exchanger.

According to the proposed dual retention mechanism the ion exchange capacity Q_{wgt}, should influence both the adsorption contribution (through σ_o and ψ_o, equations 32, 41 and second term in equation 58) and the ion exchange contribution (σ_o, equation 32 and first term in equation 58) to the sorption of a counterion Q^+. This effect is illustrated in Figure 31 which is a plot of K_{Q^+} for the sorption of NBTA$^+$ from aqueous NaCl solution onto the lower capacity 9.7 µeq/g SXAD resin (resin 2, Table 9). Note that the scale on the ordinate axis has been expanded relative to that in Figures 28-30. The parameters K_{Q^+/M^+} and $\overset{\circ}{\mu}_{Q^+,ADS}$ have been evaluated by fitting equation 58 to the five data points obtained at ionic strengths from 0.1 M to 0.6 M. The data point at c = 1.0 M NaCl was omitted since its inclusion led to poorer precision in the fitted constants. The fitted values for K_{Q^+/M^+} and $\overset{\circ}{\mu}_{Q^+,ADS}$ (Table 11) were used to calculate the individual contributions to K_{Q^+} from ion exchange ("IEX" curve, Figure 31) and adsorption ("ADS" curve). Although a quantitative comparison of the values of $\overset{\circ}{\mu}_{Q^+,ADS}$ and K_{Q^+/M^+} obtained for the counterions NBTA$^+$ and Na$^+$ on the two SXAD resins of different capacities is not possible because of the use of different thermodynamic reference states for the two resins (see p. 116), comparison of Figure 30 to Figure 28 indicates that while the ion exchange capacity of SXAD has decreased about 6-fold, the adsorption contribution to K_{Q^+} has decreased only slightly. Consequently, the decreased sorption of $NBTA^+$ observed for the lower capacity resin is almost completely due to the ion exchange process.

4.4.2 Sorption of a Coion on SXAD Resin

Figure 32 presents the experimental data obtained for sorption of the coion NBS^- on the 54.5 μeq/g SXAD resin, from aqueous NaCl solutions of various ionic strength. The sorption of NBS^- on SXAD increases with increasing c, in qualitative agreement with the predictions of the proposed model. However, equation 60 does not give a quantitative explanation for the experimentally observed sorption data for NBS^- on SXAD.

Afrashethfar and Cantwell [132] in testing an analogous model for the sorption of organic ions on a low capacity surface quaternized XAD resin (QXAD) also observed that while sorption of a counterion (NBS^-) on the anion exchanger QXAD could be quantitatively described by the model, the sorption behaviour of a coion ($NBTA^+$) showed significant deviations from theory. Ion pair formation between $NBTA^+$ and Cl^- in the aqueous solution was suggested as a possible source of this discrepency. However, in the present case, ion pair formation between NBS^- and the well hydrated Na^+ ion is not likely to occur

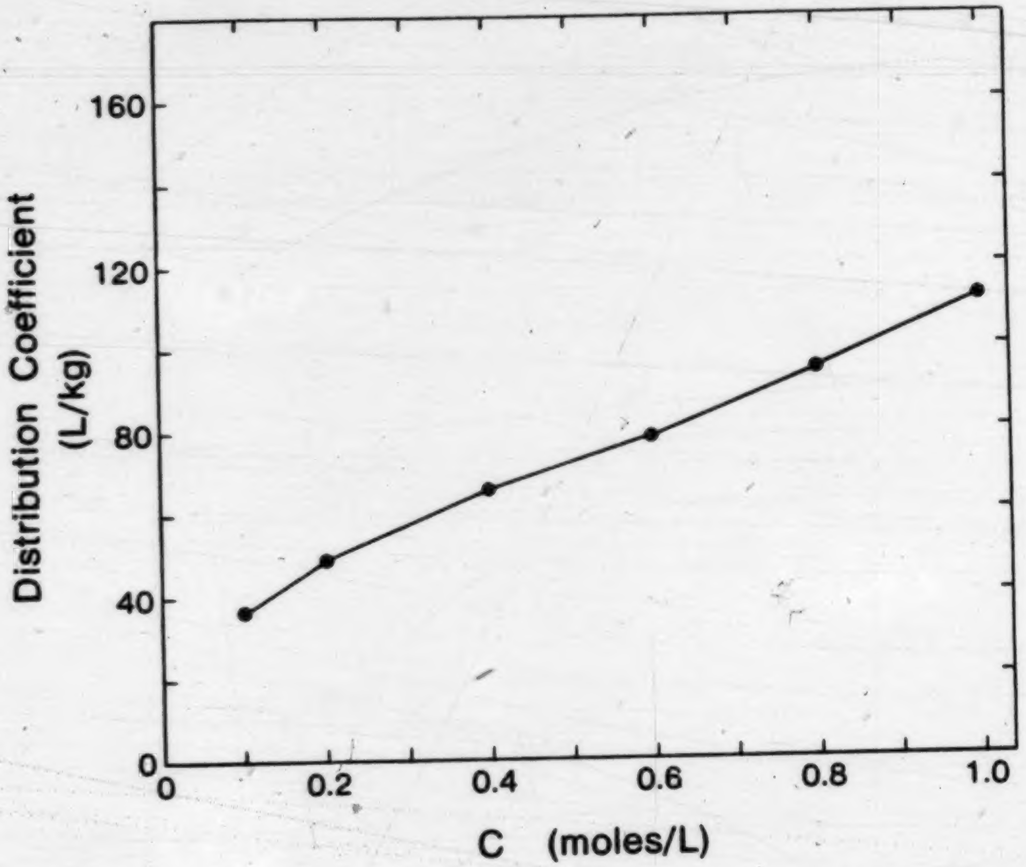

Figure 32. Distribution coefficient for the sorption of NBS^- on 54.5 μeq/g SXAD resin as a function of NaCl concentration.

[183]. Further experimental work will be required to understand the reason for this deviation from theory.

4.5 Relevance to Ion-Pair Chromatography

Over the last seven or eight years, the column packings (sorbents), which have become most popular with practitioners of high performance liquid chromatography (HPLC) are the chemically bonded alkyl-silica reversed phase sorbents [184,185]. Typically such packings are composed of 5- or 10 μm diameter, totally porous particles of silica gel onto the surface of which have been covalently bound alkylsilyl groups. Reaction of an alkyl dimethylchlorosilane for example, with surface silanol groups on the silica gel produces a siloxane bond between the silica surface and the alkyl chain (typically octyl or octadecyl). In a simplistic view, the chemically bonded organic phase can be considered equivalent to an adsorbed monolayer of the nonpolar octane or octadecane.

While chemically bonded reversed-phase sorbents show excellent retention of nonionic sample species, they typically retain ionic sample species much less strongly. However, the retention of ionic sample species on such sorbents can be greatly increased if an "ion-pairing" reagent is added to the mobile phase [186-189]. An "ion-pairing" reagent is usually a salt composed of a large organic cation or anion with a small inorganic anion or cation. If the sample ion to be retained is a cation then the "ion-pairing" reagent to be used contains a large anionic pairing ion (e.g. sodium hexadecanesulfonate), while an anionic sample requires a cationic "ion pairing" reagent (e.g. cetyltrimethylammonium chloride).

Although "ion-pairing" techniques on the chemically bonded reversed-phase sorbents have proved very successful and have become popular over the last five years [186-189], a great deal of research during this time has failed to produce a model for the physico-chemical retention mechanism which has met with anything near universal acceptance. Briefly, there are three leading models, each with its school of adherents. The "ion-pair model" assumes that an ion-pair formed in the mobile phase between the sample ion and the oppositely charged pairing ion partitions into the pseudo-liquid nonpolar bonded phase [190-192]. The physico-chemical aspects of this process are described in terms of "solvophobic interactions".

A second popular model proposes that the pairing ion from the reagent is sorbed by the chromatographic packing to produce a "dynamic ion exchanger" [163,193-197]. For example, the reagent sodium hexadecanesulfonate converts the sorbent into a dynamic cation exchanger because hexadecanesulfonate ions are sorbed and sodium ions can be exchanged for sample cations in the mobile phase.

The third model, the "ion interaction model", appeared in the literature [198,199] at the same time as did the paper by Puon and Cantwell [112] proposing the SGC model for ionic adsorption onto neutral adsorbents. In the ion interaction model the pairing ion is sorbed to the chromatographic packing in much the same way that it is in the dynamic ion exchange model, to produce a "primary ion layer". The other ion of the reagent (e.g. Na^+ or Cl^-) remains in a "secondary layer" outside the primary ion layer. Sorption of a sample ion from the mobile phase occurs because of coulombic attraction into the oppositely charged primary ion layer. Then another pairing ion from the mobile phase is sorbed to replace the one "neutralized" by the sorption of the sample ion.

While the presently reported research on low capacity cation exchangers and the two previous studies of ionic adsorption onto a neutral sorbent [112] and a low capacity anion exchanger [132] have not dealt with the chemically bonded reversed-phase sorbents, nevertheless, the fundamental principles elucidated in this work have some relevance to "ion-pair" chromatography on the chemically bonded reversed-phase sorbents. With this in mind, the following tentative observations can be made. The evidence in support of the view that the "ion-pairing reagent" is sorbed from the mobile phase onto the chromatographic packing in the absence of a sample ion is now overwhelming [197]. Thus it is very likely that an electrical double layer is present at the sorbent-solution interface. Deelder [200] has shown the utility of SGC theory in describing the retention of sample ions on chemically bonded reversed-phase sorbents, in the presence of "ion-pairing reagents". It is important to remember that when the surface charge density (σ_O) arises from sorption of an ion from the mobile phase, then not only ψ_O, but also σ_O will depend on ionic strength [112]. Assuming that the dual retention mechanism (ion exchange/surface adsorption) has some relevance to "ion-pair" chromatography on the chemically bonded reversed-phase sorbents, then this means that the ion exchange capacity depends not only on the concentration of "ion-pairing reagent" in the mobile phase but also on the overall ionic strength of the mobile phase.

A second point to come out of the present work is that models accounting for the adsorption of ions onto a charged surface should be expressed in terms of electrical potential (ψ_O) and not in terms of charge density. It has been shown that the distribution coefficient for the adsorption of a sample ion is a function of ψ_O (equation

51) and also that a given surface charge density can give rise to many different values for the surface potential depending on the ionic strength of the mobile phase (Figure 18).

A third important point to consider, based on the present work, concerns the "ion interaction model". This model postulates the sorption of a sample ion due to electrostatic attraction to the charged surface followed by sorption of a pairing ion from the mobile phase to maintain the surface charge at a constant value. The point is this: if it is assumed that the pairing ion accompanying the sample ion from the mobile phase to the interfacial region winds up also at the surface then this is energetically equivalent to the sorption of a neutral ion-pair (sample ion/pairing ion) and the corresponding free energy change will not be influenced by the electrical charge on the surface of the sorbent. Stated qualitatively, the attractive force enhancing sorption of the sample ion will be balanced by a repulsive force diminishing the sorption of another pairing ion. If, on the other hand, the pairing ion accompanying the sample ion remains in the diffuse layer then this criticism is not valid.

The above comments are made tentatively as a starting point for evaluating the data from chemically bonded reversed-phase sorbent/ion-pairing systems in terms of the ion exchange/surface adsorption double layer model proposed herein. It should be noted that ion exchange and adsorption are essentially independent processes and that, depending on the system of sorbent, ion-pairing reagent and sample, either of the two processes may predominate. Also, other processes such as ion-pair formation [201], and micelle formation in the mobile phase [184] may play a more or less important role in ionic retention in such systems.

Several other investigators have begun to invoke SGC theory to explain chromatographic retention behaviour of ions in HPLC [202-206]. This trend can be expected to continue since it represents a merging of well-established surface-chemical principles with modern chromatography.

Finally, the present research has demonstrated the speed, simplicity and accuracy of the "column equilibration" approach to studies of chromatographic systems. It is hoped that this technique will find greater use in studies of retention mechanisms. Its advantages include the following: (i) the system under study is at equilibrium, which is not true in studies involving retention volume measurements on chromatographic columns; (ii) as a result ambiguities in interpretation arising from skewed chromatographic peaks do not exist;

(iii) the technique is convenient for strongly retained compounds and for low concentrations of sample as well as for less strongly retained and more highly concentrated ones; (iv) only small quantities of expensive packings are required; and (v) it is relatively easy after equilibrium is established betwen the sorbent and sample solution to wash off and collect all of the sorbed components including sample, ion-pairing reagent, organic solvent modifier, etc., and to perform a total analysis of all of these components for any given mobile phase composition. Such studies can be expected to be very useful in providing a definitive model for the retention of ions in "ion-pair" chromatography.

BIBLIOGRAPHY

1. S. Bruckenstein and I.M. Kolthoff in Treatise of Analytical Chemistry, I.M. Kolthoff, P.J. Elving and E.B. Sandell, Eds., The Interscience Encyclopedia, New York, 1959, Chapter 12.
2. J.E. Ricci, Hydrogen Ion Concentration, Princeton University Press, Princeton, N.J., 1952.
3. R.G. Bates, Determination of pH, Theory and Practice, 2nd ed., Wiley-Interscience, 1973.
4. D. Rosenthal and P. Zuman in Treatise on Analytical Chemistry, Theory and Practice, Part I, 2nd ed., I.M. Kolthoff and P.J. Elving, Eds., John Wiley and Sons, N.Y., 1979, Chapter 18.
5. J.S. Fritz, Acid-Base Titrations in Nonaqueous Solvents, Allyn and Bacon, Boston, Mass., 1973.
6. J. Kucharsky and L. Safarik, Titrations in Nonaqueous Solvents, Elsevier, New York, 1965.
7. R.G. Bates, J. Electroanal. Chem., 29, 1 (1971).
8. B.L. Saunders and R.S. Srivastava, J. Pharm. Pharmacol., 3, 78 (1951).
9. R.G. Bates and R.M Robinson in Chemical Physics of Ionic Solutions, B.E. Conway and R.G. Barrades, Eds., Wiley, New York, 1966.

10. F.F. Cantwell, Ph.D. Thesis, University of Iowa, December, 1972.

11. F.F. Cantwell and D.J. Pietrzyk, Anal. Chem., _46_, 344 (1974).

12. Ibid, _46_, 1450 (1974).

13. S. Puon and F.F. Cantwell, Anal. Chem., _49_, 1256 (1977).

14. S. Puon, Ph.D. Thesis, University of Alberta, 1979.

15. J.A. Christensen, Acta Chem. Scand., _16_, 2363 (1962).

16. M. Donbrow and C.T. Rhodes, J. Pharm. Pharmacol., _15_, 233 (1963).

17. W.P. Evans, J. Pharm. Pharmacol., _16_, 233 (1964).

18. A.L. Underwood, Anal. Chim. Acta, _93_, 267 (1977).

19. E. Pelizzetti and E. Pramauro, Anal. Chim. Acta, _117_, 403 (1980).

20. P.A. Johansson, G. Hoffmann and U. Stefansson, Anal. Chim. Acta, _140_, 77 (1982).

21. D. Dyrssen, Svensk Kem. Tidskr., _64_, 213 (1952).

22. P.A. Johansson and K. Gustavii, Acta Pharm. Suecica., _13_, 407 (1976).

23. P.A. Johansson, Acta Pharm. Suecica., _14_, 363 (1977).

24. J.J. Kaufman, N.M. Semo and W.S. Koski, J. Med. Chem., _18_, 647 (1975).

25. T. Sekine and Y. Hasegawa, Solvent Extraction Chemistry, Dekker, N.Y., 1977, p. 320-322.

26. P.A. Johansson, Acta Pharm. Suecica., 14, 363 (1977).

27. P.A. Johansson, Acta Pharm. Suecica., 19, 137 (1982).

28. D. Ratajewicz and Z. Ratajewicz, Chem. Analityczne, 16, 1299 (1971).

29. T. Kubota and K. Ezumi, Chem. Pharm. Bull., 28, 3673 (1980).

30. P.A. Johansson and K. Gustavii, Acta Pharm. Suecica., 14, 1 (1977).

31. N.P. Komar, Zavod. Lab., 34, 513 (1968).

32. I.A. Gur'ev and N.A. Sokova, Tr. Khim. Khim. Tekhnol., 131 (1974); (C.A. 83:141518a).

33. I.M. Korenman and I.A. Gur'ev, J. Anal. Chem. U.S.S.R., 30, 1601 (1975); (English Translation).

34. I.A. Gur'ev and Z.M. Gur'eva, Tr. Khim. Khim. Tekhnol., 98, (1975); (C.A. 86:133136w).

35. I.A. Gur'ev, Izv. Vyssh. Uchebn. Zaved., Khim. Khim. Tekhnol., 20, 504 (1977); (C.A. 87:145391j).

36. I.A. Gur'ev, G.M. Lizunova and I.M. Korenman, Fiz.-Khim. Metody Anal., 1, 78 (1976); (C.A. 88:15573e).

37. I.A. Gur'ev and G.M. Lizunova, Fiz.-Khim. Metody Anal., 2, 85 (1977); (C.A. 90:197168y).

38. K. Gustavii , P.A. Johansson, and A. Brändström, Acta Pharm. Suecica, 13, 391 (1976).

39. P.A. Johansson, talk presented at Euroanalysis III Conference, Dublin, August, 1978.

40. I.A. Gur'ev, I.M. Korenman, T.G. Aleksandrova and V.V. Kutsovshaya, J. Anal. Chem. U.S.S.R., 32, 192 (1977); (English Translation).

41. I.A. Gur'ev and Z.M. Gur'eva, Zh. Anal. Khim., 32, 2442 (1977); (C.A. 89:36176p).

42. R.A. Hux and F.F. Cantwell, Anal. Chem. 52, 2388 (1980).

43. G. Schill in Ion Exchange and Solvent Extraction, J.A. Marinsky and Y. Marcus, Eds., Marcel Dekker, New York, 1974, vol. 6, Chapter 1.

44. R.R. Grinstead, Proceedings Int. Conf. Solvent Extraction Chemistry, Goteborg, 1966, D. Dyrssen, J. Liljenzin, J. Rydberg, Eds., North Holland, Amsterdam, 1967, p. 426.

45. E. Hogfeldt, Proceedings Int. Conf. Solvent Extraction Chem., Jerusalem, 1968, A.S. Kertes and Y. Marcus, Eds., Wiley, New York, 1969, p. 157.

46. G. Chuchani, J.A. Hamandez and J. Zabicky, Nature, 207, 1385 (1965).

47. H.Y. Mohammed and F.F. Cantwell, Anal. Chem., 52, 553 (1980).

48. T.J. Janjic and E.B. Milosavljevic, Anal. Chem., 50, 597 (1978).

49. T.J. Janjic , E.B. Milosavljevic and M.R. Sradvovic, Anal. Chim. Acta, 107, 359 (1979).

50. T.J. Janjic, E.B. Milosavljevic and W. Nanayakkara, Analusis, 10, 197 (1982).

51. J.V. Parke and W.W. Davis, Anal. Chem., 26, 642 (1954).

52. H.A. Laitinen and W.E. Harris, Chemical Analysis, 2nd ed., McGraw Hill, New York, 1975, p. 63.

53. Ibid, p. 45.

54. United States Pharmacopea, Mack Printing Co., Easton, PA., 1975, 19th Rev., p. 335.

55. J.L. Dye and V.A. Nicely, J. Chem. Ed., 48, 443 (1971).

56. H.A. Laitinen and W.E. Harris, Chemical Analysis, 2nd ed., McGraw-Hill, New York, 1975, p. 13.

57. J. Kielland, J. Amer. Chem. Soc., 59, 1675 (1937).

58. J.N. Butler, Ionic Equilibrium: A Mathematical Approach, Addison-Wesley, Reading, Mass., 1964, p. 428.

59. Ibid, p. 439.

60. M.J. Duffy, Endo Laboratories, private communication.

61. M.G. Natrella, *Experimental Statistics*, Handbook 91, National Bureau of Standards, Washington, D.C., 1966, pp. 5-18.

62. H.A. Laitinen and W.E. Harris, *Chemical Analysis*, 2nd ed., McGraw-Hill, New York, 1975, p. 542.

63. M. Carmichael and F.F. Cantwell, Can. J. Chem., *60*, 1286 (1982).

64. M.J. Duffy, Endo Laboratories, private communication.

65. G. Kortum, W. Vogel and K. Andrussow, *Dissociation Constants of Organic Acids in Aqueous Solution*, Butterworths, London, 1961, p. 450.

66. W. Kemula and H. Buchowski, J. Phys. Chem., *63*, 155 (1959).

67. Ya.I. Korenman, E.B. Kotelyanskaya and T.A. Nefedova, Zh. Prikl. Khim., *49*, 1112 (1976); (C.A. 85:37740x).

68. K.B. Sandell, Naturwissenschaften, *51*, 336 (1964).

69. R.F. Cookson, Chem. Rev., *74*, 5 (1974).

70. R.G. Bates, *Determination of pH, Theory and Practice*, 2nd ed., Wiley-Interscience, 1973, Chapter 8.

71. H. Ko and E.N. Petzold in *GLC and HPLC Determination of Therapeutic Agents, Part 1*, K. Tsuji and W. Morozowich, eds., Marcel Dekker, New York, 1978, Chapter 8.

72. B.J. Gudzinowicz and M.J. Gudzinowicz, Analysis of Drugs and Metabolites by Gas Chromatography-Mass Spectrometry, Marcel Dekker, New York, vol. 2, Chapter 1.

73. J.W. Dolan in L.R. Snyder and J.J. Kirkland, Introduction to Modern Liquid Chromatography, 2nd ed., Wiley, New York, 1979, Chapter 17.

74. L. Kopjack, B.S. Finkle, T.C. Lamoreaux, W.O. Pierce and F.M. Urry, J. Anal. Toxicol., 3, 155 (1979).

75. W.R. Kuelpmann, J. Clin. Chem. Clin. Biochem., 17, 115 (1979).

76. M.A. Evenson and G.L. Lensmeyer, Clin. Chem., 20, 249 (1974).

77. A. Cailleux, A. Turcant, A. Premel-Cabic and P. Allain, J. Chromatogr. Sci., 19, 163 (1981).

78. H.P. Gelbke, T.H. Grell and G. Schmidt, Arch. Toxicol., 39, 211 (1978).

79. C.N. Hodnett and R.D. Eberhardt, J. Anal. Toxicol., 3, 187 (1979).

80. M. Eichelbaum, B. Sonntag and G. Von Unruh, Arch. Toxicol., 4, 187 (1978).

81. R.W. Frei, Anal. Proc., 17, 519 (1980).

82. J. Lankelma and H. Poppe, J. Chromatogr., 149, 587 (1978).

83. G.J. DeJong, J. Chromatogr., 183, 203 (1980).

84. F. Erni, H.P. Keller, C. Morin and M. Schmitt, J. Chromatogr., 204, 65 (1981).

85. W. Roth, K. Beshke, R. Jauch, A. Zimmer and F.W. Koss, J. Chromatogr., 222, 13 (1981).

86. C.E. Werkhoven-Goewie, C. DeRuiter, U.A.Th. Brinkman, R.W. Frei, G.J. DeJong, C.J. Little and O. Stahel, J. Chromatogr., 255, 79 (1983).

87. W. Voelter, T. Kronbach, K. Zech and R. Huber, J. Chromatogr., 239, 475 (1982).

88. H.Y. Mohammed, H. Veening and D.A. Dayton, J. Chromatogr., 226, 471 (1981).

89. J.C. Gfeller and M. Stockmeyer, J. Chromatogr., 198, 162 (1980).

90. L.R. Snyder and J.J. Kirkland, Introduction to Modern Liquid Chromatography, 2nd ed., Wiley, New York, 1979, p. 281.

91. H. Adler, M. Margoshes, L.R. Snyder and C. Spitzer, J. Chromatogr., 143, 125 (1977).

92. D.D. Koch and P.T. Kissinger, Anal. Chem., 52, 27 (1980).

93. J. Lankelma and H. Poppe, J. Chromatogr., 149, 587 (1978).

94. F.F. Cantwell, Anal. Chem., 48, 1854 (1976).

95. H.Y. Mohammed and F.F. Cantwell, Anal. Chem., 50, 491 (1978).

96. D. Ishii, K. Hibi, K. Asai, M. Nagaya, K. Mochizuki and Y. Mochida, J. Chromatogr., 156, 173 (1978).

97. R.G. Baum, R. Saetre and F.F. Cantwell, Anal. Chem., 52, 15 (1980).

98. R.G. Baum and F.F. Cantwell, J. Pharm. Sci., 67, 1066 (1978).

99. R.G. Baum and F.F. Cantwell, Anal. Chem., 50, 280 (1978).

100. R.A. Hux, H.Y. Mohammed and F.F. Cantwell, Anal. Chem., 54, 113 (1982).

101. D.J. Berry, J. Chromatogr., 42, 39 (1969).

102. D.M. Patel, A.J. Visalli, J.J. Zalipsky, N.H. Reavy-Cantwell in Analytical Profiles of Drug Substances, K. Florey, Ed., Academic Press, New York, 1975, Vol. 4.

103. K. Diem, Ed., Documenta Geigy Scientific Tables, 6th ed., Geigy Pharmaceuticals, Montreal, 1962, pp. 553-555.

104. Amberlite XAD-2, Technical Bulletin, Rohm and Haas Co., Philadelphia, PA, 1972.

105. J.M. Christensen and S. Holfort, J. Pharm. Pharmacol., 25, 538 (1975).

106. G.E. Boyd, A.W. Adamson and L.S. Meyers Jr., J. Amer. Chem. Soc., 69, 2836 (1947).

107. H.P.M. van Vliet, Th.C. Bootsman, R.W. Frei and U.A.Th. Brinkman, J. Chromatogr., 185, 483 (1979).

108. L.R. Snyder and J.J. Kirkland, Introduction to Modern Liquid Chromatography, 2nd ed., Wiley, New York, 1979, Chapter 5.

109. O. Ericsson and B. Danielsson, Drug Metab. and Disposit., 5, 497 (1977).

110. O. Ericsson, Acta Pharm. Suecica, 15, 81 (1978).

111. J.K. Baker, J. Liq. Chromatogr., 4, 271 (1981).

112. F.F. Cantwell and S. Puon, Anal. Chem., 51, 623 (1979).

113. Amberlite XAD-2, Technical Bulletin, Rohm and Haas Co., Philadelphia, PA., 1972.

114. R.L. Gustafson, R.L. Albright, J. Heisler, J.A. Lirio, O.T. Reid, Jr., Ind. Eng. Chem., Prod. Res. Dev., 7, 107 (1968).

115. R.L. Gustafson and J. Paleos, Organic Compounds in Aquatic Environments, S.J. Faust and J.V. Hunter, ed., Dekker, New York, 1971, p. 213.

116. D.J. Pietrzyk, Talanta, 16, 169 (1969).

117. R. Kunin, E.F. Metzner, J.A. Oline, S.A. Fisher and N. Frisch, Ind. Eng. Chem., Prod. Res. Dev., 1, 140 (1962).

118. A.D. Wilks and D.J. Pietrzyk, Anal. Chem., 44, 676 (1972).

119. J. Paleos, J. Colloid. Interface. Sci., 31, 7 (1969).

120. D.J. Pietrzyk and C.H. Chu, Anal. Chem., 49, 757 (1977).

121. M.D. Grieser and D.J. Pietrzyk, Anal. Chem., 45, 8 (1973).

122. C.H. Chu and D.J. Pietrzyk, Anal. Chem., 46, 330 (1974).

123. H.Y. Mohammed and F.F. Cantwell, Anal. Chem., 50, 491 (1978).

124. M.D. Grieser and D.J. Pietrzyk, 45, 1348 (1973).

125. F.A. Long and W.F. McDevitt, Chem. Rev., 51, 119 (1952).

126. M.W. Scoggins and J.W. Miller, Anal. Chem., 40, 1155 (1968).

127. M.W. Scoggins, Anal. Chem., 44, 1285 (1972).

128. D.J. Pietrzyk, E.P. Kroeff and T.D. Rotsch, Anal. Chem., 50, 3 (1978).

129. E.P. Kroeff and D.J. Pietrzyk, Anal. Chem., 50, 502 (1978).

130. J.L. Lundgren and A. Schilt, Anal. Chem., 49, 974 (1977).

131. T.D. Rotsch, W.R. Cahill, Jr., D.J. Pietrzyk and F.F. Cantwell, Can. J. Chem., 59, 2179 (1981).

132. S. Afrashethfar and F.F. Cantwell, Anal. Chem., 54, 2422 (1982).

133. F.F. Cantwell in Ion Exchange and Solvent Extraction, J.A. Marinsky and Y. Marcus, eds., Dekker, New York, to be published.

134. O. Stern, Z. Elektrochem., 30, 508 (1924).

135. G. Gouy, J. Phys., 9, 457 (1910); Ann. Phys., 7, 129 (1917).

136. D.L. Chapman, Phil. Mag., 25, 475 (1913).

137. D.L. Grahame, Chem. Revs., 41, 441 (1947).

138. J.Th. Overbeek in Colloid Science, H.R. Kruyt, ed., Vol. I, Elsevier, N.Y., 1952, Chapters 4 and 5.

139. K.J. Mysels, Introduction to Colloid Chemistry, Interscience, N.Y., 1967, Chapter 15.

140. A.W. Adamson, Physical Chemistry of Surfaces, 2nd ed., Interscience, N.Y., 1967, Chapter 4.

141. J.O'M. Bockris, B.E. Conway and E. Yeager, Comprehensive Treatise of Electrochemistry, Vol. 1, Plenum Press, N.Y., 1980.

142. D.J. Shaw, Introduction to Colloid and Surface Chemistry, 3rd ed., Butterworths, London, 1980, Chapter 7.

143. R.A. Robinson and R.H. Stokes, Electrolyte Solutions, Butterworths, London, 1959.

144. W.B. Dandliker and V.A. de Saussure in The Chemistry of Biosurfaces, Vol. 1, M.L. Hair, ed., Dekker, N.Y., 1971, Chapter 1.

145. J.O'M. Bockris and A.K.N. Reddy, Modern Electrochemistry, Vol. 2, Plenum Press, N.Y., 1970.

146. Y.G. Berube and P.L. Debruyn, J. Colloid Interface Sci., 28, 92 (1968).

147. R. Reeves in Comprehensive Treatise of Electrochemistry, Vol. 1, Plenum Press, N.Y., 1980, p. 111.

148. Handbook of Mathematical Functions, M. Abramowitz and I.A. Stegun, eds., National Bureau of Standards, Applied Mathematics Series 55, 1968, p. 87.

149. F. Helfferich, Ion Exchange, McGraw-Hill, N.Y., 1962, Chapter 5.

150. R.P. Buck in Proceedings of the Symposium on Ion Exchange Transport and Interfacial Properties, R.S. Yeo and R.P. Buck, eds., Electrochemical Society, Pennington, N.J., 1981, p. 16.

151. L.R. Snyder, Principles of Adsorption Chromatography, Marcel Dekker, N.Y., 1968, Chapter 4.

152. F. Helfferich, Ion Exchange, McGraw-Hill, N.Y., 1962, Chapter 2.

153. P. Somasundaran and D.W. Fuerstenau, J. Phys. Chem., 70, 90 (1966).

154. E.H. Lucassen-Reynders in Progress in Surface and Membrane Science, D.A. Cadenhead and J.F. Danielli, eds., Academic Press, N.Y., 1976, Vol. 10, p. 317.

155. J.J. Stranahan and S.N. Deming, Anal. Chem., 54, 2251 (1982).

156. L.R. Snyder, Principles of Adsorption Chromatography, Marcel Dekker, N.Y., 1968, Chapter 3.

157. J.F.K. Huber and R.G. Gerritse, J. Chromatogr., 58, 137 (1971).

158. J.R. Conder and C.L. Young, Physicochemical Measurements by Gas Chromatography, Wiley, Toronto, 1979, Chapter 9, p. 423.

159. F. Dondi, A. Betti, G. Blo, C. Bighi and B. Versino, Ann. Chim. (Rome), 68, 293 (1979).

160. A.W.J. de Jong, J.C. Kraak, H. Poppe and F. Nooitgedacht, J. Chromatogr., 193, 181 (1980).

161. R.P.W. Scott and P. Kucera, J. Chromatogr., 175, 51 (1979).

162. E.H. Slaats, W. Makarovski, J. Fekete and H. Poppe, J. Chromatogr., 207, 299 (1981).

163. J.L.M. van de Venne, J.L.H.M. Hendrikx and R.S. Deelder, J. Chromatogr., 167, 1 (1978).

164. J.R. Conder and C.L. Young, Physiochemical Measurement by Gas Chromatography, John Wiley and Sons, N.Y., 1979, p. 72.

165. Ibid, p. 354.

166. S. May, University of Alberta, unpublished work, 1981.

167. C.A. Bennet and N.L. Franklyn, Statistical Analysis in Chemistry and the Chemical Industry, Wiley, New York, 1954, Chapter 6.

168. F.S. Acton, Analysis of Straight Line Data, Dover Publications, N.Y., 1959.

169. R.B. Dean and W.J. Dixon, Anal. Chem., 23, 636 (1951).

170. R.M. McCormick and B.L. Karger, Anal. Chem., 52, 2249 (1980).

171. C. Horvath and H. Lin, J. Chromatogr., 126, 401 (1976).

172. R.P.W. Scott and P. Kucera, J. Chromatogr., 125, 251 (1976).

173. J.S. Fritz and J.N. Story, J. Chromatogr., 90, 267 (1974).

174. H.A. Laitinen and W.E. Harris, Chemical Analysis, 2nd ed., McGraw-Hill, N.Y., 1975, Chapter 27.

175. G.E. Boyd, J. Soln. Chem., 6, 135 (1977).

176. G. Eisenman, Biophys. J., 2, 259 (1962).

177. G. Eisenman in Membrane Transport and Metabolism, A. Kleinzeller and A. Kotyk, eds., Academic Press, New York, 1961, pp. 163-179.

178. D. Reichenberg in Ion Exchange: A Series of Advances, vol. 1, J.A. Marinsky, ed., Dekker, New York, 1966, Chapter 7.

179. R.M. Diamond, J. Phys. Chem., 67, 2513 (1963).

180. R.M. Diamond and D.C. Whitney in Ion Exchange: A Series of Advances, Vol. 1, J.A. Marinsky, ed., Dekker, New York, 1966, Chapter 8.

181. J. Feitelson, ibid., Vol. 2, 1969, Chapter 4.

182. H.S. Frank and W.Y. Wen, Discussions Faraday Soc., 24, 133 (1957).

183. G. Schill in Advances in Ion Exchange and Solvent Extraction, Vol. 6, Dekker, New York, 1974, Chapter 1.

184. W.R. Melander and C. Horvath in High Performance Liquid Chromatography: Advances and Perspectives, Vol. 2, C. Horvath, ed., Academic Press, New York, 1980.

185. R.E. Majors, ibid, Vol. 1, 1980.

186. E. Tomlinson, T.M. Jeffries, and C.M. Riley, J. Chromatogr., 159, 315 (1978).

187. G. Schill and K.G. Wahlund, Proc. 9th Materials Research Symposium, Gaithersburg, Maryland, April 1978.

188. R. Gloor and E.L. Johnson, J. Chromatogr. Sci., 15, 413 (1977).

189. M.T.W. Hearn in Advances in Chromatography, Vol. 18, J.C. Giddings and R.A. Keller, eds., Dekker, New York, 1980, Chapter 2.

190. D.P. Wittmer, N.O. Nuessle, and W.G. Honey, Jr., Anal. Chem., 47, 1422 (1975).

191. C. Horvath, W. Melander, I. Molnar, and P. Molnar, Anal. Chem., 49, 2295 (1977).

192. C. Horvath, W. Melander, and I. Molnar, J. Chromatogr., 125, 129 (1976).

193. J.H. Knox and G.R. Laird, J. Chromatogr., 122, 17 (1976).

194. C.P. Terweij-Groen, S. Heemstra, and J.C. Kraak, J. Chromatogr., 161, 69 (1978).

195. P.T. Kissinger, Anal. Chem., 49, 883 (1977).

196. C.T. Hung and R.B. Taylor, J. Chromatogr., 202, 333 (1980).

197. R.H.A. Sorel and A. Hulshoff in Advances in Chromatography, Vol. 21, J.C. Giddings, ed., Dekker, New York, 1983, Chapter 3.

198. B.A. Bidlingmeyer, S.N. Deming, W.P. Price, Jr., B. Sachok, and M. Petrusek, J. Chromatogr., 186, 419 (1979).

199. B.A. Bidlingmeyer, J. Chromatogr. Sci., **18**, 525 (1980).

200. R.S. Deelder and J.H.M. Van Den Berg, J. Chromatogr., **218**, 327 (1981).

201. B.L. Karger, J.N. LePage, and N. Tanaka in *High Performance Liquid Chromatography: Advances and Perspectives*, Vol. 1, C. Horvath, ed., Academic Press, New York, 1980, p. 141.

202. J.H. Knox and R.A. Hartwick, J. Chromatogr., **204**, 3 (1981).

203. Z. Iskandarins and D.J. Pietrzyk, Anal. Chem., **54**, 1065 (1982).

204. J.J. Stranahan and S.N. Deming, Anal. Chem., **54**, 1540 (1982).

205. B. Sachok, J.R. Stranahan and S.N. Deming, Anal. Chem., **53**, 70 (1981).

206. C.M. Riley, L.A. Sternson, A.J. Repta, J. Chromatogr., **219**, 235 (1981).

APPENDIX I

APPENDIX I

A derivation is given of the equations describing the titration curve for an H_2A^+ type acid with NaOH in the presence of a two-phase (aqueous solution/immiscible solvent) system. The treatment is analogous to that given in [13,14]. The equilibria that describe the system are given as equations 1 through 7 in the text.

The equilibrium constant and distribution coefficient expressions corresponding to these equilibria may be written:

$$K_{a,H_2A} = \frac{[HA].a_H}{[H_2A^+]} \qquad (I-1)$$

$$K_{a,HA} = \frac{[A^-].a_H}{[HA]} \qquad (I-2)$$

$$K_{I,H_2AX} = \frac{[H_2AX]_o}{[H_2A^+]} \qquad (I-3)$$

$$K_{HA} = \frac{[HA]_o}{[HA]} \qquad (I-4)$$

$$K_{I,MA} = \frac{[MA]_o}{[A^-]} \qquad (I-5)$$

$$K_{I,H_2A.A} = \frac{[H_2A.A]_o}{[H_2A^+][A^-]} \qquad (I-6)$$

$$K_w = a_H \cdot a_{OH} \qquad (I-7)$$

The mass balance and electroneutrality expressions are needed in addition to equations I-1 thru I-7 to completely describe the system. The electroneutrality condition for the aqueous phase can be written:

$$[H_3O^+] + [M^+] + [H_2A^+] = [OH^-] + [X^-] + [A^-] \qquad (I-8)$$

With the assumption that dissociation of ion pairs in the organic phase is negligible (see p. 9) an electroneutrality expression is not required for the organic phase.

The mass balance expressions for H_2A^+, M^+ and X^- can be written:

$$n_{H_2A} = V([H_2A^+] + [HA] + [A^-]) + V_o([H_2AX]_o$$

$$+ [HA]_o + [MA]_o + 2[H_2A\cdot A]_o) \qquad \text{(I-9)}$$

$$[M^+] = [MX] + n_{OH}/V - (\frac{V_o}{V})\ [MA]_o \qquad \text{(I-10)}$$

$$[X^-] = [MX] + n_{H_2A}/V - (\frac{V_o}{V})\ [H_2AX]_o \qquad \text{(I-11)}$$

where n_{H_2A} is the number of moles of the salt H_2AX initially present in the titration vessel; n_{OH} is the moles of strong base titrant, MOH, added at a given point in the titration; V and V_o are the volumes (in liters) of the aqueous and organic phases respectively; and [MX] is the concentration of the inert electrolyte (e.g. NaCl) in the aqueous phase.

The electroneutrality condition (equation I-8) can be solved by substituting for $[M^+]$ and $[X^-]$ from equations I-10 and I-11.

$$n_{OH} = n_{H_2A} + V([A^-] + \frac{V_o}{V}[MA]_o - [H_2A^+] - \frac{V_o}{V}[H_2AX]_o$$

$$+ [OH^-] - [H_3O^+]) \qquad \text{(I-12)}$$

The titration equations are obtained by substituting for the species concentrations in equations I-9 and I-12 using the equilibrium constant and distribution coefficient expressions I-1 thru I-7. The electroneutrality expression gives rise to the equation:

$$n_{OH} = n_{H_2A} + (V+V_o \cdot K_{I,MA})\frac{K_{a,HA}}{a_H}[HA] - (V+V_o \cdot K_{I,H_2AX})\frac{a_H}{K_{a,H_2A}}$$

$$+ \frac{K_w V}{a_H \gamma_{OH}} - \frac{a_H V}{\gamma_H} \qquad \text{(I-13)}$$

where [HA] is found by solving the mass balance condition for H_2A^+, which takes the form of a quadratic equation:

$$a[HA]^2 + b[HA] - n_{H_2A} = 0 \qquad \text{(I-14)}$$

where

$$a = 2 \cdot V_o \cdot K_{I,H_2A} \cdot A\left(\frac{K_{a,HA}}{K_{a,H_2A}}\right) \qquad \text{(I-15)}$$

and

$$b = (V+V_o \cdot K_{HA}) + \frac{K_{a,HA}}{a_H}(V+V_o \cdot K_{I,MA})$$

$$+ \frac{a_H}{K_{a,H_2A}}(V+V_o \cdot K_{I,H_2AX}) \qquad \text{(I-16)}$$

Equations I-13 thru I-16 may be written in a simpler form by defining the "apparent dissociation constants" K^{app}_{a,H_2A} and $K^{app}_{a,HA}$ for the first and second protons of H_2A^+ in a two-phase system [48-50].

$$K^{app}_{a,H_2A} = \frac{a_H \cdot C^{app}_{HA}}{C^{app}_{H_2A}} \qquad \text{(I-17)}$$

$$K^{app}_{a,HA} = \frac{a_H \cdot C^{app}_{A}}{C^{app}_{HA}} \qquad \text{(I-18)}$$

The terms $C^{app}_{H_2A}$, C^{app}_{HA} and C^{app}_{A} are the "apparent concentrations" of H_2A^+, HA and A^-. They are defined as the total number of moles of that species in both phases divided by the aqueous phase volume. They can be written:

$$C^{app}_{H_2A} = [H_2A^+] + \frac{V_o}{V}[H_2AX]_o$$

$$= [H_2A^+]\left(1 + \left(\frac{V_o}{V}\right)K_{I,H_2AX}\right) \qquad \text{(I-19)}$$

$$C^{app}_{HA} = [HA] + \frac{V_o}{V}[HA]_o$$

$$= [HA]\left(1 + \left(\frac{V_o}{V}\right)K_{HA}\right) \qquad \text{(I-20)}$$

$$C_A^{app} = [A^-] + \frac{V_o}{V}[MA]_o$$

$$= [A^-]\left(1 + \left(\frac{V_o}{V}\right)K_{I,MA}\right) \qquad \text{(I-21)}$$

Substituting equations I-19 thru I-21 into equations I-17 and I-18 gives

$$K_{a,H_2A}^{app} = \frac{a_H[HA]}{[H_2A^+]}\left[\frac{1+\left(\frac{V_o}{V}\right)K_{HA}}{1+\left(\frac{V_o}{V}\right)K_{I,H_2AX}}\right]$$

$$= K_{a,H_2A}\left[\frac{1+\left(\frac{V_o}{V}\right)K_{HA}}{1+\left(\frac{V_o}{V}\right)K_{I,H_2AX}}\right] \qquad \text{(I-22)}$$

$$K_{a,HA}^{app} = \frac{a_H[A^-]}{[HA]}\left[\frac{1+\left(\frac{V_o}{V}\right)K_{I,MA}}{1+\left(\frac{V_o}{V}\right)K_{HA}}\right]$$

$$= K_{a,HA}\left[\frac{1+\left(\frac{V_o}{V}\right)K_{I,MA}}{1+\left(\frac{V_o}{V}\right)K_{HA}}\right] \qquad \text{(I-23)}$$

Equations I-20 and I-22 thru I-23 may be substituted into equations I-13 thru I-16 to give the titration equations in a second form:

$$n_{OH} = n_{H_2A} + V\left[\frac{K^{app}_{a,HA}}{a_H} C^{app}_{HA} - \frac{a_H}{K^{app}_{a,H_2A}} C^{app}_{HA}\right]$$

$$+ \frac{K_w \cdot V}{a_H \gamma_{OH}} - \frac{a_H \cdot V}{\gamma_H} \qquad \text{(I-24)}$$

from the mass balance condition:

$$a'(C^{app}_{HA})^2 + b'C^{app}_{HA} - n_{H_2A} = 0 \qquad \text{(I-25)}$$

where

$$a' = 2 \cdot V_o \cdot K_{I,H_2A} \cdot A\left(\frac{K_{a,HA}}{K_{a,H_2A}}\right)\left(1+\left(\frac{V_o}{V}\right)K_{HA}\right)^{-2} \qquad \text{(I-26)}$$

$$b' = V\left(\frac{K^{app}_{a,HA}}{a_H} + \frac{a_H}{K^{app}_{a,H_2A}} + 1\right) \qquad \text{(I-27)}$$

Since a' and b' are both positive while the third term in equation I-25 is negative, both positive and negative roots exist. Only the positive root has physical meaning because C^{app}_{HA} cannot be negative:

$$C^{app}_{HA} = \frac{-b' + \left((b')^2 + 4.a'.n_{H_2A}\right)^{1/2}}{2.a'} \qquad \text{(I-28)}$$

When the extraction of the ion-pair $H_2A \cdot A$ is negligible (i.e. $(b')^2 >> 4 \cdot a' \cdot n_{H_2A}$) then equation I-28 is no longer valid. However, in this case equation I-25 simplifies to a linear form:

$$C_{HA}^{app} = \frac{n_{H_2A}}{b'} \qquad \text{(I-29)}$$

APPENDIX II

TABLE 12

Sorption Isotherm Data for Acetaminophen on XAD in Aqueous 1.0×10^{-3} M NaCl (Figure 25)

C_m (moles/L)	C_s (moles/Kg)
1.003×10^{-6}	3.22×10^{-5}
2.006×10^{-6}	6.20×10^{-5}
4.012×10^{-6}	1.26×10^{-4}
6.018×10^{-6}	1.91×10^{-4}
8.024×10^{-6}	2.54×10^{-4}
1.003×10^{-5}	3.22×10^{-4}
2.006×10^{-5}	6.22×10^{-4}
4.012×10^{-5}	1.21×10^{-3}
6.024×10^{-5}	1.82×10^{-3}
8.024×10^{-5}	2.42×10^{-3}
1.003×10^{-4}	3.00×10^{-3}
2.006×10^{-4}	5.85×10^{-3}
4.012×10^{-4}	1.09×10^{-2}

TABLE 13

Sorption Isotherm Data for NBTA$^+$ on 54.5 μeq/g SXAD Resin from Aqueous 0.1 M NaCl (Figure 26)

C_m (moles/L)	C_s (moles/Kg)
0.9978×10^{-7}	4.40×10^{-4}
1.996×10^{-7}	7.34×10^{-4}
3.991×10^{-7}	1.23×10^{-3}
5.987×10^{-7}	1.62×10^{-3}
7.982×10^{-7}	2.01×10^{-3}
9.978×10^{-7}	2.35×10^{-3}
1.988×10^{-6}	3.72×10^{-3}
3.975×10^{-6}	5.37×10^{-3}

TABLE 14

Sorption Isotherm Data for NBTA$^+$ on 54.5 μeq/g SXAD Resin from Aqueous 1.0 M NaCl (Figure 26)

C_m (moles/L)	C_s (moles/Kg)
9.938×10^{-8}	7.44×10^{-5}
1.988×10^{-7}	1.38×10^{-4}
3.975×10^{-7}	2.58×10^{-4}
5.963×10^{-7}	3.77×10^{-4}
7.950×10^{-7}	4.67×10^{-4}
9.938×10^{-7}	5.64×10^{-4}
1.988×10^{-6}	9.69×10^{-4}
3.975×10^{-6}	1.73×10^{-3}

TABLE 15

Sorption Isotherm and Distribution Coefficient Data for $NBTA^+$ on 54.5 μeq/g SXAD Resin from Aqueous NaCl Solutions (Data from Figures 27 and 28)

[NaCl] (moles/L)	C_m (moles/L)	C_s (moles/Kg)	K_{Q^+} (L/Kg)
0.1000	1.988×10^{-8}	8.24×10^{-5}	4.40×10^3
	3.975×10^{-8}	1.73×10^{-4}	
	9.978×10^{-8}	4.40×10^{-4}	
0.1500	3.018×10^{-8}	1.04×10^{-4}	3.41×10^3
	5.963×10^{-8}	2.03×10^{-4}	
0.2500	4.024×10^{-8}	9.27×10^{-5}	2.11×10^3
	9.054×10^{-8}	1.88×10^{-4}	
0.4000	5.963×10^{-8}	8.69×10^{-5}	1.44×10^3
	1.292×10^{-7}	1.85×10^{-4}	
0.6000	7.950×10^{-8}	8.18×10^{-5}	1.01×10^3
	1.789×10^{-7}	1.81×10^{-4}	
1.000	9.938×10^{-8}	7.44×10^{-5}	7.05×10^2
	1.988×10^{-7}	1.38×10^{-4}	

TABLE 16

Distribution Coefficient Data for ~~the Sorption~~ of $NBTA^+$ on 54.5 μeq/g SXAD Resinfrom Aqueous KCl Solutions

(Figure 29)

[KCl] (moles/L)	K_Q+ (L/Kg)
0.100	2.50×10^3
0.160	1.67×10^3
0.240	1.12×10^3
0.400	7.37×10^2
0.600	5.44×10^2
1.000	4.10×10^2

TABLE 17

Distribution Coefficient Data for the Sorption of NBTA$^+$ on 54.5 μeq/g SXAD from Aqueous LiCl Solutions

(Figure 30)

[LiCl] (moles/L)	K_O^+ (L/Kg)
0.09985	3.29×10^3
0.1598	2.27×10^3
0.2396	1.57×10^3
0.3954	9.95×10^2
0.5991	7.08×10^2
0.9985	4.93×10^2

TABLE 18

Distribution Coefficient Data for the Sorption of $NBTA^+$ on 9.7 μeq/g SXAD Resin from Aqueous Solutions

(Figure 31)

[NaCl] (moles/L)	K_{Q^+} (L/Kg)
0.100_0	7.89×10^2
0.150_0	5.94×10^2
0.250_0	4.44×10^2
0.400_0	3.53×10^2
0.600_0	3.07×10^2
1.00_0	2.87×10^2

TABLE 19

Distribution Coefficient Data for the Sorption of NBS^- on 54.5 μeq/g SXAD Resin from Aqueous NaCl Solutions

(Figure 32)

[NaCl] (moles/L)	K_Q^+ (L/Kg)
0.100_0	3.64×10^2
0.200_0	4.92×10^2
0.400_0	6.59×10^2
0.600_0	7.84×10^2
0.800_0	9.45×10^2
1.00_0	1.12×10^3